



DISSERTATION

Iron(II) Spin Crossover Complexes: a multifaceted approach to rational design, tailor cooperativity, enhance complexity and advanced multifunctionality.

Ausgeführt zum Zwecke der Erlangung des akademischen Grades eines

Doktors der technischen Wissenschaften unter Leitung von

Associate Prof. Dipl.-Ing. Dr.techn. Peter Weinberger (E163 Institut für Angewandte Synthesechemie)

Eingereicht an der Technischen Universität Wien Fakultät für Technische Chemie

von

Dipl.-Ing. Willi Zeni Matrikel-Nr. 01529678

Willi Zeni Wien, 2024



I am among those who think that science has great beauty. A scientist in his laboratory is not only a technician: he is also a child placed before natural phenomena which impress him like a fairy tale.



Maria Skłodowska Curie



Acknowledgements

The word acknowledgement is an understatement, because in this page I want to truly thank all the people who supported me throughout the years and helped make this work a reality.

In first instance I want to thank my supervisor Assoc. Prof. Dipl.-Ing. Dr. Peter Weinberger, not only for the opportunity to carry out the work in his laboratory and the freedom in choosing the direction of my research, but also for his mentoring and friendship, for making me feel like a peer even when I was still a student and for his constant encouragement and support throughout these years. This helped me grow not only as a scientist but also as a person.

The second, major, thank you goes to my friend and former colleague and supervisor Dr. Danny Müller, who is the embodiment of a good scientist. I had the fortune, and I would also say privilege, to work alongside him for about two years, and it still astonishes me how much knowledge he was able to pass on to me in this short time. Thanks to him, I saw firsthand what it means to be a researcher and how to approach and conduct scientific research in a proper and rigorous way. His never-ending ideas, the genuine interest for chemistry and science in general, together with his astoundingly vast chemical knowledge and expertise truly enriched me and kept the spark for chemistry alive.

Thanks to all the colleagues in the research group Weinberger, especially Dr. Marco Seifried and Frieda Kapsamer, with whom a working relationship turned into a friendship, probably cemented by the countless coffee breaks. You two always ensured a pleasant work environment and alleviated the stressful work phases.

Thanks to all my non-chemist friends Andrea, Katja, Bea, Franci, Michele, Erika, Elena for bearing with my sometimes-difficult moods and listening to my rants when things at work didn't work out, and to the boulder-crew Tommy, Ines, Gitti, Patricia, Fabi, Johannes, Niki for your support and help in keeping my mind off work during our extenuating sessions.

A special thank you goes of course to you, Petra, for your patience and support especially in the last and very stressful phase of this journey (and obviously also for your help with the interpretation of crystal structures).

Finally, I want to thank my parents, who supported me in all my career choices and always believed in me. You were always there for me and gave me the strength to keep going, no matter how hard of a time I was having. This is probably my last chapter in the academia, but thanks to you I could also experience what's outside of this world and from you I have learned the meaning of work ethic, and I am prepared for whatever comes next.

Part of this work was financially supported by the Austrian Science Fund (FWF), Project P31076-N28



Abstract

Molecular bistability is a key-ingredient for the development of novel molecular materials tailored for technological applicability. One of the most illustrious examples of bistability in coordination chemistry is the spin-crossover (SCO) effect, featuring for 3d⁴-3d⁷ metal ions a reversible transition between different electronic states triggered by external stimuli as temperature, pressure, light, etc. The change of the metal centre's spin-state affects key-properties of the material including magnetic moment, colour, dielectric constant, lattice extension. These attributes make SCO compounds highly desirable for applications in sensors, data storage, and smart materials. Of the utmost importance for any possible application is an abrupt and preferably hysteretic spin transition at or above room temperature, for which a high degree of cooperativity between molecules is required.

Modern SCO research focuses mainly on two aspects: the first is a deeper understanding of the SCO phenomenon through rational design of SCO materials to achieve precise control over the SCO phenomenon and exploit the underlying magnetic behavior, but in the last three decades a new trend emerged, namely the synthesis of multifunctional SCO materials bearing an additional property which synergistically depends on the spin transition. In this work, both abovementioned aspects were tackled.

In the context of rational design, a decoupling of electronic and steric effects was attempted, by preparing $[Fe(PrIm)_6]^{2+}$ (PrIm = 1-propyl-1H-imidazole) and comparing it with $[Fe(3tz)_6]^{2+}$ (3tz=1-propyl-1H-tetrazole), one of the first and probably the most studied and comprehensively characterized SCO-compound. The study also shed light on the versatility of PrIm as ligand for Fe(II) complexes.

Multifunctionality was first approached by synthesizing and characterizing a series of ω -(1H-tetrazol-1-yl) carboxylic acids bifunctional ligands and their Fe(II) complexes aiming to obtain systems showing a strong, extended H-bond network for enhanced cooperativity, ergo improve the quality of the spin transition. In a second step, the bidentate nature of the ligands was exploited for the synthesis of mixed-metallic 3d-4f coordination polymers.

Lastly, the coupling of SCO with host-guest chemistry for chemo-sensing application was investigated, by taking a new approach to produce extended Hofmann-type SCO-PCPs. Applying a novel synthetic procedure, an enlargement of the classic structure [Fe(pz)][M(CN)₄] (M=Ni, Pd, Pt) based on cyanometallate linkers was performed, using tetrakis-cyanoacetylides linkers to obtain PCPs having the general formula $[Fe(pz)][M(C_3N)_4]$. They feature five-fold larger cavities and a drastic increase of the porosity. Most importantly, all the desired properties (hysteretic SCO, guest-dependent spin transition, bidirectional chemoswitching and memory effect) were retained.

Kurzfassung

Molekulare Bistabilität ist eine entscheidende Komponente für die Entwicklung neuartiger molekularer Materialien, die auf technologische Anwendbarkeit zugeschnitten sind. Eines der bekanntesten Beispiele für Bistabilität in der Koordinationschemie ist der Spin-Crossover (SCO)-Effekt, bei dem es bei 3d⁴-3d⁷ Metallionen zu einem reversiblen Übergang zwischen verschiedenen elektronischen Zuständen kommt, der durch äußere Einflüsse wie Temperatur, Druck, Licht usw. ausgelöst wird. Der Wechsel des Spin-Zustands am Metallzentrum beeinflusst Schlüsseleigenschaften des Materials wie magnetisches Moment, Farbe, Dielektrizitätskonstante und Gitterausdehnung. Diese Eigenschaften machen SCO-Verbindungen für Anwendungen in Sensoren, Datenspeicherung und intelligenten Materialien äußerst begehrt. Von größter Bedeutung für jede mögliche Anwendung ist ein abrupter und vorzugsweise hysteretischer Spin-Übergang bei oder über Raumtemperatur, für den ein hohes Maß an Kooperation zwischen den Molekülen erforderlich ist.

Die moderne SCO-Forschung konzentriert sich hauptsächlich auf zwei Aspekte: Der erste ist ein tieferes Verständnis des SCO-Phänomens durch das rationale Design von SCO-Materialien, um eine präzise Kontrolle über das SCO-Phänomen zu erreichen und das zugrunde liegende magnetische Verhalten auszunutzen, aber in den letzten drei Jahrzehnten ist jedoch ein neuer Trend aufgetaucht, nämlich die Synthese von multifunktionalen SCO-Materialien, die eine zusätzliche Eigenschaft aufweisen, die synergistisch vom Spin-Übergang abhängt. In dieser Arbeit wurden beide oben genannten Aspekte angegangen.

Im Kontext des rationalen Designs wurde versucht, elektronische und sterische Effekte zu entkoppeln, indem $[Fe(PrIm)_6]^{2+}$ (PrIm = 1-Propyl-1H-imidazol) synthetisiert und mit $[Fe(3tz)_6]^{2+}$ (3tz = 1-Propyl-1H-tetrazol), einer der ersten und wahrscheinlich am meisten untersuchten und umfassend charakterisierten SCO-Verbindung, verglichen wurde. Die Studie beleuchtete auch die Vielseitigkeit von PrIm als Ligand für Fe(II)-Komplexe.

Multifunktionalität wurde zunächst durch die Synthese und Charakterisierung einer Reihe von bifunktionalen ω-(1H-tetrazol-1-yl)-carbonsäure Liganden und deren Fe(II)-Komplexen angegangen, mit dem Ziel, Systeme zu erhalten, die ein starkes, erweitertes H-Brückennetzwerk für eine verbesserte Kooperativität aufweisen, um somit die Qualität des Spin-Übergangs zu verbessern. In einem zweiten Schritt wurde die bidentate Natur der Liganden zur Synthese von gemischt-metallischen 3d-4f-Koordinationspolymeren genutzt.

Schließlich wurde die Kopplung von SCO mit Wirts-Gast-Chemie für chemo-sensorische Anwendungen untersucht, indem ein neuer Ansatz zur Herstellung erweiterter Hofmannartiger SCO-PCPs verfolgt wurde. Durch ein neuartiges synthetisches Verfahren wurde eine Verlängerung der klassischen Cyanometallat-Linker durchgeführt, was zu fünfmal größeren Kavitäten und einer drastischen Erhöhung der Porosität führte. Am wichtigsten war jedoch, dass alle gewünschten Eigenschaften (hysteretisches SCO, gastabhängiger Spin-Übergang, bidirektionales Chemoschalten und Memory-Effekt) erhalten blieben.

Table of Contents

А	CKNOV	vieage	ementsv
Α	bstrad	ct	DN 1 -crossover phenomenon - Fundamentals 1 f spin crossover 1 properties, types of magnetic behavior and detection of spin-crossover 4 ater 6 e ligands 8 e ligands 8 in Crossover complexes with azole ligands 9 ubstituted Tetrazoles 9 azoles 10 ons 11 ctional SCO Materials 12
K	urzfas	ssung	VII
1	IN ⁻	TROD	UCTION1
	1.1	The	spin-crossover phenomenon - Fundamentals
	1.2	His	tory of spin crossover
	1.3	Affe	ected properties, types of magnetic behavior and detection of spin-crossover.
	1.4	Stir	nuli
	1.5	Met	cal center
	1.6	Liga	ands
	1.6.1		Azole ligands
	1.7	Fe(II) Spin Crossover complexes with azole ligands
	1.7	7.1	N1-substituted Tetrazoles
	1.7	7.2	Imidazoles
	1.8	App	blications11
	1.9	Mu	tifunctional SCO Materials
	1.9	0.1	Spin-Crossover and host-guest Chemistry: Hofmann-type networks14
2	M	AVITC	TION AND AIM OF THE WORK16
3	RE	SULT	S18
	3.1	Pul	olished Journal Articles
	3.1 , a		A New Family of Fe(II) 1-Propyl-1H-Imidazole Complexes with Mono-, Bi- tranuclear Members
	3.1 cai		Bifunctional Fe(II) spin crossover complexes based on ω -(1H-tetrazol-1-yl) lic acids

	3.2	Submitted Journal Articles	20
		.2.1 Tetrakis-cyanoacetylides as building block for a second general witchable Hofmann type-networks with enhanced porosity	-
4	C	CONCLUSIONS	89
5	R	References	91
6	A	ppendix	98
	6.1	Reprint Permissions and copyright	99
	6.9	Curriculum vitae	100

INTRODUCTION

Spin crossover research has been conducted for almost a century now, hence a detailed description of the history and development of SCO research would go far beyond the scope of this work. Only the aspects relevant for an understanding of the phenomenon and for this work will be highlighted. Interested readers are referred to the book series "Spin-Crossover in Transition Metal Compounds I-III" by P. Gütlich and H. A. Goodwin, [1-3] the book on Spin-Crossover Materials by M. A. Halcrow [4] and the cited literature for further reading.

1.1 The spin-crossover phenomenon - Fundamentals

Spin Crossover describes a phenomenon occurring in coordination compounds of transition metal with electronic configuration 3d⁴-3d⁷ in octahedral ligand field. Perturbation of the system with external stimuli such as variation of temperature, pressure, light irradiation or the application of a magnetic field trigger a reversible change in the spin state of the complex between high-spin (HS) and low-spin (LS).

As we know from ligand-field theory, the magnitude of the ligand field splitting energy (Δ_0) compared to the spin pairing energy (P) determines whether the complex will have a HS or LS ground state configuration. Specifically, if the first is greater than the latter, the LS state is stabilized, and vice versa, the HS state is stabilized if P is greater than Δ_0 . Here lies the peculiarity of SCO complexes: for this class of compounds, Δ_0 and P are of the same magnitude, consequently, the energy barrier between the HS and LS state can be easily overcome enabling a reversible spin transition.

1.2 History of spin crossover

The Spin Crossover phenomenon was first observed and described in 1931 by Cambi and Szegö^[5], when they observed a temperature-dependent change in the magnetic moment of some tris-(N,N)-dialkyldithiocarbamate-iron(III) complexes. As many other scientific discoveries, the phenomenon was initially misinterpreted, and this peculiar behavior was attributed to an equilibrium between two magnetic isomers alternating due to the change in temperature.

With the development of crystal field theory and subsequently the ligand field theory, the ligand-metal relationship could be better understood, and the coordination bond explained. Those two theories introduced the concept of spin states for transition metal coordination compounds; generally, the electron distribution follows Hund's rule in respect to the ligand field strength. A special case is represented by octahedral complexes

of first-row transition metal with electronic configurations 3d⁴-3d⁷: for these compounds, two configurations are possible, namely one with the maximum number of unpaired spins, called high-spin, and one where a minimum of unpaired electrons is reached, the low-spin configuration.

As mentioned in Chapter 2.1, two energetic contributions determine whether the complex will have a high-spin or low-spin configuration, the ligand field splitting energy (Δ_0) and the spin pairing energy (P). The comparison between these two contributions determines the complex spin state, and in most cases the spin state is unambiguous since Δ_0 is either much bigger or much smaller than P. In some cases, though, the difference between the two contributions is marginal, leading to a narrow energy difference between the HS and LS state. A slight external perturbation can then induce a change of the spin state, resulting in the phenomenon known as spin crossover (SCO).

In the case of octahedral iron(II) complexes, the LS state corresponds to the t_{2g}⁶ electronic state, and the HS state from the t_{2g}^4 e_g^2 electronic configuration. A representation of the energy diagram and orbital population for the two electronic configurations is depicted in Figure 1.

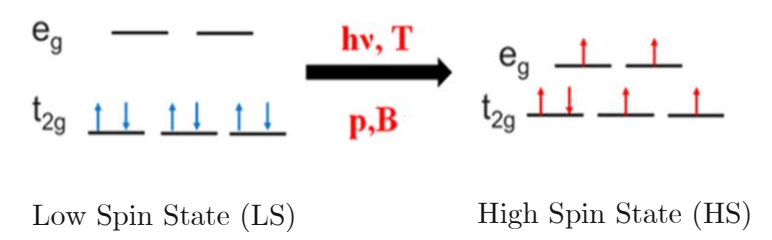


Figure 1: Electronic configuration of the LS and HS state for iron(II) in an octahedral field

1.3 Affected properties, types of magnetic behavior and detection of spin-crossover.

As one can easily imagine, the change of the spin state is accompanied by a change of different properties of the complex. These changes can be detected with different analytical techniques, which can help to determine the spin state, track changes in the spin state and define the quality of the magnetic behavior.

The most obvious affected property is the change in magnetic moment, as it was at the base of the discovery of SCO itself. The most prominent metal of choice for SCO complexes is iron(II), and the choice is based on some advantages this ion offers. With a 3d⁶ electronic configuration, it presents the biggest difference in spin multiplicity between the HS (S=2) and the LS (S=0) state, and the read-out of the spin state is quite straightforward since the LS state is diamagnetic. Magnetic measurements usually track the change in molar magnetic susceptibility as a function of temperature $(\gamma_{mol}T)$ when a constant magnetic field is applied. Evans-NMR^[6] can be applied for studies in liquid solution, solid samples are usually done with SQUID magnetometers. The spin transition can be abrupt, gradual, multi-step and with hysteresis, in some cases it is incomplete (Figure 2). Thermal spin transition is usually characterized through the $T_{1/2}$ temperature, which is defined as the temperature where 50% of the metal centers are in the HS state and 50% in the LS state. In the case of a hysteretic transition, T↑ represents $T_{1/2}$ in the heating process and $T\downarrow$ represents $T_{1/2}$ in the cooling process. The value γ_{HS} represents the fraction of metal centers in the HS state.

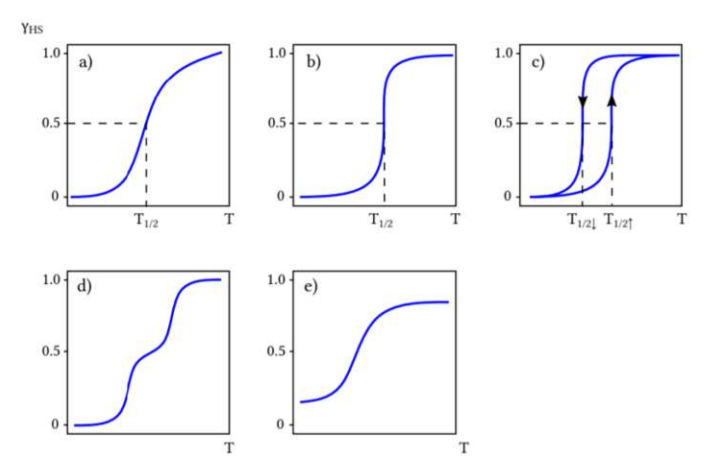


Figure 2: possible types of spin-transition; a) gradual b) abrupt c) abrupt with hysteresis d) two-step e) incomplete

The transition from a LS ground state to a HS excited state means a population of the antibonding eg* orbitals, and with that an elongation of the metal-ligand bond occurs, making X-ray crystallography another suitable technique to monitor the spin state of a complex. In the case of iron(II) complexes, the change in bond length is around 10%. The elongation of the metal ligand bonds entails an expansion of the molecular volume, and in crystalline materials the volumetric expansion of one molecule can be "transmitted" in the lattice and trigger the change of spin state of the neighboring molecules. This effect is described as cooperativity and is one of the main aspects taken into account in the design of new SCO complexes, so much that it could be considered as a sub-field of SCO research. Structural factors have demonstrated to be the dominant factor in determining the magnetic properties, and numerous studies have been conducted to see the influence of ligands and anions in the molecular packing. A more detailed discussion of these aspects will be given in the next chapters.

The degree of cooperativity is determined by lattice properties and determines the form of the spin transition curve: gradual spin transitions are caused by weak cooperative interactions, whereas abrupt transitions indicate the presence of strong cooperativity. If the cooperativity is particularly high, hysteresis is observed. Hysteresis is a particularly significant aspect of the SCO phenomenon because it confers bistability (ability of a system to be observed in two different states in a certain range of external perturbation,

in this case temperature) and thus memory effect, which are necessary for any application of SCO systems.

Another property that often changes along with the spin state is color, due to a change in the absorption bands in the UV-vis-NIR region. Electronic spectroscopy can therefore be used to detect changes in the spin state. For octahedral iron(II) complexes, the LS state presents the ${}^{1}A_{1g} \rightarrow {}^{1}T_{1g}$ electronic transition at 545nm in the visible region (magenta), whereas the HS state presents the ${}^{5}T_{2g} \rightarrow {}^{5}E_{g}$ transition at 860nm in the nearinfrared region, thus invisible to the human eye. The change in color was used as output in the first application of SCO in a real device, namely a monochrome magenta/white display device.^[7]

Changes in spin-state can also be tracked by means of variable-temperature infrared spectroscopy. Two bands can be used as a reference: the metal-ligand bond stretch and the absorption bands of the ligands for atoms near the coordination site. With the electronic rearrangement caused by the spin-transition, the strength of these bonds changes, and that is reflected in a shift of the absorption bands in the infrared spectra. This characterization method is an extremely useful tool, because with a very fast and routine-method one can quickly obtain information about the spin-state in SCO complexes. In a study by Weinberger and Grunert it was demonstrated, that for systems presenting large enough hysteresis even the $T_{1/2}$ can be determined by means of variabletemperature IR spectroscopy.^[8]

For iron complexes, Mössbauer spectroscopy is another useful characterization method. The isomer shift δ and the quadrupole splitting ΔEQ , two of the most important parameters derived from a Mössbauer spectrum^[9], are significantly different for the HS and LS states of both Fe(II) and Fe(III), hence with this technique one can retrieve information about both spin state and oxidation state of the iron atoms present in the sample. Mössbauer spectroscopy also offers direct means of determining the relative concentrations of the spin states in the sample. A drawback of this technique are the long measurement times.

1.4 Stimuli

The spin transition can be triggered by a plethora of stimuli involving different mechanisms. It would go far beyond the scope of this work to treat each of them in detail, hence only the most used, studied and of great significance for potential application will be mentioned.

The most accessible and thus the most used type of perturbation is the variation of temperature. The energy difference between the HS and LS state can be expressed as the product of temperature and the Boltzmann constant (eq. 1), hence, an increase in temperature gives the system enough energy to cause a transition to the HS state. Vice versa, cooling the system triggers a transition to the LS state.

$$\Delta E_{LS \to HS} \approx k_B T$$
 (eq.1)

Another possible stimulus to trigger the spin transition is pressure, which acts on the different molecular volume between the two states to favor one spin state over the other. [10] Since the HS state presents a higher volume than the LS state, an increase in pressure favors the LS state. The $\Delta E_{LS\to HS}$ for systems under higher pressure is increased, because the energy of the potential well for the HS increases much more in relation to the low spin state. Ewald et al reported one of the first attempts for a mathematical description of a system under high pressure. [11] A model suitable for more complex system was developed by Klokishner et $al^{[12]}$, which takes into account long-range electrondeformational and short-range interaction to predict the bistability of SCO systems under pressure. Unfortunately, a general model able to describe the behavior under pressure of all systems cannot be given and needs to be specifically developed for each studied system. A report on the different experimental methods to generate pressure, track the spin state and theoretical concepts regarding SCO under high-pressure condition can be found in the work by Gaspar et al.[13]

The probably most exciting and most interesting trigger for SCO compounds is the perturbation by light, which represented a real breakthrough in SCO research. McGarvey and Lawthers reported in 1982 the first photo-induced spin transition in solution, [14] and two years later Decurtins et al expanded on this study and observed the same process in solid state. [15-17] With this study, the term Light-Induced-Spin-State-Trapping (LIESST) was coined, and since then the spin transition triggered by light was studied extensively.LIESST consists in the excitement of the LS ¹A₁ state to a higher ¹T₁ or ¹T₂ energy state through irradiation with a 514nm green laser, and the following relaxation back to the HS ⁵T₂ state via two successive intersystem-crossing steps. If sufficiently low temperature is maintained, the HS state has an infinite lifetime. The reverse process can be triggered by a NIR light of 820nm (the reported wavelengths are for iron(II)). A schematic representation of the electronic transitions involved in the two processes is given in Figure 3.

The LIESST effect represented a real breakthrough because it allows a switch on a nanosecond scale, allowing application in sensing, data storage and switching devices with a much higher efficiency compared to the common technology used today. Furthermore, the data storage capacity could be dramatically increased, in the best case with a single molecule fixed on a surface, which can store a bit of information, with the possibility of reading/writing within nanoseconds. The biggest drawbacks are the necessity to continuously provide low temperature, and the fact that in most reported cases, the HS can be trapped for satisfying duration only at temperatures below that of liquid nitrogen, making in fact any application impossible.





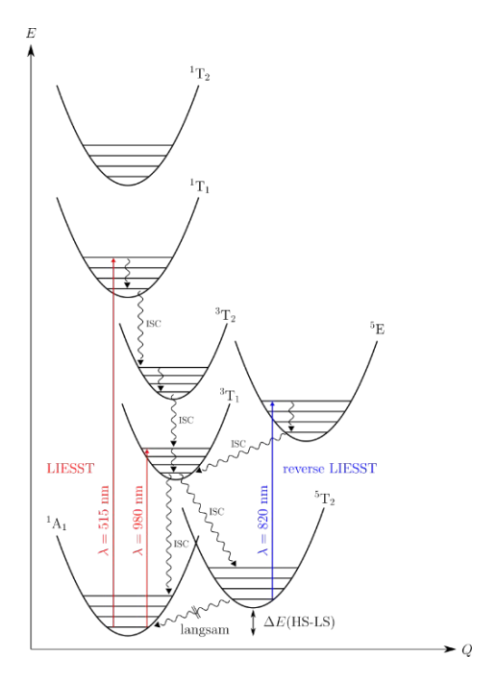


Figure 3: Schematic representation of the electronic states and the electronic transition processes involved in LIESST and reverse LIESST

The vast potential for technological applications offered by this effect pushed researchers to try to overcome the aforementioned problems, and many LIESST-like phenomena were discovered and reported.

Two other approaches addressing the central atom as in LIESST were reported, namely the nuclear-decay-induced excited spin-state trapping (NIESST)^[18] and the hard-X-ray-induced excited spin-state trapping (HAXIESST)^[19]. In the first one, nuclear decay is used as intrinsic excitation source and the relaxation is used to trap the excited HS state, whereas in the second one hard X-rays are used as energy source instead of vis-NIR light.

A different approach was reported in 1994 by Zarembowitch et al., called liganddriven light-induced spin change (LD-LISC). [20-22] With this approach, instead of targeting the metal atom, the ligands undergo a photo-induced modification which results in a change of the ligand field strength that triggers the spin transition.

1.5 Metal center

The SCO phenomenon is theoretically possible for every first-row transition metal with configuration 3d⁴-3d⁷, but looking at the research done in the field one can clearly see how the pool of used metal is restricted.

The most prominent metal of choice for SCO complexes is iron(II), and the choice is based on some advantages this ion offers. With a 3d⁶ electronic configuration, it

presents the biggest difference in spin multiplicity between the HS (S=2) and the LS (S=0) state, and the read-out of the spin state is quite straightforward since the LS state is diamagnetic. These factors constitute an advantage not only from an experimental point of view due to the ease of characterization and determination/tracking of the spin state, but also for potential applications. Furthermore, this metal ion is suitable for Mössbauer spectroscopy.

The library of known Fe(II) SCO compounds is therefore extremely vast, and it rapidly expanded form mononuclear compounds used in early studies to dinuclear^[23-24], trinuclear^[25-27], tetranuclear^[28] and polynuclear^[29-30] complexes using ligands of different denticity.

SCO has also been investigated for other metals, mostly Co and Mn.

Several Co(II) and some Co(III) complexes were reported [31-39]; the main differences compared to Fe(II) compounds are the smaller change in spin multiplicity, a smaller difference in metal-ligand bond length between HS and LS and the presence of Jahn-Teller effect. SCO complexes with Co(III) are rare because the higher nuclear charge, compared to the isoelectronic Fe(II), stabilizes the S=0 state. In general, the spin transition for these compounds requires smaller amount of energy compared to Fe(II), but in most cases it is rather gradual.

The use of Mn as metal center for SCO compounds has been reported, but its role is still marginal. Both Mn(II) and Mn(III) are in principle susceptible of SCO, but examples of SCO compounds with these ions are extremely rare, and especially for Mn(III) the occurrence of spin transition is considered exceptional. Reason for this is that in Mn(II) the HS state is usually stabilized, and a spin transition for d⁴ ions as Mn(III) is in general difficult to achieve. This is also confirmed by the fact that the best-known example for Mn(III) SCO compounds is still the first ever reported, despite it dating back to 1981. [40] The R-Sal₂323 generic Schiff-base has been identified as an ideal ligand to promote SCO in Mn(III) compounds. Morgan et al. investigated these systems extensively, showing how changing substituents on the ligand and varying their position (geometric tuning), using different anions and guest inclusion play a key role in the packing in the crystal, which in turn determines the SCO behavior, resulting in some cases in multi-step spin transitions due to multiple symmetry breaking. [41-48]

Metal salts are generally used as source of metal ions for SCO complexes. In most cases the choice falls on metal salts of weak-coordinating anions, such as BF₄-, ClO₄- or SbF₆, since it will avoid competition for coordination to the metal center allowing control over the reaction's outcome. In some cases salts of coordinating anions such as SCN⁻, NO₃ or Cl are used, and in that case, the anion will act as anionic ligand in the resulting complex.

1.6 Ligands

The choice of the appropriate ligand system is crucial, since it has a major impact on the strength of the ligand field. Ligands creating too weak or too strong ligand fields need to be avoided, since they would just stabilize one spin state. The metal of choice and its oxidation state also need to be taken into consideration in the choice of the ligand.

Other relevant aspects, especially for synthetic chemists, are the ligands' ease of preparation and yields, possibility for post-synthetic modification and the different coordination modes of the ligand when more potential donor atoms are present.

For SCO compounds, the use of nitrogen-based ligands (particularly heterocyclic azole ligands but also mono- and multi-dentate N-heterocyclic ligands, NCS-, CN-ligands) has proven to be very suitable, and the research on systems based on these types of ligands has been and still is extensive.

Since a discussion of all literature-reported ligand systems and ligand-metal combinations in SCO compounds would take far too long, only the aspects relevant for this work, namely suitable ligands for Fe(II) SCO compounds, will be discussed.

Azole ligands 1.6.1

The most commonly used azole ligands for iron(II) SCO complexes are reported in Figure 4. Among them, triazoles and tetrazoles play the main role.

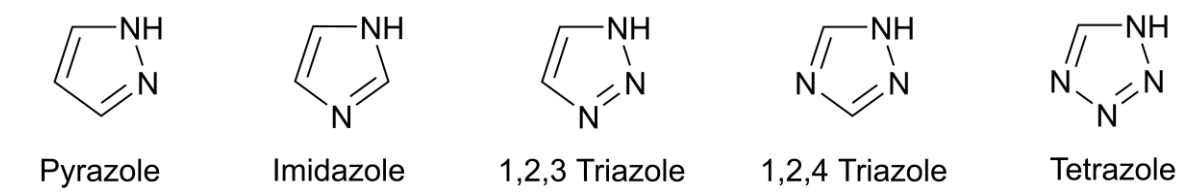


Figure 4: Common azole ligands used for Fe(II) SCO compounds

Triazoles have gained the interest of chemists in the SCO field due to the facile synthesis, good yields and the ease of functionalization.

1,2,3 Triazoles are usually prepared via the azide alkyne Huisqen cycloaddition^[49], a 1,3-dipolar cycloaddition between an alkyne and an azide. With time, the yield and regioselectivity improved dramatically, especially thanks to the improvement of copper(I) catalysts by Sharpless.^[50]

For 1,2,4 triazoles, two synthetic pathways can be used: cyclization of an alkyl hydrazine and an imide, known as the Einhorn-Brunner reaction^[51], or the condensation of an acyl hydrazine with an amide, known as Pellizzari reaction.

A major drawback in the use of triazoles is their bidentate nature arising from their tautomerism, resulting in different possible coordination modes which are not always predictable. In addition to that, triazoles can also act as bridging ligands between two metal centers.

Tetrazoles are usually prepared through a cyclization process, known as the Franke synthesis^[52], involving an amine, triethyl orthoformate and sodium azide, the organic rest attached to the amino-group will be the substituent on the N1 atom of the tetrazole ring. N1 substituted tetrazoles present a big advantage, namely the restricted monodentate coordination through the exo-N4 nitrogen atom^[53], and are therefore the most used ligands. Substitution on the carbon atom results in bridging coordination between two metal centers.^[54] N1-substituted tetrazole can also be prepared via [2+3] cycloaddition of isonitriles and azides^[55] or functionalization of 1H-tetrazole using tosylates^[56].

Ligands having two or more tetrazole units connected by linkers yield coordination polymers with 1D,^[57] 2D^[58] or 3D dimensionality.^[59-60]

The Weinberger research group has a long history and a strong background in the investigation of N1-substituted tetrazoles as ligand for SCO complexes. This also led to the development of new synthetic routes for their preparation, such as the microwave alkylation of lithium tetrazolates, [61] a modified phase-transfer-catalyst-assisted pathway that allowed the synthesis of so-far inaccessible bis-tetrazoles^[62] and the development of Suzuki and Heck cross coupling protocols for the synthesis of (unsaturated) aryl- and heteroaryl N1 tetrazoles^[63-64].

SCO complexes have been reported also for other azole ligands, such as isoxazole 65-^{68]}, pyrazole^[69-71] and imidazole.^[72-74]

1.7 Fe(II) Spin Crossover complexes with azole ligands

Although the pool of suitable ligands for SCO complexes is in principle vast, some considerations restrict the focus on specific systems. Homoleptic complexes are preferred to limit the number of variables. Fe(II)-N₆ homoleptic complexes have also, in most cases, proved to provide an appropriate ligand field for SCO. The system should also allow for modification of the ligands and offer different physico-chemical methods for characterization.

N1-substituted Tetrazoles 1.7.1

Hasnoot et al. introduced homoleptic Fe(II) octahedral complexes of N1-substituted tetrazoles for SCO studies, [52] following the studies on [Fe(1-propyl-1H-tetrazole)₆]²⁺ by Gütlich [75]. This lead to systematic investigations of homologous series aiming for a detailed understanding of structure-property relationships, with the goal of a precise understanding and thus prediction of the SCO behavior, which would allow a rational design of complexes.

Tetrazole complexes of Fe(II) are probably the most studied and well-characterized SCO compounds. One reason is because, unlike e.g. triazole complexes, most of the tetrazole-based systems show some kind of SCO behavior. The combination of Fe(II) and tetrazole ligands seems therefore to be in the sweet spot of a ligand field of appropriate strength for SCO. Several studies have been done, mostly in the context of rational design, to gather a deeper understanding of the factors influencing the spin transition.

The studies took different approaches to the subject, e.g effect of changing the substitution pattern on 2-haloethyl- and 3-halopropyl-tetrazole ligands^[76-77], comparative studies on homologous series^[60, 62, 76, 78-81], electronic^[76] and steric^[82-84] impact of the ligand's structures. Other studies investigated the use of different weakly-coordinating anions and solvents^[85-86] and their impact on the molecular packing and hence the cooperativity.

N1-substituted tetrazoles are also an ideal platform for infrared-characterization. The v_{CH} and $v_{N2=N3}$ undergo a shift upon coordination as well as upon spin transition, making a fast and routine analysis such as infrared spectroscopy a powerful tool for their characterization. The v_{CH} band also has the advantage of not being afflicted by band overlap of other CH bonds.

Imidazoles 1.7.2

Imidazoles are lesser-known ligands for Fe(II) SCO complexes. One reason is that, beside their ability to form hexacoordinated complexes, they tend to stabilize the [M₄-µ₃-O₄ (M=metal) cubane-type clusters. Especially with iron, multiple synthetic oxo-clusters with imidazole ligands have been prepared and characterized, [87-90] recently some were also reported by the Weinberger group.^[91-92]

Imidazoles are mostly used in the form of Schiff-bases, [93-94] or attached to pyridine moieties; [95-96] simple alkyl substitution patterns are not as common as they are for tetrazoles. Recently, a new Hofmann—type coordination polymer with imidazole ligands was reported.^[97]

Another interesting class of imidazole ligands are the so-called scorpionates, tripodal ligands based on the tris-imidazolyl-borate and-methane motif. [73, 98-99]

Unlike tetrazoles, imidazoles have multiple CH-bonds on the ring, which in the infrared spectra feature overlapping bands. The characterization and tracking of the spinstate is still possible, but it is not as unambiguous as for tetrazoles, as one cannot use a single band as reference but just observe the shift of the group of bands.

1.8 Applications

Regardless of the envisioned application, there are some prerequisites a SCO compound should fulfill to be suitable for any of them: the spin transition must occur at or above room temperature, and it needs to be abrupt and complete, meaning the HS and the LS state have to be fully reached at the corresponding temperature regimes.

The applicability of SCO has been extensively discussed since the discovery of this phenomenon. Kahn and Martinez first envisioned a potential application for SCO polymers in memory devices^[7], since the two different spin states of SCO compounds can act as a binary switch as in common memory devices. The limitations for the construction of SCO-based memory devices are the temperature regimes of the spin transition, which are often way below room temperature. As mentioned in chapter 2.3, Kahn and Martinez also built the first SCO-based display device. This constituted the first hand-on application of SCO, but the construction of display-devices based on SCO materials cannot be realistically considered as a future application: on one hand, there is no demand for monochrome display systems, and on the other hand the preparation of the SCO system, even for the most basic implementations, would be far too expensive.

For a concrete and competitive technological application, the spin-transition needs to be triggered via the LIESST effect, but also for this case there are some limitations. The SCO material needs to show perfect cycle stability, hysteretic behavior and the transition needs to occur in an extremely short timescale, otherwise there is no real gain compared to the current technology.

Another possibility for the application of SCO systems is their use as sensors. Compared to their implementation in data storage, the construction of sensing devices can be considered as straightforward, but there is one aspect that cannot be neglected: to compete with already existing technology, there is the need to evolve from simple I/O sensors and include quantification. It was demonstrated that, in principle, SCO materials could act as sensor materials in a small dynamic range by combining thermal SCO with fluorescence, the latter showing a proportional response. [100]

Independently from the chosen applications, a crucial aspect for the implementation of SCO systems is a non-destructive readout of the spin state. The commonly used techniques, from spectroscopical methods (Mössbauer, Raman, IR, UV-vis/NIR...) to the determination of the magnetic moment, structural characterization etc. allow a simple detection of the spin-state, but clearly, they are not suitable for technological applications. This also constitutes a limiting factor in the construction of LIESST-based devices, since all the mentioned techniques require large equipment that can hardly be miniaturized.

All mentioned concepts for applications face two main challenges: they would have to compete with already existing technology, which production costs are by far lower as what could be expected for SCO-based systems, and also, the way to get to a competitive product is still long and demands further and intensive research efforts, with the risk of ending with a product that matches but doesn't improve on the existing technology.

To overcome these obstacles and avoid these risks, basic research is taking another direction, and instead of solely focusing on creating a product to compete with an already existing one, different ways to exploit the SCO phenomenon for new applications are being explored.

The introduction of the concept of multifunctionality is a key aspect in this context. The idea is to combine SCO with an additional property, whose response is synergistically correlated with the spin transition. [101]

Another fascinating and more recent concept is the use of SCO compounds as molecular actuators. In this case, the cooperative molecular expansion/retraction that accompanies the spin transition is used as output in form of mechanical motion. Especially in the group of Bousseksou this concept is being investigated, and some promising results were already obtained. Aside from studies to establish feasibility of the concept, [102] concrete applications are also being investigated. One example is the use of SCO compounds as bending actuators, a famous class of artificial muscle: an electrochemically-actuated bilayer bending actuator based on SCO compounds showed extremely short response time even with a load up to five times the actuator weight. [103]

1.9 Multifunctional SCO Materials

The introduction of an additional property to combine with SCO seems to be the most promising approach to expand the SCO field outside of strictly academic research and towards its actual implementation in real devices. The investigation of multifunctionality led to various combinations, such as porosity and host-guest chemistry^[104-112], conductivity^[113], non-linear optics (NLO)^[114], luminescence^[115-117], liquid-crystal transformation [118] etc.

The combination of SCO with porosity is mainly achieved through polymeric compounds, known as Porous Coordination Polymers (PCP) or Metal Organic Frameworks (MOF). It was shown that some classes of PCPs, e.g. Hofmann-type networks, there is a true synergy between SCO and host-guest chemistry. With the observation of a guest dependent spin-transition, the stabilization of either HS or LS based on the nature of the guest and retention of the spin-state after desorption, meaning a guest-induced memory effect, this class of compound has proven to be truly environment responsive^[111]. Studies on the effect of gaseous guests suggest a possible use as gas-sensors or gas-separators.[101, 109]

Conductive SCO materials are for the most part double salts, with the anions building stacked layers and allowing for conduction through the layers.[113]

Combination of SCO and luminescence gained significant interest in the last 10 years for the potential applications in thermometry^[100], biomarkers^[119], photonic switches^[120] and gas sensors^[121]. A major obstacle to overcome is the fact that 3d metals, especially Fe(II), promote luminescence quenching.

The interest in NLO is driven by theoretical studies, predicting an increase in the quadratic ($\propto E^2$) NLO response upon spin transition. [122] This still remains a theoretical prediction, as so far the expected effect could not be observed.

Combining SCO with liquid-crystals properties was motivated by the idea of simple material preparations and processability, with easy film preparation with simultaneous conservation of the crystalline properties. The major difficulty here is finding an adequate temperature range for the coexistence of SCO and liquid crystalline properties.[118]

Independently from the chosen additional properties, a common aspect of all multifunctional SCO compounds is the necessity to synthesize the system before testing its properties. Two major strategies can be identified:

- covalent modification of the ligand backbone, in which the moiety bearing the additional functionality is connected to the existing SCO entity via chemical bond,
- using a PCP as SCO entity, and adding the additional properties by incorporation in the framework

The second strategy is generally preferred because it presents some advantages compared to the first one.

Synthetically speaking, the preparation of the ligands alone can be rather tedious, and its post-synthetic modification even more so. Aside from being time consuming, some syntheses also show low yields, and with increasing number of synthetic steps it can result in extremely low overall yield. Lastly, for each selected additional property a new ligand must be prepared, and in some cases that can represent a true synthetic challenge.

Aside from these synthetic aspects, SCO systems are in general extremely sensitive to even the slightest changes in the steric and electronic properties of the ligands, and especially steric influences on the molecular packing have a far larger impact on the SCO properties than electronic ones. The covalent attachment of the second functionality to the SCO compound results in a system that is structurally completely different from the



parent compound, hence one can reasonably expect for the SCO behavior to not be retained.

Using the second approach these problems can be overcome, and since the two functional building blocks are not chemically bonded/modified, there is more flexibility in the design of the system. Furthermore, the use of polymeric structures in which the metal centers are linked to one another via covalent bonds allows for a better communication of the intramolecular structural changes that occur with the spin transition, hence enhanced cooperativity and possibly hysteretic spin transition.

One issue persists: while the two separate properties are preserved, there is no guarantee that their response will be synergistic.

This chapter about multifunctionality has again no claims on completeness, but it aims on giving the reader an overview of this research area in the field of SCO. The aspects relevant for this work will be treated more in detail in the following chapters.

1.9.1 Spin-Crossover and host-quest Chemistry: Hofmann-type networks

The combination of SCO with porous properties seems something that was just meant to be: if SCO research is more and more focusing on multifunctionality, so is the research in porous materials, aiming to create systems in which the guest-absorption is accompanied by a change in solid state properties. PCPs are therefore very attractive materials because they offer regular, designable porosity and thus great versatility. The host-guest chemistry properties can be exploited for the incorporation of functional molecules, and the same "scaffold" can be used for different combinations without the necessity of synthetic modifications for each functionality.

Among all the polymeric compounds, when it comes to combining SCO with porosity and host-guest chemistry, the class of Hofmann-type networks is without doubt the most intensively studied one. As the name suggests, they are based on the $M1(L)_2[M2(CN)_4]$ (M1=M2=Ni²⁺ L=NH₃) clathrate reported in 1897 by Hofmann and Küspert. [123] About 100 years later, a breakthrough was achieved when Kitazawa et al. reported the first SCO-PCP, namely the 2D $Fe(py)_2[Ni(CN)_4]$ (py=pyridine), [124] and in 2001 a new milestone was reached when Real and co-workers reported the synthesis of Fe(pz)[MII(CN)₄] (M=Ni, Pd, Pt). [125] The substitution of py with pz resulted in $\{Fe[M^{II}(CN)_4]\infty\}$ layers stacked by pz ligands, giving the network 3D dimensionality and with that achieving the desired regular porosity and enhanced rigidity, enabling strongly cooperative SCO behavior.

The regular pore structure allows for ample host-guest chemistry, and the networks showed robustness to absorption and desorption of a wide range of guest molecules. [109, ¹¹¹ The sorption/desorption of guests has a notable impact on the magnetic behavior,

which can express itself in different ways: some guests can improve the magnetic behavior compared to the empty framework, some other cause gradual spin transition, and there are also guests who stabilize either the HS (e.q. benzene) or the LS state (e.q. CS₂) at all temperatures. [111] According to the nature of the guest, the stabilized spin-state is retained even after guest-desorption, giving a memory effect which allows a memory system and guest-sensing. In a study published by Ohba et al., in-situ bidirectional chemoswitching was also observed for $[Fe(pz)][Pt(CN)_4]$. A synergistic interplay between SCO and guestexchange was also observed for [Fe(pz)][Ni(CN)₄] by Kepert et al. [109]

A limitation of these systems is represented by the small size of the pores, only allowing the absorption of small molecules, hence making the scope of possible applications rather limited. The creation of Hofmann-type networks with enhanced porosity represented, therefore, the logical next-step in this field, and different strategies were used.

The most common is the substitution of pyrazine with longer, ditopic N-ligands. This is mostly because, from a synthetic point of view, it can be easily achieved, since the ligands do not require tedious synthesis or are already commercially available. Literature-reports include for example the use of bpac^[126] or bpeben^[127] (bpac=bis(4pyridyl)acetylene, bpeben=1,4-bis(4-pyridylethynyl)benzene). This strategy was in principle successful, since the desired complexes were obtained and the desired 3D structure preserved, but they showed a major drawback: the compounds often show poor magnetic behavior, suggesting that the elongation of the pillar ligands decrease the effectiveness of transmission of SCO cooperativity. For bpac, incorporation of the ligand itself was observed.

The second strategy is the substitution of the $[M^{II}(CN)_4]^{2-}$ linkers, hence an elongation within the ab plane. To the best of our knowledge, the only reported example is the use of $[M^{I}(CN)_{2}]$ (M=Ag, Cu, Au) linkers; the use of $[Ag(CN)_{2}]^{-}$ yields $[Fe(L)_n \{Ag(CN)_2\}_2]$, with a structure consisting of two interpenetrating 3D networks with edge-shared {Fe[Ag(CN)₂]₄} rhombuses in the 2D sheets^[128]. In the case of Au, 3D triply interpenetrated networks are formed. [129-131] This approach successfully enlarged the voids so that even a ferrocene molecule could be incorporated^[131], but again, the compounds showed poor magnetic behavior. Furthermore, network interpenetration takes away the regular porosity, making the system less flexible for possible modifications.

MOTIVATION AND AIM OF THE WORK

As outlined in the previous chapters, spin-crossover research faces multiple and very different challenges. In the last decades the preparation of multifunctional system aiming for applicability of SCO compounds has shifted the interested in this field, but there still are some unanswered fundamental questions about the factors governing the spin transition.

The present work was conceived with the idea of tackling both these aspects.

The first part of the work focuses on rational design. The SCO phenomenon has been known and studied for almost a century now, but aside the exception of homologous series of compounds with well-defined variations where certain trend may be predicted 132- 133 , the phenomenon is de facto still unpredictable. Several research teams concentrate on the correlation between ligand-design and substitution and the impact of the anion and incorporated solvent on the observed magnetic behavior. The target is not a general recipe for the synthesis of SCO compounds, but rather gaining insight on the factors governing the spin transition and using the information for a target-oriented design.

For this work a different approach is selected, namely a decoupling of electronic and steric effect. This was achieved by changing the azole ring in a complex geometrically as similar as possible to $[Fe(PrTz)_6]^{2+}$, one of the most studied and well-characterized SCO compounds. The analogue 1-propyl-1H-imidazole complex was synthesized. Since the position of the propyl chain in respect to the coordinating N-atom is the same in both ligands, the regular octahedral geometry is expected to be retained, and differences in magnetic behavior should be caused purely by electronic effects. Magnetic, structural and spectroscopic characterization will help to get insight on the differences between the two compounds, and hopefully define the impact on the different azole ring on the spintransition behavior of the complex.

In the second part of the work, both aspects of multifunctionality and rational design are investigated. As mentioned in previous chapters, cooperativity is a key aspect for an abrupt spin transition, and a tight packing is essential in this sense. Different studies conducted in the Weinberger group focused on the fine-tuning of ligands' geometry and flexibility in shaping the cooperativity and the transition temperature on a molecular scale, as well as on modifications of the ligand's backbone. To expand on this studies, a series of ω -(1H-tetrazol-1-vl) carboxylic acids bifunctional ligands are considered for the preparation of homoleptic Fe(II) SCO-complexes. The choice of the ligands is based on different features expected from the introduction of a carboxylic function. First, the formation of a very dense H-bond network which will enhance the cooperativity, impacting the spin transition in a positive manner. Second, the carboxylic function constitutes a second coordination site on the ligand, allowing for the preparation of mixed-metallic complexes with either a second transition metal or rare-earth elements. Third, the terminal carboxylic function could allow deposition of the material on oxide

surfaces. The first part of the study will consist in the synthesis and characterization of the Fe(II) complexes of the ω -(1H-tetrazol-1-yl) carboxylic acids with weak coordinating anions (ClO₄, BF₄). In the second part, an exploitation of the carboxylic coordination site will be attempted, specifically for the synthesis of mixed-metallic complexes with rare-earth elements. The designated metal is Gd³⁺, and the choice is made based on some simple considerations: since this is somewhat uncharted territory, a metal whose coordination compounds are already known for luminescence properties constitutes an advantage and could potentially lead to a multifunctional SCO-compounds, and in second instance the affinity of Gd³⁺ for O-donor ligands should facilitate the process of post-This can be considered as a hybrid approach to synthetic modification. multifunctionality, since the addition of the second functionality is post-synthetic, but it will happen through coordination to the carboxylic function and not via synthetic modification.

The third and last part of the work will entirely focus on multifunctionality. As outlined in Chapter 1.9.1, porous SCO compounds seem to be the most promising candidates for the realization of multifunctional SCO systems, and the class of Hofmanntype network above all. The incorporation of larger, bulkier functional molecules has until now been difficult due to the limited pore size, and the attempts to obtain larger pores and enhance the porosity resulted in a loss of magnetic behavior. For this reason, a new approach is considered, namely an extension of the networks on the ab plane by insertion an acetylenic unit in the M-CN bond of the tetracyanometallate linkers. The resulting tetrakis-cyanoacetylide-metallates will be used as linkers to give Hofmann-type networks of the general formula $[Fe(pz)][M^{II}(C_3N)_4]$ (M=Ni, Pd, Pt). Some preliminary work was already done in the Weinberger group by Danny Müller, who gave proof of concept for the synthesis of the compounds, but it did not expand on investigating the influence of guest molecules on the SCO properties, and some synthetic procedures needed improvement due to the relatively low yields. [134] In this work, an optimization of the synthetic protocols and a complete characterization of the compounds is performed, as well as an investigation of the guest effect on the spin-transition and the synergistic interplay between guest-absorption and SCO.

RESULTS

The present PhD thesis is written in a cumulative fashion, and the results are presented as a collection of published articles. The reproduction of these publications was kindly authorized by their corresponding journals and the reprint permissions are given in the appendix. The last work is currently under review and listed as submitted journal article.

3.1 Published Journal Articles

3.1.1 A New Family of Fe(II) 1-Propyl-1H-Imidazole Complexes with Mono-, Bi-, and **Tetranuclear Members**

Authors

Willi Zeni, Danny Müller, Marco Seifried, Jan Welch, Berthold Stöger, Gerald Giester, Michael Reissner, Ronald Miletich, Peter Weinberger

European Journal of Inorganic Chemistry, 2024

DOI 10.1002/ejic.202400358

Abstract

The synthesis of $[Fe(PrIm)_6](BF_4)_2$ with the intention of investigating its magnetic and structural properties led to the discovery of a new family of Fe(II) 1-propyl-1H-imidazole complexes, which were obtained by simply changing the reaction conditions. The structural, magnetic and electronic properties were investigated.

Contribution

Conception of the study, synthesis and characterization of the reported compounds, writing of the manuscript.

Bifunctional Fe(II) spin crossover complexes based on ω -(1H-tetrazol-1-yl) 3.1.2 carboxylic acids

Authors

Willi Zeni, Marco Seifried, Christian Knoll, Jan M. Welch, Gerald Giester, Berthold Stöger, Werner Artner, Danny Müller and Peter Weinberger

Dalton Transactions, 2020, 49, 17183-17193 DOI 10.1039/D0DT03315D

Abstract

To increase the supramolecular cooperativity in Fe(II) spin crossover materials based on N1-substituted tetrazoles, a series of ω -(1*H*-tetrazol-1-yl) carboxylic acids with chainlengths of C₂-C₄ were synthesized. Structural characterization confirmed the formation of a strong hydrogen-bond network, responsible for enhanced cooperativity in the materials and thus largely complete spin-state transitions for the ligands with chain lengths of C₂ and C₄. To complement the structural and magnetic investigation, electronic spectroscopy was used to investigate the spin-state transition. An initial attempt to utilize the bifunctional coordination ability of the ω -(1*H*-tetrazol-1-yl) carboxylic acids for preparation of mixed-metallic 3d-4f coordination polymers resulted in a novel onedimensional gadolinium-oxo chain system with the ω -(1*H*-tetrazol-1-yl) carboxylic acid acting as μ_2 - η^2 : η^1 chelating-bridging ligand.

Contributions

Synthesis and characterization of the reported compounds, partial writing of the manuscript.

3.2 Submitted Journal Articles

3.2.1 Tetrakis-cyanoacetylides as building block for a second generation of spinswitchable Hofmann type-networks with enhanced porosity

Authors

Willi Zeni, Danny Müller, Werner Artner, Gerald Giester, Michael Reissner, Peter Weinberger

ACS Inorganic Chemistry, unpublished results, 2024

Abstract

The combination of Spin Crossover (SCO) with guest incorporation properties has attracted the interest of researchers in the last couple of decades, and lead to the design of numerous SCO-porous coordination polymers (SCO-PCP). The most famous class of SCO-PCP is the one of Hofmann-type networks, which are very promising materials for (chemo) sensing applications. Different strategies have been carried out to expand the classic structure Fe(pz)[M(CN)4] (M=Ni, Pd, Pt) to get larger cavities, but the resulting compounds often showed poor magnetic behavior. In this work, we present wide mesh spin-switching Hofmann-type networks based on tetrakis(cyanoacetylides) synthesized with a newly developed method, resulting in compounds of the general formula Fe(pz)[M(C3N)4]. The compounds were characterized in their structural, magnetic, and spectroscopic properties. They present five-fold larger cavities and a drastic increase in porosity. The desired hysteretic and guest-dependent Spin-crossover behavior is retained, in-situ chemoswitching of the spin state and memory effect are also observed

Contributions

Conception of the study, optimization of the synthetic protocols, synthesis and characterization of the reported compounds, writing of the manuscript.

EurJIC

European Journal of Inorganic Chemistry





Accepted Article

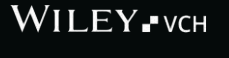
Title: A New Family of Fe(II) 1-Propyl-1H-Imidazole Complexes with Mono-, Bi-, and Tetra-Nuclear Members

Authors: Willi Zeni, Danny Müller, Marco Seifried, Jan Welch, Berthold Stöger, Gerald Giester, Michael Reissner, Ronald Miletich, and Peter Weinberger

This manuscript has been accepted after peer review and appears as an Accepted Article online prior to editing, proofing, and formal publication of the final Version of Record (VoR). The VoR will be published online in Early View as soon as possible and may be different to this Accepted Article as a result of editing. Readers should obtain the VoR from the journal website shown below when it is published to ensure accuracy of information. The authors are responsible for the content of this Accepted Article.

To be cited as: Eur. J. Inorg. Chem. 2024, e202400358

Link to VoR: https://doi.org/10.1002/ejic.202400358



Bibliothek Die approbierte gedruckte Originalversion dieser Dissertation ist an der TU Wien Bibliothek verfügbar. Your knowledge hub The approved original version of this doctoral thesis is available in print at TU Wien Bibliothek.

A New Family of Fe(II) 1-Propyl-1H-Imidazole Complexes with Mono-, Bi-, and Tetra-Nuclear Members

Willi Zeni,[a]* Danny Müller,[a] Marco Seifried,[a] Jan M. Welch,[b] Berthold Stöger,[c] Gerald Giester,[d] Michael Reissner, [e] Ronald Miletich, [d] and Peter Weinberger [a]*

Abstract: The synthesis of [Fe(PrIm)₆](BF4)₂ with the intention of investigating its magnetic and structural properties led to the discovery of a new family of Fe(II) 1-propyl-1H-imidazole complexes, which were obtained by simply changing the reaction conditions. The structural, magnetic and electronic properties were investigated.

Introduction

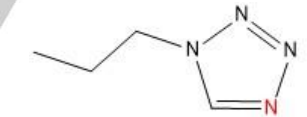
The intrinsic molecular bistability of selected first-row 3d4-3d7 transition metal complexes inspires application of those materials in display-devices, [1] sensors, [2-4] molecular switches [5-7], and many other forms of device, requiring a controllable transition between two states. 11-13 The perceived potential is based on the various properties affected by the spin crossover (SCO), describing this transition between high-spin (HS) and low-spin (LS) state: Triggered by external stimuli as temperature. [8-9] pressure, [4, 8-9] light, [10-11], etc. the change of the metal centre's spin-state affects key-properties including magnetic moment, [8-9] colour.[1] dielectric constant.[12-13] lattice extension.[14] etc. Heading towards molecular materials for applicability, the application of the LIESST-effect^[10-11, 15] offers a huge potential: The "light induced excited spin state trapping"-effect allows the interchange of the spin states by a single-shot laser pulse within femtoseconds.[16-17] Parallel to this application-driven research, fundamental investigation on the spin crossover effect is providing a better understanding of the factors impacting the spin crossover phenomenon. Major obstacle in broadening the selection of suitable materials is the unpredictability of the spin crossover behaviour.^[18-19] Strongly dependent on ligand- and substituent

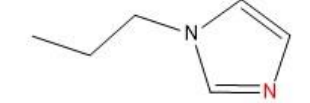
effects, the anion used (if any), (non-stoichiometric) solvent inclusion into the packing, steric effects imposed by the packing, crystallite sizes, etc., only for homologous series of compounds with clearly defined variations a "rule-of-thumb" may be observed and, therefore, trends predicted.[20-21]

Focusing on lessons learned by a rational design approach, correlation between ligand design and substitution, [21-26] the effect of dilution of the spin state changing metal with other nonswitching metals,[27] the impact of the anion[20, 28-30] and incorporated solvent,[29,31] provide enhanced understanding of the various factors governing the spin transition properties.

Our group focused in the past mainly on Fe(II) SCO systems with N1-substituted tetrazoles as ligands: A suitable design of the ligands varies nuclearity of the resulting compounds, [32-34] homologous series [34-40] shed light on the electronic[37] and steric impact[41-43] of the ligand structures, as well as on the impact of weakly-coordinating anions and solvents. [44-45] Nevertheless, the constant in all those studies was the utilization of N1-substituted tetrazoles as N-donor ligand set.

Additional to variations of the tetrazole substitution pattern a potential way to impact the spin crossover behavior of the system is found in a variation of the azole, impacting the electronics of the ligand more heavily and direct than by any substitution on its backbone. For this purpose - widely retaining the coordination angle and coordination geometry around the Fe(II)-centre - an exchange of two N-atoms in the azole, leading to N1-substituted imidazoles was attempted (see Figure 1).





1-propyl-1*H*-tetrazole (3tz)

1-propyl-1*H*-imidazole (*PrIm*)

Figure 1. 1-propyl-1H-imidazole (right), the ligand used in the current study with 1-propyl-1H-tetrazole as parent ligand. Coordinating nitrogen in red.

 $[Fe(3tz)_6]^{2+,[15, 32]}$ 3tz = 1-propyl-1*H*-tetrazole, is one of the first and probably the most comprehensively characterized SCOcompound. Therefore, 1-propyl-1H-imidazole (Prlm) was selected as ligand for a study on homoleptic Fe(II)-Imidazole complexes, allowing for a comparison between the two systems. In literature only one report on homoleptic Fe(II)-imidazole systems was published, reporting among others the synthesis of [Fe(Prlm)₆](ClO₄)₂, but without including a magnetic or structural characterization.^[46] Starting from [Fe(PrIm)₆](BF₄)₂, 1-propyl-1Himidazole in combination with Fe(II) revealed a very versatile coordination chemistry, giving rise to a new family of Fe(II) 1propyl-1H-imidazole complexes with mono-, bi-, and tetra-nuclear members.

DI Willi Zeni, Dr. Danny Müller, Dr. Marco Seifried, Associate-Prof. Dr. Peter Weinberger Institute of Applied Synthetic Chemistry, TU Wien

Getreidemarkt 9/163-AC, 1060 Vienna, Austria

E-mail: willi.zeni@tuwien.ac.at; peter.e163.weinberger@tuwien.ac.at

Dr. Jan M. Welch [b] Atominstitut, TU Wien Stadionallee 2, 1020 Vienna, Austria

Privatdoz. Dipl.-Ing. Dr.techn. Berthold Stöger

X_Ray Center, TU Wien, Getreidemarkt 9, 1060 Vienna, Austria

Ao. Univ. Prof. Dr. Gerald Giester, Univ.-Prof. Dr. Ronald Miletich Department of Mineralogy and Crystallography University of Vienna, Josef-Holaubek-Platz 2, 1090 Vienna, Austria

Ao. Univ. Prof. Dr. Michael Reissner Institute of Solid State Physics, TU Wien Wiedner Hauptstraße 8-10/050, 1040 Vienna, Austria

> Supporting information for this article is given via a link at the end of the document.



FULL PAPER

Results and Discussion

Synthesis

Figure 2 depicts the reaction scheme for all the reported 1-propyl-1H-imidazole based compounds. Reaction of Prlm with $Fe(BF_4)_2 \cdot 6H_2O$ in MeOH under inert atmosphere and $50^{\circ}C$ temperature over 6 hours results in the formation of the expected homoleptic complex $[Fe(Prlm)_6](BF_4)_2$ (1). The same reaction conducted at $140^{\circ}C$ over 12 hours results in the formation of the cubane-like iron-oxo cluster $[Fe_4(\mu_2-OH)_4(Prlm)_{12}](BF_4)_4$ (2). Redissolution of 1 in MeOH and heating to $140^{\circ}C$ also leads to 2. Reaction of Prlm with $Fe(NCS)_2 \cdot 4MeCN$ leads to different products depending on the solvent: if the reaction is carried out in MeCN, it results in the mononuclear complex $[Fe(Prlm)_4(NCS)_2]$ (3), whereas in MeOH the binuclear, methoxo-bridged complex $[Fe(Prlm)_2(NCS)_2]_2(\mu_2-MeO)_2]$ (4) is formed.

To better understand what drives the reaction towards the cluster formation and what the oxygen source is, other synthetic pathways were tried out (b and c were performed in the glovebox):
a) shortening the reaction time to 2h

- b) using anhydrous $Fe(BF_4)_2$ and stirring the mixture for 18h
- c) using anhydrous $Fe(BF_4)_2$ and dry MeCN as solvent, stirring for 18h.

All three syntheses led to compound 1. These results suggest that the solvate water molecules in the Fe(II) salt serve as oxygen source, and that compound 1 is the kinetic product formed over shorter reaction time, whereas 2 is the thermodynamic product being formed by longer reaction time.

Magnetic Characterization

Temperature dependent magnetic susceptibility was measured for compounds **1-4**; the compounds do not show spin-crossover and are in the HS state over the whole measured temperature range (10 to 300 K). For **1,3** and **4** χ_{mol} T values vary between 2.64 and 3.65 cm³Kmol⁻¹, which are typical for Fe(II) ions in the HS state. The faster decrease below 50K is to be attributed to zero field splitting. The results are shown in Figure 3, χ_{mol} T for the reference system [Fe(3Tz)₆](BF₄)₂ is reported as well for comparison.

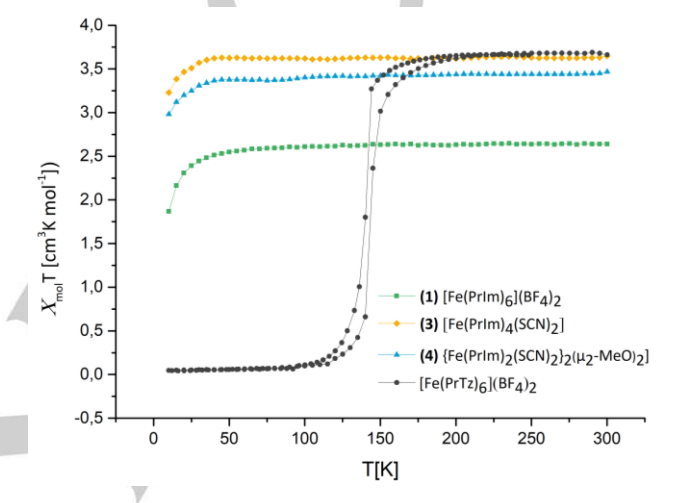


Figure 3. Temperature dependent magnetic susceptibility of compounds **1-3**, [Fe(3Tz)₆] is reported for comparison.

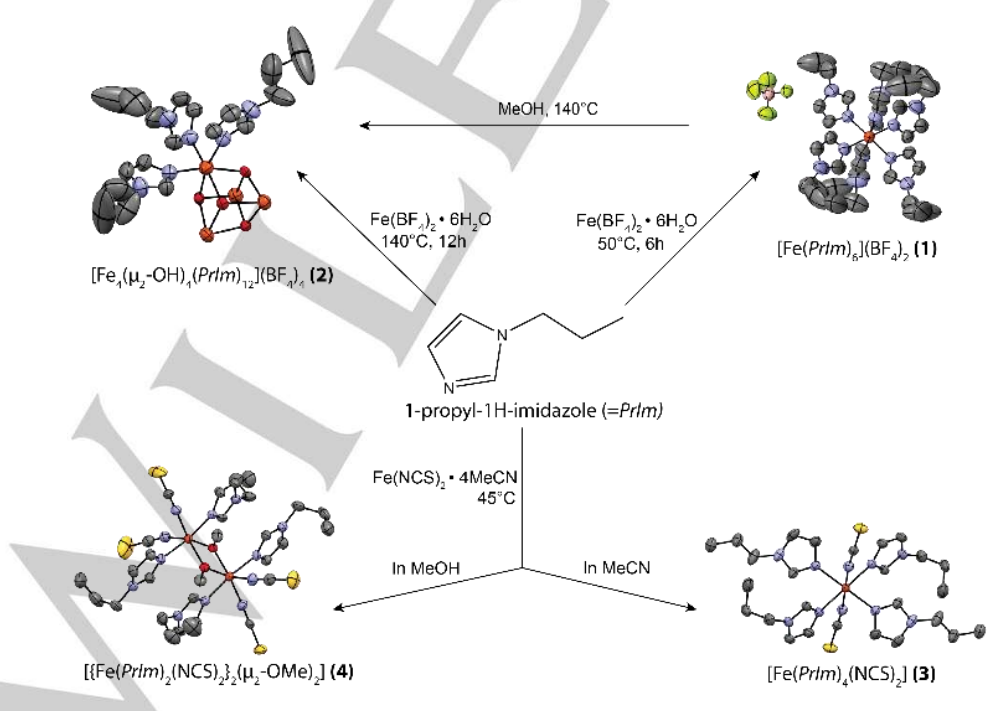


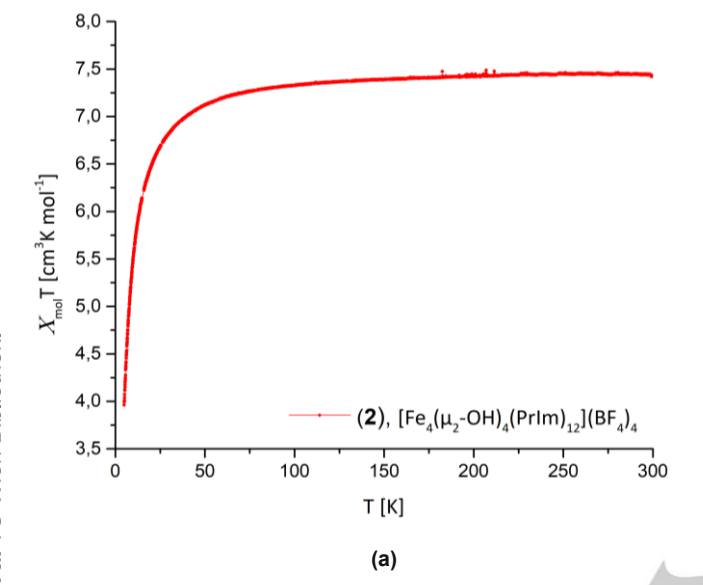
Figure 2. Reaction scheme and synthetic pathways for compounds 1-4 starting from *Prlm*. Hydrogens are omitted for clarity, for 2 only three ligands are shown, the rest is omitted for clarity.



FULL PAPER

WILEY-VCH

 $\chi_{mol}T$ values of compound **2** present a slight variation between 7.12 and 7.48 cm³ K mol⁻¹. The value at room temperature is smaller than that of four uncoupled Fe(II) in the HS state with a ground state S=8, and the slight decrease observed by cooling demonstrates the presence of antiferromagnetic interactions. An absence of intramolecular ferromagnetic interactions was further



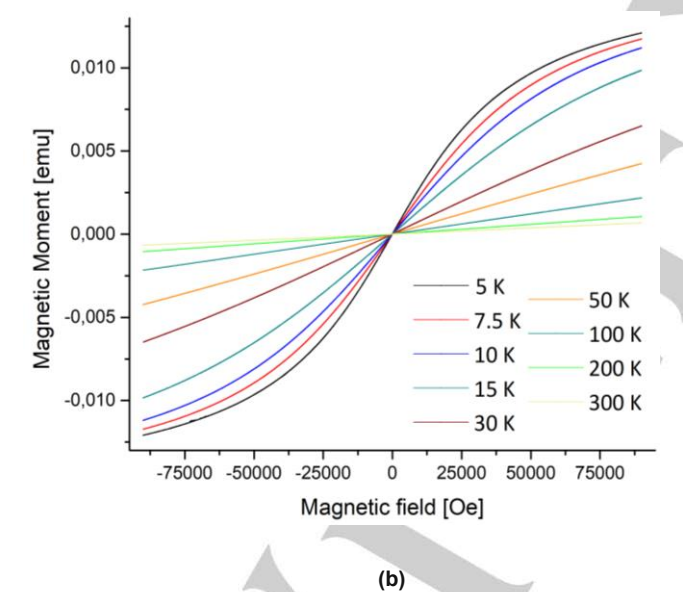


Figure 4. (a) temperature dependent magnetic susceptibility of 4. (b) field dependent magnetic moment of a crystalline sample of 4 mounted in arbitrary orientation in the field.

confirmed by field-dependent measurement of the magnetic moment for a crystalline sample (Figure 4).

Structural Characterization

Single crystals were grown for all the reported compounds by vapor diffusion of Et_2O in a concentrated MeOH (1,2 and 4) or MeCN (3) solution of the corresponding compound.

Compound 1 crystallizes in the cubic space group $Pa\overline{3}$ as a mononuclear octahedral complex, with four molecules per unit cell. The complex is located on a $\overline{3}$ position, therefore all ligands are related by symmetry thus exhibiting six symmetry-equivalent bonds. The Fe—N distance of 2.209 Å is in good agreement with typical values for Fe(II) in the HS state. The N—Fe—N angle between cis-ligands deviates by 3.7° from the regular 90°.

The BF₄⁻ anion is located on a threefold axis and fills the voids between the complex molecules. Comparison of **1** with the reference system [Fe(3Tz)₆](BF₄)₂ shows that coordination angle and geometry around the Fe(II) center are retained (Figure 5), but [Fe(3Tz)₆](BF₄)₂ crystallizes in a different space group, namely the trigonal space group $R\overline{3}$. Since the molecules packing in the crystal influences the cooperativity between the Fe(II) centers, which in turn plays a key role in the abruptness of the spin transition, this difference must be taken into account as it impacts the overall magnetic behavior of the complexes.

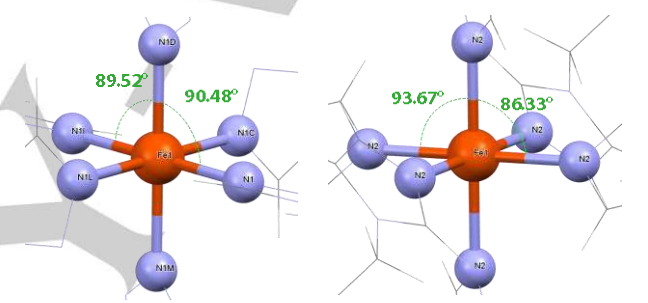


Figure 5. Comparison of the coordination geometry around the Fe(II) centre for $[Fe(3Tz)_6](BF_4)_2$ (left) and $[Fe(PrIm)_6](BF_4)_2$ (right) with selected bond angles. Ligands -except coordinating N atoms- are represented as wireframe for clarity. Anions are omitted for clarity.

Compound 2 likewise crystallizes in the cubic space group Pa3, with eight molecules per unit cell located on the threefold axes. The [Fe₄(µ₂-OH)₄]-cubane core presents Fe(II) ions and OH bridging anions located at alternate vertices of a distorted cube. The distortion is well reflected in the Fe—O—Fe and O—Fe—O angles, which vary between 100.98°-102.04° and 76.76°-77.30°, respectively. Consequently, the Fe-centers present a distorted octahedral coordination geometry, with one octahedral face occupied by three bridging OH- ligands and the other one by the imidazoles, which decorate the surface of the core. The N-Fe-N and N—Fe—O bond angles vary between 89.79° and 97.64°, thus closer to those of an ideal octahedron but still affected by the distortion of the $[Fe_4(\mu_2-OH)_4]$ core. The substantial deviation from an ideal octahedral geometry is well expressed by the angular deviation parameter Σ (defined as the sum of the deviation from an ideal octahedral angle of 90° of the 12 cis angles in the coordination sphere) [47], with values of Σ =76.5° for Fe1 and Σ =94.7° for Fe2. Bond lengths vary between 2.135 and 2.154 Å for the Fe—O bonds, and between 2.128 and 2.155 Å for the Fe— N bond. Both bond angles (specifically O-Fe-O and Fe-O-Fe) and Fe—O bond lengths are in accordance with typical values for Fe(II) in the HS state reported in literature for similar cubane

WILEY-VCH

FULL PAPER

 Table 1. Crystallographic parameters for compounds 1-4

	1	2	3	4
Formula	C ₃₆ H ₆₀ B ₂ F ₈ FeN ₁₂	C ₇₂ H ₁₂₄ B ₄ F ₁₆ Fe ₄ N ₂₄ O ₄	C ₂₆ H ₄₀ FeN ₁₀ S ₂	C ₃₀ H ₄₆ Fe ₂ N ₁₂ O ₂ S ₄
Weight [g mol ⁻¹]	890.43	1960.58	612.65	846.72
T [K]	100	250	200	296.15
Colour	white	white	white	orange
Shape	platelet	platelet	platelet	block
Crystal System	cubic	cubic	monoclinic	monoclinic
Space Group	Pa 3	Pa 3	P2 ₁ /c	P2 ₁ /c
a [Å]	17.3177(13)	26.657(5)	9.4925(12)	16.155(3)
<i>b</i> [Å]	17.3177(13)	26.657(5)	11.0060(14)	15.082(2)
c [Å]	17.3177(13)	26.657(5)	15.4112(19)	33.864(6)
α [°]	90	90	90	90
β [°]	90	90	98.182(3)	95.386(2)
γ [°]	90	90	90	90
V [Å ³]	5193.6(12)	18942(10)	1593.7(3)	8214(2)
Z	4	8	2	4
$ ho_{calc.}$ [g cm $^{-3}$]	1.139	1.375	1.277	1.369
μ [mm ⁻¹]	0.354	0.689	0.637	0.953
Measured Refl's.	62417	210975	36679	114419
Unique Refl's	1075	4543	3977	14694
F(000)	1872	15914	648	3528
Rint	0.0782	0.0808	0.0446	0.0484
GooF	2.757	1.01	1.008	1.101
R ₁	0.0958	0.0709	0.0348	0.0684
wR ₂	0.2602	0.2364	0.0854	0.1472
No. of parameters	91	377	181	913
CCDC	2035093	2035095	2035091	2035094

iron-oxo clusters^[48-51]. The two crystallographically unique BF₄ anions are located on the one hand on a threefold axis on the other hand on a general position.

Compound 3 crystallizes in the monoclinic space group $P2_1/c$ as a mononuclear octahedral complex, with two molecules per unit cell located on a center of inversion. Fe is coordinated by four 1H-1-propyl-imidazoles and two isothiocyanate anions, that occupy both apical positions and coordinate through their N-atom. The Fe—N_{im} bond lengths vary between 2.213 and 2.171 Å, which again is in agreement with the presence of Fe(II) in the HS state. The Fe—N_{NCS} bond length is 2.157Å. Compound 4 crystallizes in the monoclinic space group $P2_1/c$ as a binuclear complex, with two crystallographically different molecules located on general positions. Fe centers show octahedral geometry and are each coordinated by two 1-propyl-1H-imidazoles, two isothiocyanate anions and two OMe anions which act as bridging ligands. The Fe-N_{im} bond lengths vary between 2.120 and 2.138Å, again typical values for Fe(II) in the HS state. The imidazole groups are placed in an orthogonal fashion relative to the plane formed by the [Fe₂-(µ₂-OMe)₂] unit, the NCS moieties are aligned within the plane. The bridging -OMe ligands cause a significant deviation from an ideal octahedral coordination around the Fe atoms, with O—Fe—O bond angles varying between 74.69° and 75.71°. As for 2, the Σ parameter gives a good sense of the distortion, with values of 52.8° for Fe1, 48.1° for Fe2, 51.6° for Fe3 and 54.0° for Fe4.

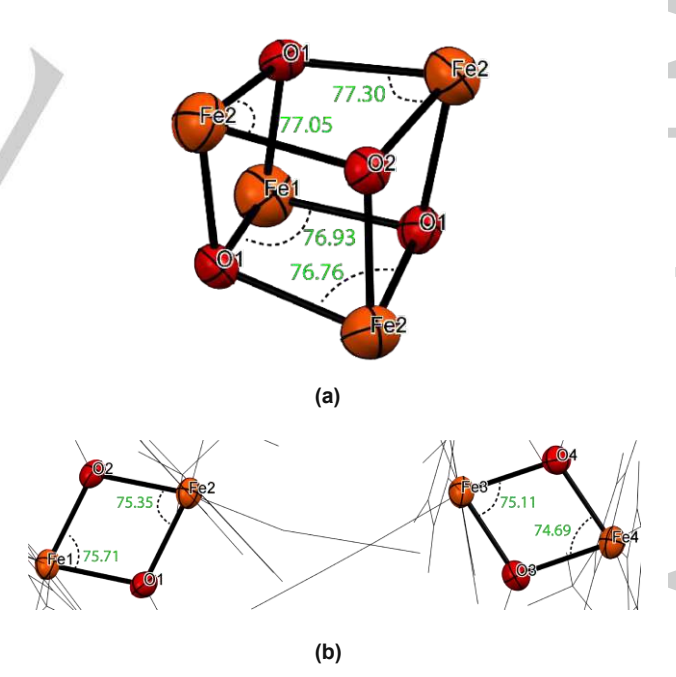


Figure 6. (a) distorted [Fe₄(μ_2 -OH)₄] core of **2** with selected O-Fe-O bond angles (ligands, anions and hydrogens are omitted for clarity). (b) [Fe₂(μ_2 -OMe)₂] cores of both crystallographic molecules of **4** with O-Fe-



FULL PAPER

WILEY-VCH

By looking at the structures, one can see that the carbon atoms of the propyl chain -particularly in **1** and **2**- show huge ellipsoids. We attempted to locate the carbon atoms at a specific position, but we were not able to do so. This is obviously an indication of poor packing, which as mentioned above, has with all probability repercussions on the magnetic behavior of the complexes, causing scarce cooperativity. The disorder in **1** was present even at 100K, hence the problem seems be intrinsic to the substances which show a scarce tendency to pack; this hypothesis is also supported by the difficulty encountered in growing single crystals for **1** and **2**, and the submitted structures were the best results we could obtain.

Infrared Spectroscopy

ATR-FT-IR spectra were measured for the free ligand (liquid) and compounds **1-4** (powder samples).

Characteristic vibrations for the imidazole ring are found in the mid-infrared at 3107cm^{-1} and 1507 cm^{-1} for the free ligand. The first band represents the $v_{(\text{CH Im})}$ of the CH at the rings 2 position, its asymmetric form and the slight shoulder are caused by the stretching modes -both symmetric and asymmetric- of the CH bonds in the 4 and 5 positions, which are not so strong and thus do not appear as separate absorption bands. The second band represents the in-plane ring deformation. Further bands for the ligand are found in the range 2965-2877 cm⁻¹ and arise from the different vibration modes of the propyl chain. Upon coordination, the bands are affected due to the formation of the Fe-N3 bond, resulting in a band shift; the results are reported in Table 2.

Table 2: Characteristic vibrations for Prlm as free ligand and in complexes 1-4

IR mode	PrIm (cm ⁻¹)	1 (cm ⁻¹)	2 (cm ⁻¹)	3 (cm ⁻¹)	4 (cm ⁻¹)
VCH Im	3107	3132	3133	3114	3101
in-plane ring	1507	1522	1518	1517	1514

For 1-3, the v_{CH Im} band shifts as expected to higher wavenumbers, showing an increase of about 7 up to 26 cm-1. In 4, the different coordination environment and the geometric distortion caused by the bridging OMe groups result in a shift to lower wavenumbers, with a decrease of 6 cm⁻¹. Although bridging O-ligands are present in 2 as well, the shift for this compound is to higher wavenumber due to weak H---F interactions between the BF₄- anions and the imidazolic CH. The in-plane ring deformation band is also heavily affected by coordination and shows a shift to higher wavenumbers of 7 up to 15 cm⁻¹. Being in a peripheral position, the propyl chain is much less affected by coordination, and shows a smaller shift up to 4 cm⁻¹ (range 2962-2873 cm⁻¹). For compounds 3 and 4 the v_{NCS} of the -NCS ligand is observed at its typical frequencies, 2069 and 2070 cm⁻¹, respectively. Characteristic for complexes with the BF₄ anion are broad, intense B-F stretching vibrations with a maximum at 1052 and 1053 cm⁻¹ for 1 and 2, respectively. Spectra are depicted in Figure 7.

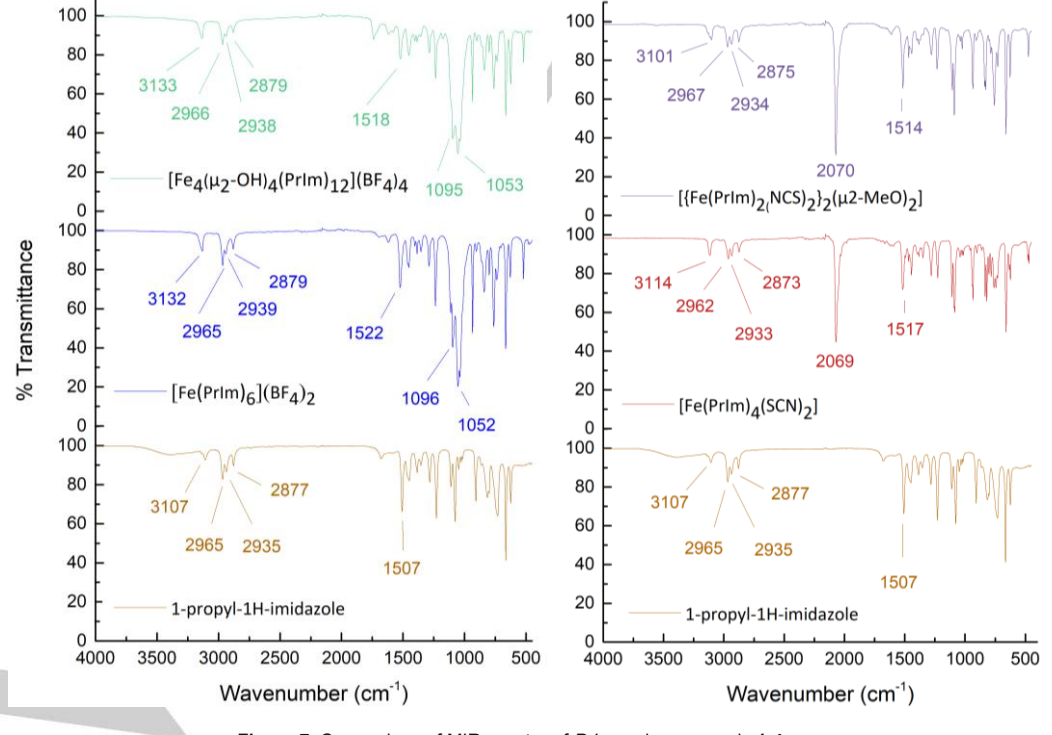


Figure 7. Comparison of MIR spectra of *Prlm* and compounds 1-4



FULL PAPER

WILEY-VCH

UV-VIS / NIR Spectroscopy

Solid state UV-VIS / NIR spectroscopy in diffuse reflection was used to obtain the ligand-field spectra of the Fe(II)-complexes. For Fe(II)-complexes octahedrally coordinated by azoles, in the HS-state at room-temperature the characteristic $^5T_2 \rightarrow ^5E$ transition occurs around 850 nm in the near infrared. Since the complexes do not show spin-crossover at ambient conditions, the $^1A_1 \rightarrow ^1T_1$ and $^1A_1 \rightarrow ^1T_2$ transitions observed at lower temperature at around 550 nm and 380 nm typical of Fe(II) LS, and which are responsible for the bright magenta color, are not observed. Since all the compounds are in the HS state, the ligand field splitting parameter 10Dq can be directly obtained from the absorption bands. Results are reported in Table 3.

Table 3: UV-VIS-NIR Absorption bands and ligand field strength for compounds 1-4

	1	2	3	4
${}^5\text{T}_2 \rightarrow {}^5\text{E (nm)}$	850	-	850	852
10 Dq (cm ⁻¹)	11765	-	11765	11737

The 10Dq value for $[Fe(3Tz)_6](BF_4)_2$ is almost the same, namely 11760cm^{-1[52]}; this suggests that the energy difference between the LS and HS state for $[Fe(Prlm)_6](BF_4)_2$ is too big to observe a thermal spin-transition.

Although the crystal-structure refinement suggests Fe is in the +2-oxidation state, the presence of the ${}^5T_2 \rightarrow {}^5E$ band cannot be observed in compound **2**. This is because the coordination geometry of Fe(II) centers is heavily distorted, resulting in the loss of the orbital degeneracy of the ${}^5T_{2g}$ octahedral states and 5A -like ground states[51]. Spectra are depicted in Figure 8.

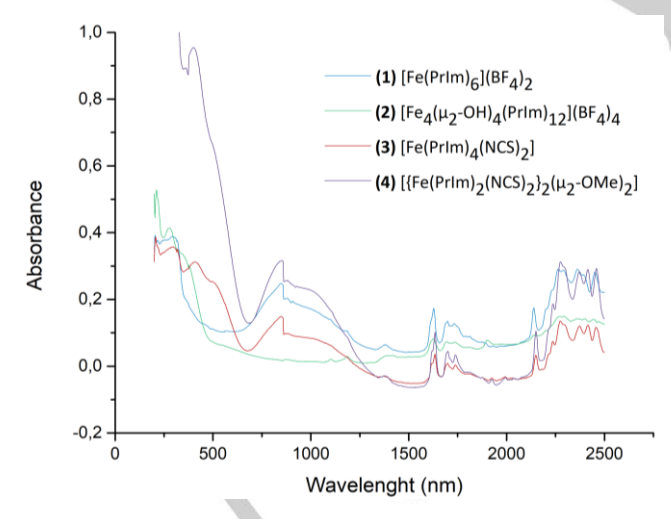


Figure 8. UV-VIS-NIR Spectra of compounds 1-4

In addition to the investigations under various temperatures, compound 1 was also compressed under hydrostatic conditions

to a maximum pressure of 11 GPa. The visual observation of the pressurized crystal specimen revealed a rather sluggish transition with the colour change gradually propagating across the crystal between approximately 9.5 and 11 GPa. The colour change to bright magenta (Figure 9) is typical for the HS-to-LS transition of Fe(II) centers in octahedral coordination. Due to the upcoming differential stress and non-hydrostaticity > 9 GPa of densified argon being used as the pressure-transmitting medium, the transformation was initiated on the side of the crystal specimen that faces the center of the pressure chamber, which usually exhibits comparatively slightly higher pressure.

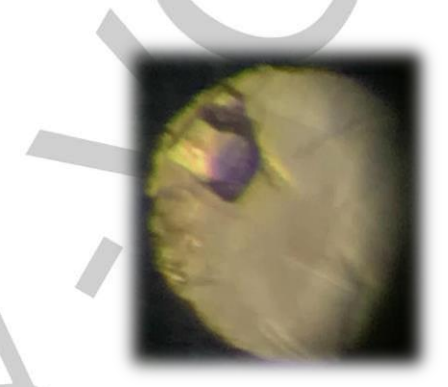


Figure 9. Image of a crystal specimen of sample 1 hydrostatically pressurized in a diamond-anvil cell to 11GPa. The sample shows a HS-LS spin transition, associated with the typical colour change from colourless to deep purple. The pressure-induced transition has only partially taken place within the crystal shown here as due to pressure gradients within the sample chamber.

Conclusions

The target compound 1 was successfully synthesized and characterized in both its structure and magnetic behavior. The complex does not show thermal spin-transition, but it seems to be susceptible of spin transition when subjected to high-pressure condition. In-situ investigations revealed a color change to deep purple, as typical for the pressure induced HS-to-LS spin crossover of Fe(II) complexes. The comparison between [Fe(3Tz)₆](BF₄)₂ and **1** in the light of the reported experimental results shows that the different magnetic behavior has with all probability a dual nature: on one hand, the different electron density distribution within the ligand changing the ligand field strength and the energy difference between HS and LS state, and on the other hand the different packing which affects the cooperativity between molecules during the spin transition. The use of different anions and/or substituents on the imidazole ring, namely bulkier ligands as benzyl groups, which can better fill the void and possibly give rise to π - π interaction, could result in a more ordered structure and hence better packing and increased cooperativity. However, as stated in the introduction, the goal of the study was to decouple the impact of electronic from steric factors on the magnetic behavior of a Fe(II) complex comparable

WILEY-VCH

FULL PAPER

to $[Fe(3Tz)_6](BF_4)_2$, and changing anion and/or substituent on the azole ring would defeat the purpose.

The combination of the two abovementioned factor makes complex 1 not susceptible to thermal SCO. This remains true for the heteroleptic complexes 3 and 4 as well. The two isothiocyanate ligands in 3 obviously cause a complete change in both the electron density distribution of the system and the packing, due to the linearity of the ligand and absence of anions, and so do the bridging OMe ligands in 4, which furthermore cause a significant distortion from an ideal octahedral geometry. The key role played by the poor packing in the magnetic behavior of 1 seems to be confirmed by the results of the high-pressure experiment: by subjecting a crystal specimen to high hydrostatic pressure, hence forcing a tighter packing, the typical color change from white to magenta associated with the HS to LS transition for Fe(II) was observed. The study also shed light on the versatility of Prlm as ligand for Fe(II) coordination compounds, giving rise to a new family of mono-, bi- and tetranuclear compounds, which can all be synthesized by simply changing the reaction conditions. The cubane-like Fe₄O₄ cluster **2** was the most interesting discovery. Several synthetic iron-oxo clusters with the Fe₄O₄ cubane motif have been prepared to study the feasibility of their occurrence in nature and compare their behavior with the known iron-sulfur proteins. Clusters with both single-valent cores, mostly Fe(II), and mixed valence core with Fe(II/III) have been prepared, for the major part with carboxylate ligands and often as a part of large polynuclear complexes.^[48-51, 53-62] Recently, a Fe₄O₄ cluster with a single valence Fe(II) core and tridentate imidazole ligands was reported from our group^[63], but to the best of our knowledge, compound 2 is the first reported cluster with the Fe₄O₄ motif where azole ligands coordinate in a monodentate fashion to the Fe(II) atoms of the core. As mentioned in "Results and Discussion", other synthetic pathways were carried out to better understand what drives the reaction towards the formation of 2, and the observed experimental results suggest that 1 is the kinetic product and 2 the thermodynamic one. Further investigation of 2, especially electrochemical measurements to investigate its redox properties, is to be carried out, but this is beyond the scope of the current publication. As for 2, solvent plays a key role in the outcome of reactions involving Fe(SCN)2: MeOH acts in this case as bridging ligand leading to the formation of the dinuclear compound 4, whereas the use of MeCN leads to the mononuclear compound 3.

Experimental Section

Methodology

All operations involving Fe(II) were carried out under inert gas atmosphere (argon 5.0). The glassware used was oven dried at 120 °C before use for at least 2 hours. All solvents for the complexation reactions were dried before use and stored over 3 Å molecular sieves under argon. [64] Unless otherwise stated, all starting materials were commercially obtained and used without further purification. All NMR spectra were recorded in dry deuterated solvents on a Bruker Avance UltraShield 400 MHz. Chemical

shifts are reported in ppm; ¹H and ¹³C shifts are referenced against the residual solvent resonance. For the measurement of MIR and FIR spectra. a Perkin-Elmer Spectrum 400, fitted with a coolable/heatable PIKE Gladi ATR unit was used within the range of 4000-100 cm⁻¹. Solid state UV/Vis/NIR spectra were recorded with a Perkin-Elmer Lambda 900 spectrophotometer between 300 and 2500 nm in diffuse reflectance against BaSO₄. A Harrick coolable/heatable powder sample holder in "Praying Mantis" configuration was used. Melting points were determined by differential scanning calorimetry, using a Netzsch STA 449 C Jupiter® with heating rates of 2 K min-1. The magnetic moment of the Fe(II) complexes was measured using a Physical Property Measurement System (PPMS®) by Quantum Design. The experimental setup consisted of a vibrating sample magnetometer attachment (VSM), bearing a brass sample holder with a quartz-glass powder container. The magnetic moment was determined in an external field of 1 T in the range of 10 K to 300 K. Variable temperature mid-range (4000 - 450 cm⁻¹) infrared spectra were recorded by the ATR technique on a Perkin Elmer Spectrum 400, fitted with a coolable/heatable PIKE Gladi ATR Unit. [65] Single crystals were attached to a glass fiber by using perfluorinated oil and were mounted on a Bruker KAPPA APEX II diffractometer equipped with a CCD detector with Mo K_{α} radiation (Incoatec Microfocus Source IµS: 30 W, multilayer mirror, λ=0.71073 Å) and an Oxford Cryosystems Cryostream 800 Plus LT device. For all measurements data were reduced to intensity values by using SAINT Plus[66], and an absorption correction was applied by using the multi scan method implemented by SADABS.[66] For the iron(II) complexes, protons were placed at calculated positions and refined as riding on the parent C atoms. All non-H atoms were refined with anisotropic displacement parameters. In-situ high pressure experiments were carried out in a ETH-type diamond anvil cell^[67], using Boehler-Almax type diamond anvils, a standard steel gasket, and cryogenically loaded argon as pressure-transmitting medium. Ruby spheres were used for calibration through optical laser-luminescence excitation techniques[68], by means of a 632.8 He-Ne laser, and measuring the R₁ line shifts on a Horiba Jobin Yvon LabRAM-HR 800 spectrometer.

Synthesis

[Fe(PrIm)₆](BF₄)₂ (1): Fe(BF₄)₂·6H₂O (0.5 g, 1.5 mmol, 1 eq.) and PrIm (1 g, 9 mmol, 6.1 eq.) were dissolved in 10 mL MeOH and stirred at 50 °C for 6 h. After evaporation of the solvent, the yellow residue was triturated twice with 10 ml CH₂Cl₂ to remove residual free ligand. The solid was dried in vacuum, yielding the product as an off-white solid. (980 mg, 74.3 %) $v_{CH(Im)}$ cm⁻¹: 3132

elemental analysis calcd (%) for $C_{36}H_{60}FeN_{12}B_4F_8$: C 47.41, H 6.63, N 18.43; found: C 46.35, H 6.63, N 17.36

[Fe₄(μ_2 -OH)₄(*PrIm*)₁₂](BF₄)₄ (2), path I: [Fe(*PrIm*)₆](BF₄)₂ (0.2 g, 225 μ mol) were dissolved in 5 ml wet MeOH and heated for 24 h to 140 °C. After evaporation of the solvent the yellow residue was washed with 10 ml CH₂Cl₂ and dried in vacuum. **2** was obtained as beige solid, 76 mg 69 %. ν CH(m) cm⁻¹; 3133

elemental analysis calcd (%) for $C_{72}H_{124}Fe_4N_{24}O_4B_4F_{16}$: C 44.11, H 6.38, N 17.15; found: C 45.06, H 6.81, N 16.93

[Fe₄(μ₂-OH)₄(*PrIm*)₁₂](BF₄)₄ (2), path II: Fe(BF₄)₂·6 H₂O (0.25 g, 741 μmol, 1 eq.) and *PrIm* (245 mg, 2.2 mmol, 3 eq.) were dissolved in 10 ml wet MeOH and stirred for 24 h at 140 °C. After evaporation of the solvent the oily residue was triturated with 10 ml CH₂Cl₂ and dried in vacuum at 40 °C. 2 was obtained as beige solid, 134 mg, 36.9 %.

v_{CH(Im)} cm⁻¹: 3133

[Fe(PrIm)₄(SCN)₂] (3): Fe(SCN)₂·4 MeCN (0.25 g, 744 µmol, 1 eq.) and PrIm (336 mg, 3 mmol, 4.1 eq.) were dissolved in 10 mL dry MeCN and stirred at room-temperature for 3 h. After evaporation of the solvent, the



WILEY-VCH

FULL PAPER

remaining slightly orange residue was triturated two times with Et₂O and once with CH₂Cl₂, resulting 3 (980 mg, 31.4 %) as a yellow solid, which was dried in vacuum. The product is very sensitive towards moist air. VCH(Im) cm⁻¹: 3114, V(SCN) cm⁻¹ 2069 elemental analysis calcd (%) for C₂₆H₄₀FeN₁₀S₂: C 50.97, H 6.58, N 22.86,

S 10.47; found: C 49.71, H 6.34, N 22.50, S 10.61

 $\label{eq:ferminal} \mbox{[{Fe}(\textit{PrIm})_2(NCS)_2}_2(\mu_2\mbox{-OMe})_2\mbox{] (4): $Fe(SCN)_2$$^-4 MeCN (0.25 g, 744 \mu mol, 1.25 g, 1.25 g,$ 1 eq.) and Prlm (336 mg, 3 mmol, 4.1 eq.) were dissolved in 10 mL MeOH and stirred at room-temperature for 3 h. During this time, the reaction solution turned bright orange. After evaporation of the solvent, the remaining residue was triturated two times with Et₂O and once with CH₂Cl₂, resulting 4 (187 mg, 29.7 %) as an orange solid.

v_{CH(Im)} cm⁻¹: 3101, v_(SCN) cm⁻¹ 2070

elemental analysis calcd (%) for $C_{30}H_{46}Fe_2N_{12}O_2S_4$: C 42.56, H 5.48, N 19.85, S 15.15; found: C 43.03, H 5.82, N 20.15, S 14.56

Deposition Number(s) 2035093 (1), 2035095 (2), 2035091 (3) and 2035094 (4) contain(s) the supplementary crystallographic data for this

https://www.ccdc.cam.ac.uk/services/structures?id=doi:10.1002/ejic.2024 00358. These data are provided free of charge by the joint Cambridge Crystallographic Data Centre and Fachinformationszentrum Karlsruhe http://www.ccdc.cam.ac.uk/structures

Acknowledgements

We acknowledge financial support of the Austrian Science Fund (FWF Der Wissenschaftsfond) project P 31076-N28.

Keywords: Magnetic Materials • Iron • Imidazole • Oxo-Cluster•

References

[8]

[9]

- [1] [2] O. Kahn, C. J. Martinez, Science 1998, 279, 44-48. C. Bartual-Murgui, A. Akou, C. Thibault, G. Molnar, C. Vieu, I Salmon, A. Bousseksou, Journal of Materials Chemistry C 2015, 3, 1277-1285
- J. Linares, E. Codjovi, Y. Garcia, Sensors 2012, 12, 4479-4492. H. J. Shepherd, C. Bartual-Murgui, G. Molnar, J. A. Real, M. C Munoz, L. Salmon, A. Bousseksou, New Journal of Chemistry 2011, 35, 1205-1210.
- [5] G. J. Halder, C. J. Kepert, B. Moubaraki, K. S. Murray, J. D. Cashion, *Science* **2002**, *298*, 1762-1765.

 J. A. Real, E. Andres, M. C. Munoz, M. Julve, T. Granier, A.
- [6] Bousseksou, F. Varret, Science 1995, 268, 265-267. S. M. Neville, G. J. Halder, K. W. Chapman, M. B. Duriska, B [7] Moubaraki, K. S. Murray, C. J. Kepert, Journal of the American
 - Chemical Society 2009, 131, 12106-+ P. Gütlich, H. A. Goodwin, in *Topics in Current Chemistry*,, Springer Berlin Heidelberg,, Berlin, Heidelberg, **2004**. P. Gütlich, European Journal of Inorganic Chemistry 2013, 581-
- 591. [10] S. Decurtins, P. Gutlich, K. M. Hasselbach, A. Hauser, H. Spiering,
- Inorganic Chemistry 1985, 24, 2174-2178.
 S. Decurtins, P. Gutlich, C. P. Kohler, H. Spiering, Journal of the [11] Chemical Society-Chemical Communications 1985, 430-432.
- T. Mahfoud, G. Molnar, S. Cobo, L. Salmon, C. Thibault, C. Vieu, P. Demont, A. Bousseksou, *Applied Physics Letters* **2011**, 99. L. Zhu, F. Zou, J. H. Gao, Y. S. Fu, G. Y. Gao, H. H. Fu, M. H. Wu, J. T. Lu, K. L. Yao, *Nanotechnology* **2015**, 26. M. D. Manrique-Juarez, S. Rat, F. Mathieu, D. Saya, I. Séguy, T. [12] [13]
- [14] Leïchlé, L. Nicu, L. Salmon, G. Molnár, A. Bousseksou, Applied
- Physics Letters 2016, 109, 061903. [15] S. Decurtins, P. Gutlich, C. P. Kohler, H. Spiering, A. Hauser,
- Chemical Physics Letters 1984, 105, 1-4. G. Aubock, M. Chergui, Nature Chemistry 2015, 7, 629-633. [16]

- S. Cobo, D. Ostrovskii, S. Bonhommeau, L. Vendier, G. Molnar, L. [17] Salmon, K. Tanaka, A. Bousseksou, Journal of the American Chemical Society 2008, 130, 9019-9024.
 - C. Gandolfi, G. G. Morgan, M. Albrecht, Dalton Transactions 2012,
- K. Nishi, S. Arata, N. Matsumoto, S. Iijima, Y. Sunatsuki, H. Ishida, [19]

[18]

[33]

[34]

[35]

[36]

[37]

[38]

[44]

- M. Kojima, *Inorganic Chemistry* **2010**, *49*, 1517-1523. M. M. Dîrtu, A. Rotaru, D. Gillard, J. Linares, E. Codjovi, B. Tinant, [20] Y. Garcia, *Inorganic Chemistry* **2009**, *48*, 7838-7852. C. J. Johnson, G. G. Morgan, M. Albrecht, *J. Mater. Chem. C* [21]
 - **2015**, *3*, 7883-7889.
- J. Cirera, E. Ruiz, *Inorganic Chemistry* **2016**, *55*, 1657-1663. H. L. C. Feltham, C. Johnson, A. B. S. Elliott, K. C. Gordon, M. [22] [23]
- Albrecht, S. Brooker, *Inorganic Chemistry* **2015**, *54*, 2902-2909. M. A. Goodman, M. J. DeMarco, S. E. Tarasek, A. Y. Nazarenko, [24] W. Brennessel, M. S. Goodman, Inorganica Chimica Acta 2014, 423, 358-368.
- [25] Y.-H. Luo, Y. Sun, Q.-I. Liu, L.-J. Yang, G.-J. Wen, M.-X. Wang, B.-W. Sun, ChemistrySelect 2016, 1, 3879-3884.
- J. Okabayashi, S. Ueno, T. Kawasaki, T. Kitazawa, *Inorganica Chimica Acta* **2016**, *445*, 17-21. [26]
- C. Baldé, C. Desplanches, J. François Létard, G. Chastanet, [27] Polyhedron 2016
- Y.-H. Luo, G.-J. Wen, L.-S. Gu, M.-N. Wang, B.-W. Sun, [28] Polyhedron 2017, 121, 101-106.
- M. Steinert, B. Schneider, S. Dechert, S. Demeshko, F. Meyer, [29] Inorganic Chemistry 2016, 55, 2363-2373
- [30] S. Wang, W.-T. Xu, W.-R. He, S. Takaishi, Y.-H. Li, M. Yamashita,
- W. Huang, Dalton Trans. 2016, 45, 5676-5688. X.-R. Wu, H.-Y. Shi, R.-J. Wei, J. Li, L.-S. Zheng, J. Tao, *Inorganic Chemistry* **2015**, *54*, 3773-3780. [31]
- [32] N. Hassan, P. Weinberger, K. Mereiter, F. Werner, G. Molnar, A. Bousseksou, M. Valtiner, W. Linert, Inorganica Chimica Acta 2008,
 - M. Valtiner, H. Paulsen, P. Weinberger, W. Linert, Match-Communications in Mathematical and in Computer Chemistry
 - 2007, 57, 749-761. C. M. Grunert, J. Schweifer, P. Weinberger, W. Linert, K. Mereiter, G. Hilscher, M. Müller, G. Wiesinger, P. J. van Koningsbruggen, Inorganic Chemistry 2004, 43, 155-165.
 - A. B. Koudriavtsev, A. F. Stassen, J. G. Haasnoot, M. Grunert, P. Weinberger, W. Linert, Physical Chemistry Chemical Physics **2003**, 5, 3676-3683.
 - A. Absmeier, M. Bartel, C. Carbonera, G. N. L. Jameson, F. Werner, M. Reissner, A. Caneschi, J. F. Letard, W. Linert, European Journal of Inorganic Chemistry **2007**, 3047-3054. A. F. Stassen, M. Grunert, E. Dova, M. Müller, P. Weinberger, G. Wiesinger, H. Schenk, W. Linert, J. G. Haasnoot, J. Reedijk, European Journal of Inorganic Chemistry 2003, 2273-2282. P. J. van Koningsbruggen, M. Grunert, P. Weinberger, Monatshefte Fur Chemie 2003, 134, 183-198.
- M. Muttenthaler, M. Bartel, P. Weinberger, G. Hilscher, W. Linert, [39] Journal of Molecular Structure 2005, 741, 159-169. D. Müller, C. Knoll, B. Stoger, W. Artner, M. Reissner, F
- [40] Weinberger, European Journal of Inorganic Chemistry 2013, 984-
- [41] N. Hassan, J. Stelzl, P. Weinberger, G. Molnar, A. Bousseksou, F. Kubel, K. Mereiter, R. Boca, W. Linert, Inorganica Chimica Acta 2013, 396, 92-100.
- N. Hassan, P. Weinberger, F. Kubel, G. Molnar, A. Bousseksou, L. [42] Dlhan, R. Boca, W. Linert, Inorganica Chimica Acta 2009, 362, 3629-3636
- [43] M. Quesada, H. Kooijman, P. Gamez, J. S. Costa, P. J. van Koningsbruggen, P. Weinberger, M. Reissner, A. L. Spek, J. G.
 - Haasnoot, J. Reedijk, Dalton Transactions 2007, 5434-5440. N. T. Madhu, P. K. Radhakrishnan, M. Grunert, P. Weinberger, W.
- Linert, Thermochimica Acta 2003, 407, 73-84. A. Absmeier, M. Bartel, C. Carbonera, G. N. L. Jameson, P. [45]
- Weinberger, A. Caneschi, K. Mereiter, J. F. Letard, W. Linert, Chemistry-a European Journal 2006, 12, 2235-2243. [46] T. Huxel, S. Riedel, J. Lach, J. Klingele, Zeitschrift für
- anorganische und allgemeine Chemie 2012, 638, 925-934 M. G. B. Drew, C. J. Harding, V. McKee, G. G. Morgan, J. Nelson, Journal of the Chemical Society, Chemical Communications 1995, 1035-1038
- [48] K. L. Taft, A. Caneschi, L. E. Pence, C. D. Delfs, G. C. Papaefthymiou, S. J. Lippard, Journal of the American Chemical Society 1993, 115, 11753-11766.
- [49] D. Lee, L. Sorace, A. Caneschi, S. J. Lippard, Inorganic Chemistry **2001**, 40, 6774-6781



FULL PAPER

WILEY-VCH

- [50] H. Oshio, N. Hoshino, T. Ito, M. Nakano, Journal of the American Chemical Society 2004, 126, 8805-8812
- T. A. Hudson, K. J. Berry, B. Moubaraki, K. S. Murray, R. Robson, [51] Inorganic Chemistry 2006, 45, 3549-3556.
- [52] [53] A. Hauser, The Journal of Chemical Physics 1991, 94, 2741-2748.
- B. F. Abrahams, T. A. Hudson, R. Robson, Journal of the
- American Chemical Society 2004, 126, 8624-8625. P. Baran, R. Boča, I. Chakraborty, J. Giapintzakis, R. Herchel, Q. Huang, J. E. McGrady, R. G. Raptis, Y. Sanakis, A. Simopoulos, [54] Inorganic Chemistry 2008, 47, 645-655.
- [55] D. Belli Dell'Amico, D. Boschi, F. Calderazzo, S. Ianelli, L. Labella, F. Marchetti, G. Pelizzi, E. G. F. Quadrelli, Inorganica Chimica Acta 2000, 300-302, 882-891.
- N. Bibi, E. G. R. de Arruda, A. Domingo, A. A. Oliveira, C. Galuppo, Q. M. Phung, N. M. Orra, F. Béron, A. Paesano, Jr., K. [56] Pierloot, A. L. B. Formiga, Inorganic Chemistry 2018, 57, 14603-
- [57] J. M. Clemente-Juan, C. Mackiewicz, M. Verelst, F. Dahan, A. Bousseksou, Y. Sanakis, J.-P. Tuchagues, Inorganic Chemistry 2002, 41, 1478-1491
- I. A. Gass, C. J. Milios, A. G. Whittaker, F. P. A. Fabiani, S. Parsons, M. Murrie, S. P. Perlepes, E. K. Brechin, *Inorganic* [58] Chemistry 2006, 45, 5281-5283.
- H. Oshio, N. Hoshino, T. Ito, Journal of the American Chemical [59] Society 2000, 122, 12602-12603.
- S. C. Shoner, P. P. Power, Inorganic Chemistry 1992, 31, 1001-[60]
- [61] K. L. Taft, G. C. Papaefthymiou, S. J. Lippard, Science 1993, 259, 1302-1305
- K. L. Taft, G. C. Papaefthymiou, S. J. Lippard, *Inorganic Chemistry* **1994**, 33, 1510-1520. [62]
- [63] M. Seifried, F. M. Kapsamer, M. Reissner, J. M. Welch, G. Giester,
- D. Müller, P. Weinberger, Magnetochemistry 2022, 8, 95.
- D. D. P. W. L. F. Armarego, Butterworth-Heinemann, Oxford 1997. [65]
 - D. Müller, C. Knoll, M. Seifried, P. Weinberger, Vibrational Spectroscopy 2016, 86, 198-205.
- [66] [67]
- [68]





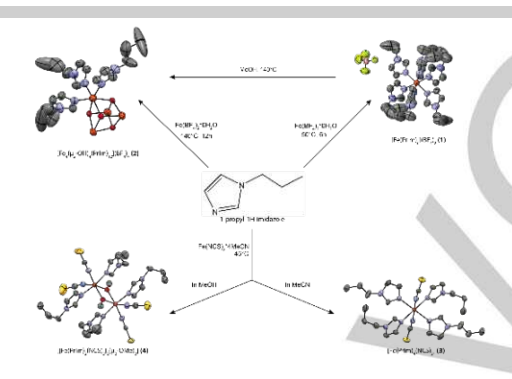
FULL PAPER

Entry for the Table of Contents

Layout 1:

FULL PAPER

With the intention of decoupling the effect of sterics and electronics in Spin-Crossover compounds, 1-propyl-1H-imidazole was used as ligand for Fe(II) complexes, for a comparison with the Fe(II) complexes of the parent ligand 1-propyl-1H-tetrazole. Its extreme versatility as ligand was unveiled, as it gave rise to a new family of Fe(II) complexes with mono-, bi-and tetranuclear members.



Willi Zeni*, Danny Müller, Marco Seifried, Jan M. Welch, Berthold Stöger, Gerald Giester, Michael Reissner, Ronald Miletich, and Peter Weinberger*

Page No. - Page No.

A new family of Fe(II) 1-propyl-1Himidazole complexes with mono-, bi-, and tetra-nuclear members





SUPPORTING INFORMATION

Table S1. Selected Bond lengths and bond angles for 1

Atom1	Atom2	Length
Fe1	N2	2.209

Atom1	Atom2	Atom3	Angle
N2	Fe1	N2	93.7
N2	Fe1	N2	180.0
N2	Fe1	N2	86.3

Table S2. Selected bond lengths and bond angles for 2

Atom1	Atom2	Length
Fe1	01	2.144(3)
Fe1	N1	2.128(5)
Fe2	01	2.154(3)
Fe2	O2	2.135(3)
Fe2	N3	2.136(5)
Fe2	N5	2.131(5)
Fe2	N7	2.155(5)
Fe2	01	2.142(3)
Fe2	01	2.154(3)
Fe2	N3	2.136(5)
Fe2	N5	2.131(5)
Fe2	N7	2.155(5)
01	Fe2	2.142(3)
Fe2	01	2.154(3)
Fe2	N3	2.136(5)
Fe2	N5	2.131(5)
Fe2	N7	2.155(5)

Ì	Atom1	Atom2	Atom3	Angle
	01	Fe1	N1	89.9(2)
	01	Fe1	01	76.9(1)
	01	Fe1	N1	97.6(2)
	01	Fe1	N1	166.5(2)
	N1	Fe1	N1	94.7(2)
	01	Fe2	02	77.1(1)
	01	Fe2	N3	106.1(2)
	01	Fe2	N5	85.5(2)
	01	Fe2	N7	164.4(2)
	01	Fe2	01	76.8(1)
	02	Fe2	N3	165.8(2)
	02	Fe2	N5	102.9(2)
	02	Fe2	N7	87.8(2)
	02	Fe2	01	77.3(1)
	N3	Fe2	N5	91.3(2)
	N3	Fe2	N7	89.4(2)
	N3	Fe2	01	89.8(2)
	N5	Fe2	N7	94.5(2)
	N5	Fe2	01	161.8(2)
	N7	Fe2	01	103.6(2)
	Fe1	01	Fe2	101.7(1)
	Fe1	01	Fe2	102.0(1)
	Fe2	01	Fe2	101.0(1)
	Fe2	02	Fe2	101.8(1)

Table S3. Selected bond lengths and bond angles for 3

Atom1	Atom2	Length
Fe1	N1	2.171
Fe1	N3	2.157
Fe1	N4	2.213

Atom1	Atom2	Atom3	Angle
N1	Fe1	N3	89.08
N1	Fe1	N4	91.67
N1	Fe1	N3	90.92
N1	Fe1	N4	88.33
N3	Fe1	N4	88.86
N3	Fe1	N4	91.14

Table S4. Selected bond lengths and bond angles for 4

Atom1	Atom2	Length
Fe1	01	1.981(3)
Fe1	02	1.994(3)
Fe1	N1	2.137(3)
Fe1	N3	2.024(4)
Fe1	N4	2.039(5)
Fe1	N5	2.120(3)
Fe2	01	2.011(3)
Fe2	02	1.980(3)
Fe2	N7	2.029(5)
Fe2	N8	2.037(4)
Fe2	N9	2.132(3)
Fe2	N11	2.138(3)
Fe3	O3	1.986(3)
Fe3	04	1.991(3)
Fe3	N13	2.129(3)
Fe3	N15	2.023(5)
Fe3	N16	2.025(5)
Fe3	N17	2.133(5)
Fe4	O3	2.015(3)
Fe4	N20	2.027(5)
Fe4	N21	2.128(3)
Fe4	N23	2.132(5)

	ingles for		
Atom1	Atom2	Atom3	Angle
01	Fe1	02	75.7(1)
01	Fe1	N1	95.1(1)
01	Fe1	N3	92.1(2)
01	Fe1	N4	169.6(2)
01	Fe1	N5	93.0(1)
02	Fe1	N1	91.5(1)
02	Fe1	N3	167.4(2)
02	Fe1	N4	94.0(2)
N1	Fe1	N3	86.5(2)
N1		N4	. ,
	Fe1		85.8(2)
N1	Fe1	N5	171.5(1)
N3	Fe1	N4	98.3(2)
N3	Fe1	N5	90.6(2)
N4	Fe1	N5	86.7(2)
01	Fe2	O2	75.3(1)
01	Fe2	N7	94.7(1)
01	Fe2	N8	168.7(2)
01	Fe2	N9	91.3(1)
01	Fe2	N11	91.0(1)
02	Fe2	N7	170.1(1)
02	Fe2	N8	93.5(2)
02	Fe2	N9	93.1(1)
02	Fe2	N11	93.6(1)
N7	Fe2	N8	96.4(2)
N7	Fe2	N9	86.8(1)
N7	Fe2	N11	
			86.7(1)
N8	Fe2	N9	91.1(2)
N8	Fe2	N11	87.9(2)
N9	Fe2	N11	173.3(1)
Fe1	01	Fe2	104.1(1)
Fe1	02	Fe2	104.8(1)
O3	Fe3	04	75.1(1)
О3	Fe3	N16	168.4(2)
O3	Fe3	N17	92.8(2)
04	Fe3	N13	92.1(1)
04	Fe3	N15	168.6(2)
04	Fe3	N16	93.3(2)
N13	Fe3	N15	87.4(2)
N13	Fe3	N16	88.2(2)
N13	Fe3	N17	172.5(2)
N15	Fe3	N16	98.1(2)
N15	Fe3	N17	87.5(2)
N16	Fe3	N17	87.1(2)
03	Fe4	04	74.7(1)
O3	Fe4	N19	92.2(2)
O3	Fe4	N20	170.1(2)
O3	Fe4	N21	94.2(1)
O3	Fe4	N23	92.9(2)
04	Fe4	N19	166.9(2)
04	Fe4	N20	95.5(2)
04	Fe4	N21	93.4(1)
N19	Fe4	N20	97.7(2)
N19	Fe4	N21	87.6(2)
N20	Fe4	N21	87.2(2)
N21	Fe4	N23	171.9(2)
Fe3	O3	Fe4	104.5(1)
	03	Fe4	
Fe3	- 04	1-64	105.6(1)



Prof. Peter Weinberger (Institute of Applied Synthetic

 $\stackrel{\underline{\omega}}{\Longrightarrow}$ ifunctional Fe(11) spin crossover-complexes based on $\overset{\cdot \cdot \cdot}{\cdots}$. .

ω-(1*H*-tetrazol-1-yl) carboxylic acids

Supramolecular cooperativity resulting in more abrupt spin state transitions is governed by a subtle interplay of ligand functionalization with carboxylic acid moieties, spacer length,





Dalton Transactions



View Article Online **PAPER**



Cite this: Dalton Trans., 2020, 49.

Received 23rd September 2020, Accepted 26th October 2020 DOI: 10.1039/d0dt03315d

rsc.li/dalton

Bifunctional Fe(II) spin crossover-complexes based on ω -(1*H*-tetrazol-1-yl) carboxylic acids†

Willi Zeni, Marco Seifried, Christian Knoll, Da Jan M. Welch, Gerald Giester, C Berthold Stöger, d Werner Artner, d Michael Reissner, Danny Müller b *a and Peter Weinberger (1) *a

To increase the supramolecular cooperativity in Fe(II) spin crossover materials based on N1-substituted tetrazoles, a series of ω -(1H-tetrazol-1-yl) carboxylic acids with chain-lengths of C₂-C₄ were synthesized. Structural characterization confirmed the formation of a strong hydrogen-bond network, responsible for enhanced cooperativity in the materials and thus largely complete spin-state transitions for the ligands with chain lenghts of C2 and C4. To complement the structural and magnetic investigation, electronic spectroscopy was used to investigate the spin-state transition. An initial attempt to utilize the bifunctional coordination ability of the ω -(1H-tetrazol-1-yl) carboxylic acids for preparation of mixed-metallic 3d-4f coordination polymers resulted in a novel one-dimensional gadolinium-oxo chain system with the ω -(1Htetrazol-1-yl) carboxylic acid acting as μ_2 - η^2 : η^1 chelating-bridging ligand.

Introduction

First row transition metals with 3d4-3d7 electron configurations allow for population of their 3d-orbitals with either a maximum, or a minimum of paired electrons. Depending on the coordinative environment around the metal centre, the energetic difference between these electron configurations (high-spin (HS) and low-spin (LS) state) may be small enough to be governed by an external stimulus such as temperature, 1,2 pressure, 1-3 light 4 or external electric field, 5-8 among others. 1 This phenomenon was first observed in the 1930s by Italian researchers, working on iron(III) N,N-dialkyldithiocarbamates and has since been known as spin crossover (SCO), or spin state transition.9-11

The intrinsic correlation between the bistability of SCO materials and several of their physical properties makes them appealing candidates for novel miniaturized sensors, 12,13 memory/storage devices, 14 and a key technology in spintronics. 15 Today, SCO materials are primarily investigated by an academic bottom-up approach, resulting in highly specialized materials for devices on a nanoscale. Molecular actuators, 16 their utilization in quenching and affecting luminescence and fluorescence, 17,18 their sensing capacity in form of porous switchable materials, 12,19 or their combination with chirality^{20–22} have recently been reported.

Since the occurrence of SCO under ambient conditions is very sensitive to the ligand field, it is strongly affected by the nature of the ligand system, the presence or absence of solvates²³ and counter anions applied.²⁴ (Substituted) azole ligands, including N1-substituted tetrazoles, are a promising platform for systematic development of SCO-materials.¹

Homoleptic hexa-coordinated Fe(II)-complexes based on N1substituted tetrazoles are often spin switchable, as coordination of Fe(II) by tetrazoles results in an appropriate ligand field strength. In this case, Fe(II) switches between a paramagnetic HS state with S = 2 and a diamagnetic LS state with S = 0.

In previous work, we have emphasized fine-tuning of the ligands' geometry and flexibility, shaping cooperativity and transition temperature on a molecular scale, 25,26 as well as post functionalization of the ligand backbone.²⁷ Therefore, in this work, a carboxylic acid moiety has been introduced to the ligand system, allowing for the investigation of the SCO in [Fe (ω -(1*H*-tetrazol-1-yl) carboxylic acid)₆]²⁺-cations. Alkylcarboxylic acid substituted tetrazoles provide three useful features: On a molecular level the COOH-group should establish a network of hydrogen bonds, increasing cooperativity and governing the

peter.e163.weinberger@tuwien.ac.at

[†] Electronic supplementary information (ESI) available. CCDC 2024140 (4, HS), 2024142 (4, LS), 2024146 (6, HS), 2024147 (6, LS), 2024143 (7, HS), 2024141 (7, LS), 2024144 (9, HS), 2024145 (9, LS) and 2024832 (10). For ESI and crystallographic data in CIF or other electronic format see DOI: 10.1039/d0dt03315d



^aInstitute of Applied Synthetic Chemistry, TU Wien, Getreidemarkt 9/163-AC, 1060 Vienna, Austria. E-mail: danny.mueller@tuwien.ac.at,

^bCenter for Labelling and Isotope Production, TRIGA Center Atominstitut, TU Wien, Stadionallee 2, 1020 Vienna, Austria

^cDepartment of Mineralogy and Crystallography, University of Vienna, Althanstraße 14 (UZA 2), 1090 Vienna, Austria

^dX-Ray Center, TU Wien, Getreidemarkt 9, 1060 Vienna, Austria

^eInstitute of Solid State Physics, TU Wien, Wiedner Hauptstraße 8-10/138, 1040 Vienna, Austria

abruptness of the spin state transition, 28-30 the COOH-group may act as an additional ligand allowing for the formation of multi-metallic networks with a second transition metal, or rare-earth element and, finally, the COOH termination of the ligand may allow for deposition on oxide surfaces.

In this contribution, we report the ω -(1*H*-tetrazol-1-yl) carboxylic acids with C2-C4 alkyl chains and the magnetic, structural and spectroscopic characterization of their Fe(II)-SCO complexes, as well as an initial attempt to prepare a multimetallic 3d-4f coordination polymer.

Results and discussion

Synthesis

The spin crossover behaviour of Fe(II)-N1-alkyl-substituted tetrazole complexes has been shown to be governed by the length of the N1-alkyl substituent and the choice of weakly coordinating anion.^{24,31} Therefore, in the current study, the length of the alkyl-skeleton was varied from C2-C4 (see Scheme 1) and BF₄ and ClO₄ were used as weakly coordinating tetrahedral anions of comparable volume (BF₄ 49 Å³; ClO₄ 54 Å³).

The ligands 2-4COOHTz (1-3) were prepared from the corresponding amino-acids based on the Franke-tetrazole synthesis, 32 in analogy to the reported synthesis of (1H-tetrazol-1yl)-2-acetic acid (2).33-35 Treatment of the resulting N1-alkylsubstituted tetrazoles with FeX2·6H2O (X = BF4-, ClO4-) in acetonitrile (MeCN) followed by subsequent washing with THF results in the desired complexes. ¹H NMR analysis of the bulk samples of all prepared complexes shows that only [Fe $(2COOHTz)_6$ ²⁺ incorporated solvent molecules, for both X = BF₄⁻and ClO₄⁻ amounting to 2 MeCN per Fe²⁺ center.

Magnetic properties

The dependence of molar magnetic susceptibility on temperature (10 to 300 K) was investigated for all six Fe(II)-complexes (Fig. 1a). The resulting $\chi_{\rm mol}T$ curves show three distinct tendencies: partial, incomplete spin crossover (5), complete spin crossover (4, 6, 7 and 9) and no spin crossover (8). All changes in $\chi_{\text{mol}}T$ below 50 K may be attributed to zero-field splitting, expected for residual HS $Fe(\pi)$.

 $\chi_{\text{mol}}T$ decreases for 5 gradually below 170 K from 3.51 cm³ K mol⁻¹ at 300 K to 2.86 cm³ K mol⁻¹ at 50 K. This seems to correspond to ~25% of Fe(II) sites in a LS state. [Fe $(2COOHTz)_6$ $(BF_4)_2 \cdot 2$ MeCN (4) shows the highest $T_{1/2}$ of the series with 227 K and decreases to a full LS-state below 180 K.

Scheme 1 ω-(1H-Tetrazol-1-yl) carboxylic acids used in this study, the number before the name displaying the chain-length.

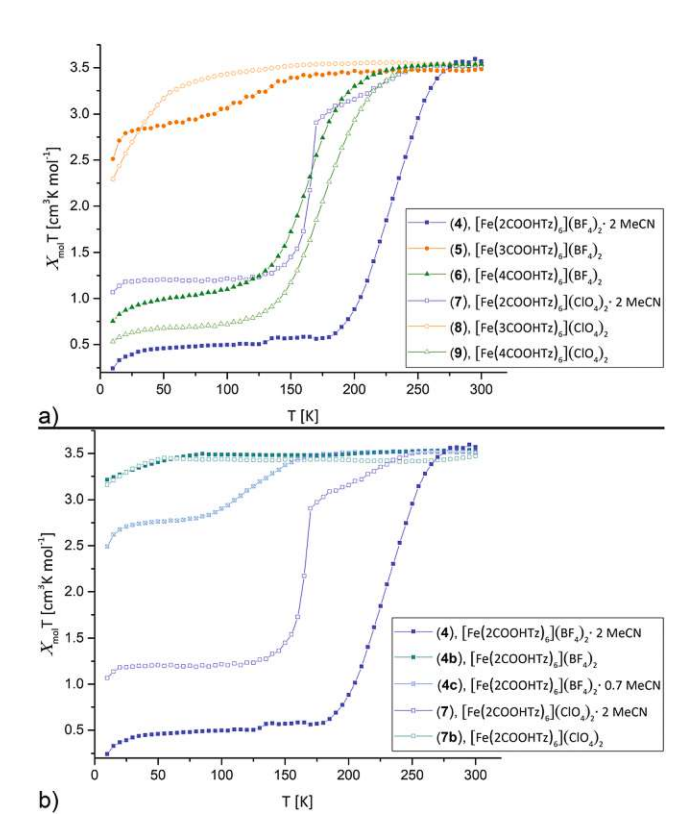


Fig. 1 Thermal variation of the molar magnetic susceptibility $\chi_{mol}T$ for $[Fe(nCOOHTz)_6]X_2$, n = 2-4, $X = BF_4^-$, ClO_4^- in the solid state between 10 K-300 K. Cooling and heating curves were found identical for all materials, so only the cooling data are displayed. (a) Overview on all materials. (b) Comparison for the solvated, partially solvated and desolvated samples of 4 and 7.

 $[Fe(4COOHTz)_6](BF_4)_2$ (6) has a $T_{1/2}$ of 163 K, the spin-state transition taking place gradually from below 235 K to a final $\chi_{\rm mol}T$ of 0.98 cm³ K mol⁻¹ at 50 K. This corresponds to ~72% of LS-state.

Within the ClO_4^- compounds, $[Fe(2COOHTz)_6](ClO_4)_2 \cdot 2$ MeCN (7) reveals a two-step transition, featuring a kink at 170 K. Below 245 K $\chi_{\text{mol}}T$ of 7 decreases gradually to 2.9 cm³ K mol⁻¹ at 170 K, pointing to a first HS-LS transition of ~18% of the Fe(II) sites. A sharp decrease of $\chi_{mol}T$ to a constant value of 1.2 cm³ K mol⁻¹ below 115 K is attributed to further 50% of the Fe(II) sites undergoing the HS-LS transition. [Fe(3COOHTz)₆] (ClO₄)₂ (8) remains all HS-state. [Fe(4COOHTz)₆](ClO₄)₂ (9) shows by far the completest HS-LS transition with a $T_{1/2}$ of 175 K and a final $\chi_{\text{mol}}T$ of 0.66 cm³ K mol⁻¹ at 50 K, corresponding to only ~18% of Fe(π)-centres remaining in the HS state.

The spin state transition in the BF₄ and ClO₄ complexes of 2COOHTz, both incorporating two molecules acetonitrile, are overly sensitive towards loss of the solvate. 4 partially loses the solvate already during drying in vacuum during the synthesis, or on shelf storage. This resulted in an intermediate with 0.7 MeCN molecules incorporated (4c, determined by ¹H NMR) and on subsequent drying in vacuum in a non-solvate (4b), shown in Fig. 1b. For 0.7 MeCN molecules incorporated in 4c the spin state transition is shifted to lower temperatures

with $T_{1/2}$ at 132 K and a final $\chi_{\text{mol}}T$ of 2.75 cm³ K mol⁻¹, corresponding to a ~25% LS-state. The completely desolvated compound 4b is spin crossover inactive, remaining in the HS-state for all temperatures. Similarly, the desolvated ClO₄-complex 7b shows no spin crossover anymore (Fig. 1b). This demonstrates, how crucial the incorporated solvate molecules are in this case additional to the H-bonding network.

All in all, the differing picture obtained from this comparison of the SCO-behaviour is not only caused by the weak-coordinating anion (as obvious by comparing 4 vs. 7, or 6 vs. 9), but rather attributed to a combination of different effects. Additional to the impact of the anion, as discussed in the case 2COOHTz the 2 MeCN solvate makes the game. Furthermore, there is the variation in the length of the alkylspacer, which for 4COOHTz seems to be a good fit between establishing cooperativity and preventing too much motional freedom in form of a shock-absorber effect, 24,31 which was evidenced in the past for increasing chain-lengths. Missing the structural characterization of the 3COOHTz-compounds, the differing SCO-behaviour is probably related to the odd number of C-atoms, which already for unsubstituted alkyl-tetrazoles were found challenging in the past. 24,31

Crystallographic analysis

Dalton Transactions

Single crystals suitable for determination of the molecular structure could be grown for 4, 6, 7 and 9 by vapour-diffusion of diethyl ether (Et2O) into a concentrated MeCN-solution of the corresponding compounds. No suitable crystals of 5 and 8 could be obtained by similar means. Single crystal diffraction data were collected at 100 and 200 K for 4, 6, 7 and 9 in order to determine both low- and high-spin molecular structures. In addition variable temperature P-XRD patterns were acquired for 4 and 7 from 100-300 K.

[Fe(2COOHTz)₆](BF₄)₂·2 MeCN (4). 4 crystallizes as MeCN solvate in the trigonal R3 space group and this symmetry is retained both at 100 K (low-spin, see Fig. 2) and 200 K (highspin). The iron-centre is octahedrally surrounded by six 2COOHTz-ligands coordinating via the exo N4-nitrogen. The Fe-N bond lengths for all six ligands are equal (1.987 Å), typical for a Fe(II) LS-state. At 200 K the distance increases \sim 9% to 2.176 Å, characteristic for the Fe(II) HS-state (see Table S1†). The packing in the crystal is governed - as predicted for a COOH-group - by an H-bond network composed of infinite C(5) type chains between the COOH-groups. Viewed along the b axis, the $[Fe(2COOHTz)_6]^{2+}$ -cations stack in layers, with three of the ligands pointing upwards and three downwards (see Fig. 2) to the adjacent layer. This arrangement is further stabilised by the above-mentioned H-bonds (see Fig. 3). The Fe-atoms are located on the Wyckoff-position 3a, alternating with an acetonitrile, an apex-up and an apex-down BF₄ group. The BF₄ groups interact strongly with the [Fe(2COOHTz)₆]²⁺-cations through C-H···F-bonds with both the tetrazolic CH and CH2-group (see Fig. 4) in both the highand low-spin states.

[Fe(2COOHTz)6](ClO4)2·2 MeCN (7). 7 crystallizes isotypically to 4 with slightly larger cell parameters (see Table 1) as

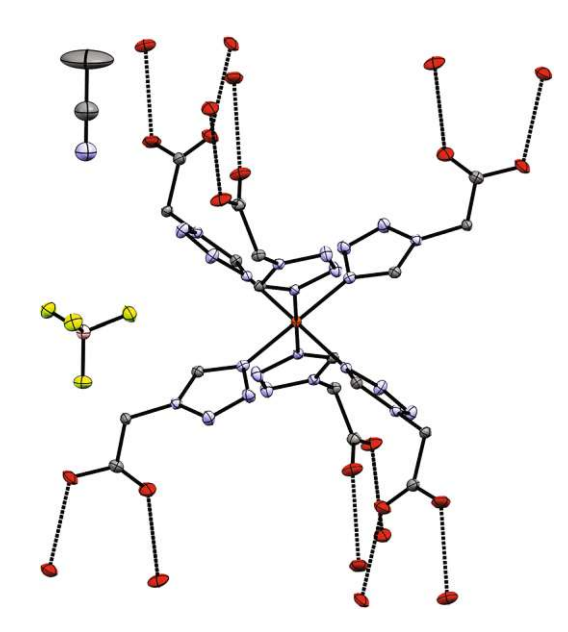


Fig. 2 Molecular structure of 4 at 100 K in the LS-state showing H-bond contacts at the carboxylic acid groups; H-atoms omitted for clarity.

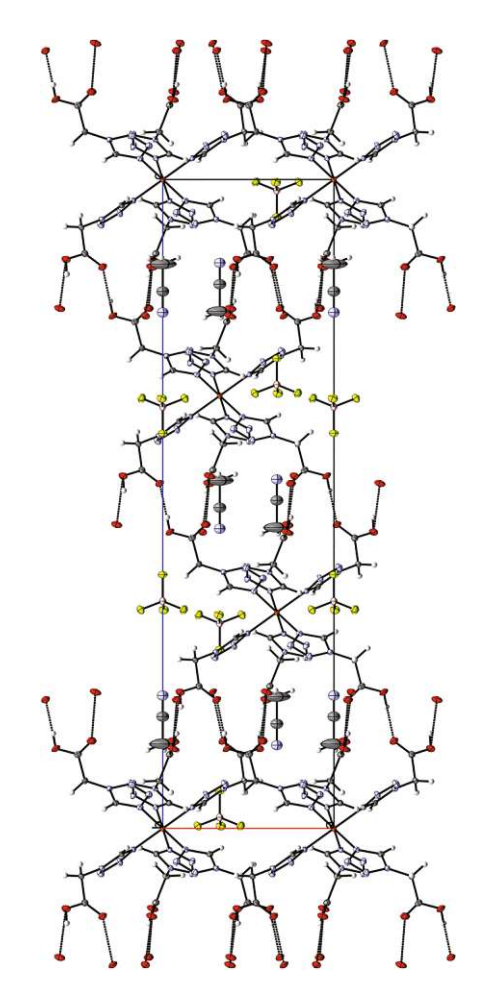


Fig. 3 H-Bonding network in 4 at 100 K, seen along the b-axis.



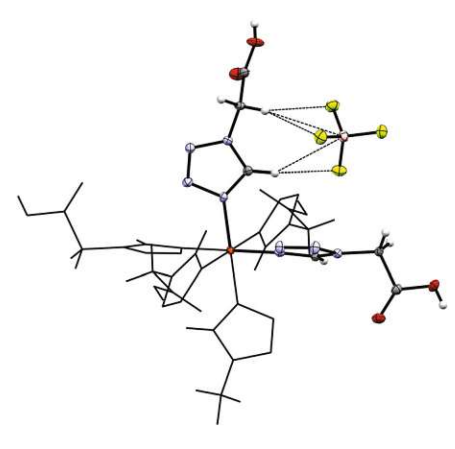


Fig. 4 H...F bonds between the tetrazolic CH and the CH₂-groups in 4 at 100 K.

an MeCN solvate in the trigonal R3 space group. In 7 the Fe-N distances (2.004 Å, 100 K, LS-state; 2.184 Å, 200 K, HS-state, see Table S2†) are slightly longer than in 4, but still compar able and characteristic for Fe(II) in the corresponding spinstate. Also, in 7 both at 100 K and 200 K the ClO₄-anion is not disordered and stabilized through interaction with the [Fe $(2COOHTz)_6$ ²⁺-cation (see Fig. 5).

Variable temperature P-XRD of bulk (4) and (7). Magnetic measurements of bulk 4 and 7 show an incomplete spin transition, whereas the Fe-N bond distances obtained from the single crystal data suggest a largely complete transition. Therefore, variable temperature P-XRD was used to follow any structural changes of the bulk material during the SCO (see Fig. 6). For both compounds, the calculated diffractograms obtained from the HS and LS molecular structures are in reasonable agreement with the powder-patterns of the bulk material. For both 4 (Fig. 6a) and 7 (Fig. 6b) the temperature dependent PXRD measurements show more pronounced changes in the powder pattern (dotted lines as a guide) than to those just expectable from thermal contraction. On this basis it seems clear that both bulk and single crystalline samples are the same compound.

[Fe(4COOHTz)₆](BF₄)₂·Et₂O (6). 6 crystallizes as an Et₂O solvate, as a result of vapour-diffusion crystallization, in the triclinic P1 space group. The structure was determined at 100 K (LS-state) and 200 K (HS-state). The asymmetric unit (see Fig. 7) includes the Fe-centre with three 4COOHTz ligands, one crystallographic independent BF₄-anion, as well as half of the Et₂O-solvate. The Fe-N distances of the three coordinated ligands are slightly different (1.961 Å (N4), 1.979 Å (N4a) and 1.989 Å (N4b), see Table S3†). In the HS-state at 200 K the Fe-N distances increase to 2.185 Å (N4), 2.182 Å (N4a) and 2.185 Å (N4b). As for 4 and 7, the supramolecular structure is governed by an H-bond network with the COOHgroups forming a three-dimensional network of R_2^2 (8) type ring motifs joining layers of [Fe(4COOHTz)₆]²⁺-cations (see Fig. 8). The voids between the ligand alkyl-chains are occupied by Et₂O, which also interacts with the COOH-groups via a

single H-bond. Comparing the supramolecular arrangement of 4/7 to 6 it becomes evident, that in this case only due to the longer alkyl-chains Et₂O could be incorporated as solvate molecule. In the former case the voids between the cationic Fe-layers would not have been large enough to fit the Et2Omolecules. Whereas at 100 K the BF₄-anions are stabilized by the H···F bonds similar to 4 preventing a potential disorder, at 200 K in the HS-state those interactions are no longer strong enough, resulting in an apex up-down disorder of the BF₄-

Structure of [Fe(4COOHTz)₆](ClO₄)₂·Et₂O (9). 9 crystallizes as Et₂O solvate like 6 in the triclinic P1 space group but has two crystallographic independent Fe-centres and two ClO₄⁻-anions in the asymmetric unit. Both Fe1 and Fe2 are surrounded by each three independent 4COOHTz-ligands, which do not interact with each other via H-bonds. The solvate molecule is located in the cavity formed by the ligands, stabilized by an H-bond (see Fig. 9). At 100 K, all Fe-N bond lengths (1.984 Å Fe1-N4, 1.987 Å Fe1-N4a, 1.982 Å Fe1-N4b, 1.987 Å Fe2N4c, 1.987 Å Fe2-N4d, 1.984 Å Fe2-N4e) are characteristic for Fe(II) in its low-spin state. In contrast, at 200 K the bonds extend to typical HS distances (2.181 Å Fe1-N4, 2.178 Å Fe1-N4a, 2.173 Å Fe1-N4b, 2.174 Å Fe2N4c, 2.185 Å Fe2-N4d, 2.178 Å Fe2-N4e, see Table S4†). In 9 the [Fe(4COOHTz)₆]²⁺-cations form layers connected through the H-bond network to each other and the ClO₄⁻-anions.

The relevant crystallographic parameters for all Fe-containing structures are given in Table 1.

Spectroscopic characterization

MIR and FIR spectroscopy. For homoleptic Fe(II)-tetrazolecomplexes IR-spectroscopy allows for confirmation of successful SCO-complex formation, as well as gaining insight into the spin state present, since the tetrazolic CH-vibration is sensitive to the N4 coordination environment.36 In Fig. 10, the IR spectra of 2COOHTz (1) and its ClO₄-complex (7) in the HSstate (red) and LS-state (blue) are compared. At 3156 cm⁻¹ the free ligand shows its tetrazolic CH-vibration, which upon successful coordination is split and shifted to 3159 cm⁻¹ and 3152 cm⁻¹. On cooling to the LS-state, at 100 K the CHvibration is shifted to 3164 cm⁻¹ and 3159 cm⁻¹, respectively. Around 1600 cm⁻¹ the $\nu_{\rm N2=N3}$ stretching vibration of the tetrazole after coordination is similarly affected by the spin-state transition, shifting from 1612 cm⁻¹ to 1616 cm⁻¹ in the LSstate. The change of the carbonyl-vibration at 1731 cm⁻¹ on coordination and afterwards during SCO may be attributed to interaction within the H-bond network, transferring the volume work of the spin-state transition. The broad absorption around 1030 cm⁻¹ corresponds to the B-F stretching vibrations of the BF₄-anion. The CN-absorption of the MeCN solvate in 7 is very weak, and is only observable in the LS-spectrum of 7 in Fig. 10 around 2250 cm^{-1} .

In the FIR-region of the spectra, both spin-states show the characteristic displacement of the Fe-centre towards the centroid of the trigonal faces of the N6-coordination octahedron.



Dalton Transactions Paper

Table 1 Crystallographic parameters for the crystal structures of 4, 6, 7 and 9

	4·MeCN, HS	4·MeCN, LS	7·MeCN, HS	7·MeCN, LS
Formula	$C_{22}H_{30}B_2F_8FeN_{26}O_{12}$	$C_{22}H_{30}B_2F_8FeN_{26}O_{12}$	$C_{22}H_{30}Cl_2FeN_{26}O_{20}$	C ₂₂ H ₃₀ Cl ₂ FeN ₂₆ O ₂₀
Weight [g mol ⁻¹]	1080.19	1080.19	1105.47	1105.47
T[K]	200	100	200	100
Colour	White	Pink	White	Pink
Shape	Platelet	Platelet	Platelet	Platelet
Crystal system	Trigonal	Trigonal	Trigonal	Trigonal
2 2	R3	R3	R3	R3
Space group				
a [Å] b [Å]	10.6588(7)	10.4735(5)	10.747(3)	10.587(2)
	10.6588(7)	10.4735(5)	10.747(3)	10.587(2)
c [Å]	34.838(3)	34.480(2)	34.689(9)	34.314(7)
<i>α</i> [°]	90	90	90	90
β [\circ]	90	90	90	90
γ [ο]	120	120	120	120
$V[\mathring{A}^3]$	3427.7(5)	3275.6(4)	3470(2)	3330.8(14)
Z	3	3	3	3
$\rho_{\rm calc.} [{\rm g \ cm}^{-3}]$	1.570	1.643	1.587	1.653
$\mu \left[\text{mm}^{-1} \right]$	0.445	0.466	0.543	0.565
Measured refl's.	22 250	21 166	27 060	26 274
Indep't refl's	1573	1495	1935	1859
Refl's $I \ge 2\sigma(I)$	1421	1374	1389	1444
$R_{\text{int}} \le 20(1)$	0.0308	0.0309	0.0952	0.0798
GooF	1.068	1.072	1.071	1.115
wR_2	0.0804	0.0673	0.1449	0.1329
R_1	0.0318	0.0271	0.0569	0.0550
CCDC†	2024140	2024142	2024146	2024147
	6 ⋅Et ₂ O, HS	6·Et₂O, LS	$9 \cdot \text{Et}_2\text{O}$, HS	9·Et ₂ O, LS
Formula	$C_{34}H_{58}B_2F_8FeN_{24}O_{13}$	$C_{34}H_{58}B_2F_8FeN_{24}O_{13}$	$C_{34}H_{58}Cl_2FeN_{24}O_{21}$	C ₃₄ H ₅₈ Cl ₂ FeN ₂₄ O ₂₁
Weight [g mol ⁻¹]	1240.45	1240.45	1265.79	1265.79
T[K]	200	100	200	100
Colour	White	Pink	White	Pink
Shape	Platelet	Platelet	Platelet	Platelet
Crystal system	Triclinic	Triclinic	Triclinic	Triclinic
2 2	PĪ	PĪ	PĪ	PĪ
Space group				
a [Å]	10.630(3)	10.530(3)	10.6262(13)	10.6120(12)
$b \begin{bmatrix} \mathring{\mathbf{A}} \end{bmatrix}$	10.971(3)	10.576(3)	11.0192(13)	10.6186(12)
c [Å]	14.235(4)	13.836(4)	27.044(3)	26.596(3)
<i>α</i> [°]	74.796(6)	75.400(8)	96.080(4)	95.237(3)
β \circ	71.624(6)	73.122(7)	93.160(4)	95.276(3)
γ [°]	63.563(6)	64.974(7)	116.571(3)	114.758(3)
$V[\mathring{\mathbf{A}}^3]$	1396.1(6)	1321.2(7)	2797.5(6)	2681.9(5)
z	1	1	2	2
$\rho_{\rm calc.} [{\rm g \ cm}^{-3}]$	1.512	1.665	1.503	1.567
$\mu [\text{mm}^{-1}]$	0.377	0.396	0.459	0.479
Measured refl's.	32 025	28 095	61 136	53 754
Indep't refl's	6916	6513	13 866	13 356
Refl's $I \ge 2\sigma(I)$	2942	2733	6407	6404
- ()	0.1497		0.0757	0.0644
R _{int}		0.2107		
GooF	1.014	1.002	1.051	1.010
wR_2	0.3257	0.1728	0.2197	0.1016
R_1	0.1327	0.0910	0.0874	0.0596
CCDC†	2024143	2024141	2024144	2024145

Those vibrations are nearly entirely decoupled from other vibrational modes and therefore indicative of spin state. For the HS-state, this vibration is found at 226 cm⁻¹, for the LSstate the characteristic vibrations are located at 470 and 443 cm⁻¹ (see Fig. 11).

UV-VIS/NIR spectroscopy. Electronic transitions are also affected by the spin state transition. For homoleptic Fe-tetrazole SCO complexes the HS-state absorbs around 850 nm in the near-infrared, causing a broad and often weak absorption in the ligand field spectrum. This ${}^5T_2 \rightarrow {}^5E$ transition weakens with cooling and spin-state transition, giving rise to two

absorptions in the visible region of the spectrum at 545 nm and 386 nm, responsible for the pink colour of the LS-state. These absorption bands correspond to the ${}^{1}A_{1} \rightarrow {}^{1}T_{1}$ transition, as well as the ${}^{1}A_{1} \rightarrow {}^{1}T_{2}$ transition. From the maxima observed in the HS and the LS state, a ligand-field strength 10 Dq can be estimated.³⁷ In the case of 7, measured in the solid state, a value of 1.65 Dq is obtained (Fig. 12).

Towards a mixed-metallic 3d-4f coordination polymer

The functionalization of alkyl-tetrazoles with a COOH-group introduces an H-bond donor-acceptor system thereby enhan-

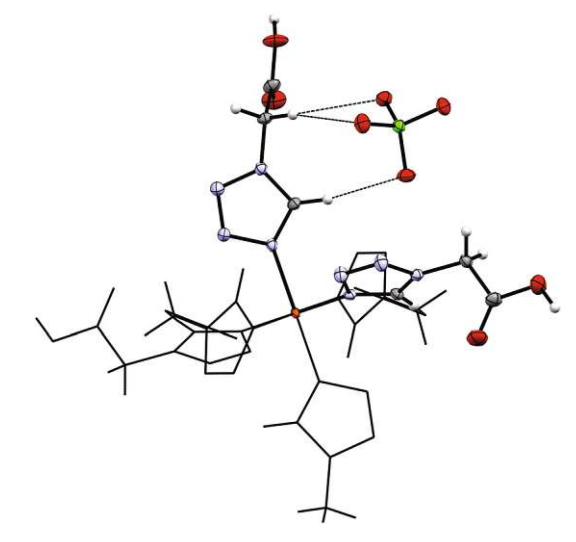


Fig. 5 Hydrogen-bonds between the tetrazolic CH and the ClO₄-anion, as well as short interactions with the CH2-group in 7 at 100 K.

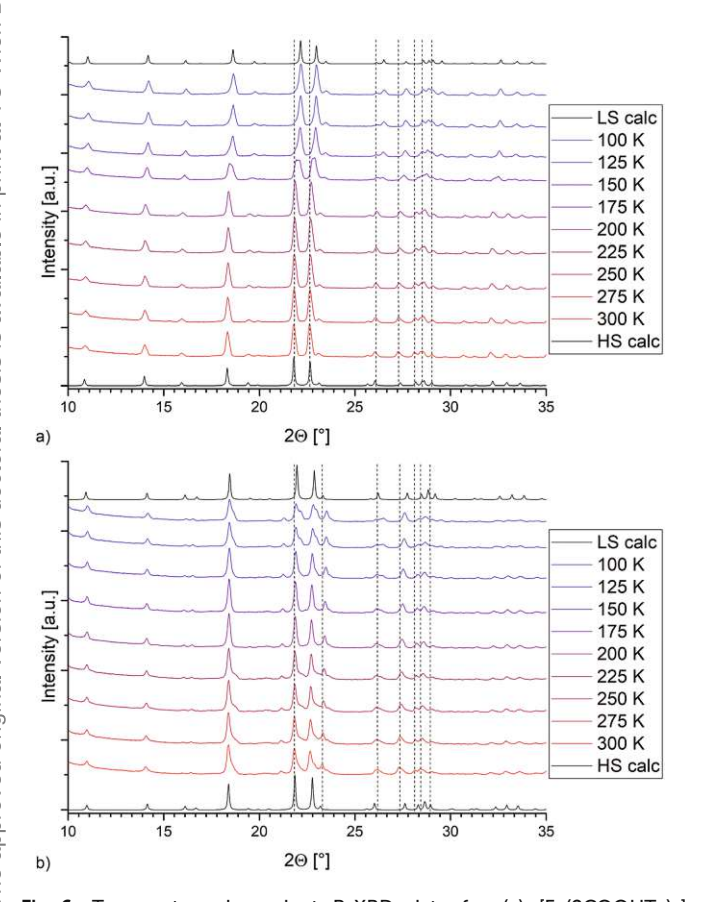


Fig. 6 Temperature-dependent P-XRD data for (a) [Fe(2COOHTz)₆] $(BF_4)_2 \cdot 2MeCN$ (4) and (b) $[Fe(2COOHTz)_6](ClO_4)_2 \cdot 2MeCN$ (7).

cing supramolecular cooperativity of SCO. To take advantage of the coordination ability of the COOH-group and the bifunctional ligand, we attempted to prepare a multi-metallic 3d-4f coordination polymer. Coronado et al. have success-

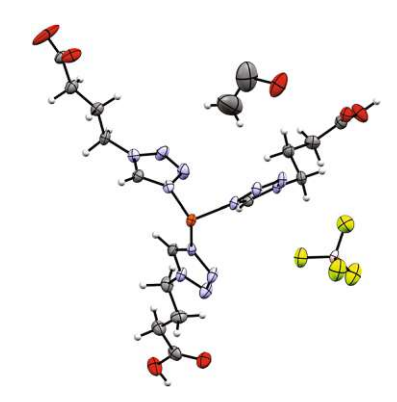


Fig. 7 Asymmetric unit of [Fe(4COOHTz)₆](BF₄)₂·Et₂O (6) at 100 K.

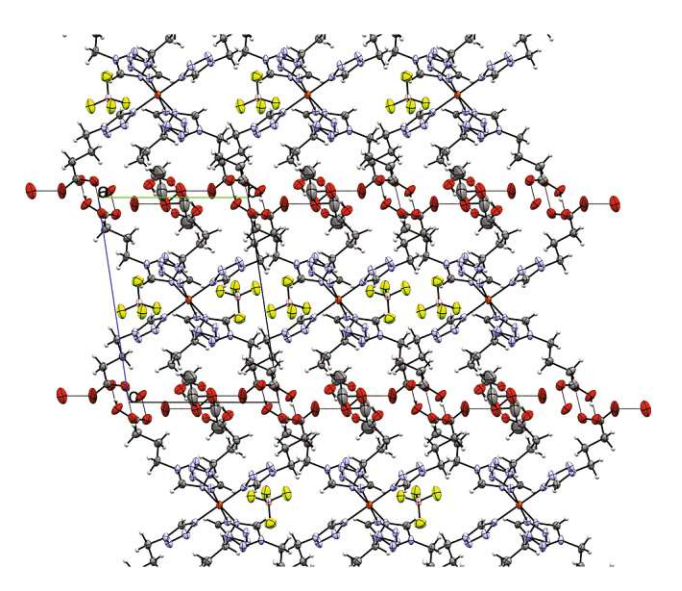
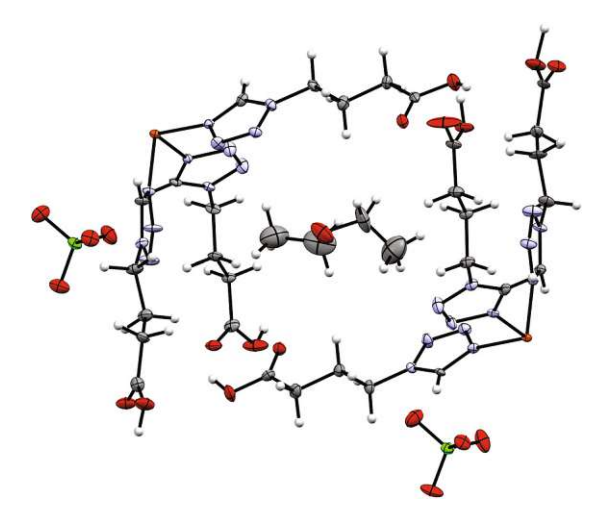


Fig. 8 Supramolecular H-bonding network in 6 at 100 K, seen along the a-axis

fully applied such an approach to the formation of a mixed Fe(III)-Fe(II) SCO compound using a COOH-functionalized ligand.38

By reacting 3COOHTz (2) with Fe(ClO₄)₂·6H₂O and GdCl₃·6H₂O in aqueous MeOH and subsequent evaporation a slightly yellow oil was obtained, which did not be solidify. After a few weeks at 4 °C a few colourless crystals had formed, allowing for determination of the structure by X-ray diffraction. Instead of a mixed-metallic coordination polymer, [Gd $(3COOTz)_2(H_2O)_3$ Cl (10) had crystallized in the monoclinic C2/ c space group. During the reaction/crystallization process the COOH-groups were deprotonated and the resulting carboxylate groups act as chelating, bridging ligands to the gadoliniumatoms in a μ_2 - η^2 : η^1 fashion (see Fig. 13). Each gadolinium atom is coordinated nine-fold by oxygen-donors as the centre of a monocapped square antiprismatic coordination polyhedron. Due to the μ_2 - η^2 : η^1 coordination of the carboxylateligands one-dimensional chains are formed, in which the Gd-atom is coordinated by four 3COOTz-ligands: two of them



Dalton Transactions

Asymmetric unit of [Fe(4COOHTz)₆](ClO₄)₂·Et₂O (9) at 100 K.

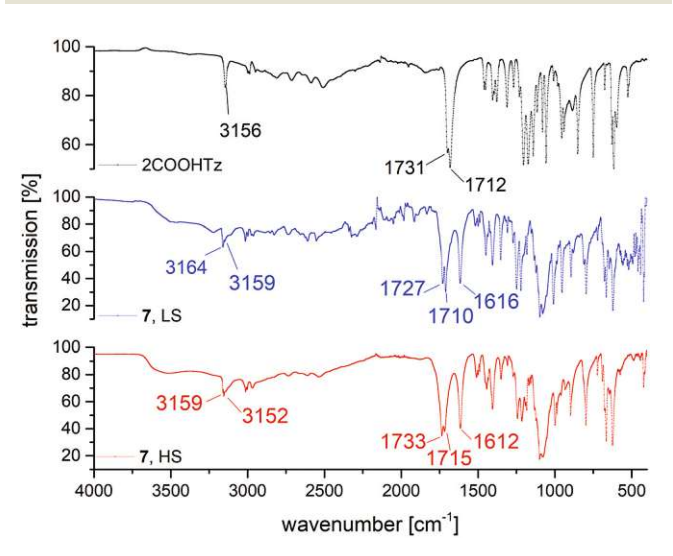


Fig. 10 Comparison of MIR spectra for 2COOHTz (1), [Fe(2COOHTz)₆] (ClO₄)₂·2 MeCN (7) in the HS-state (red) and LS-state (blue).

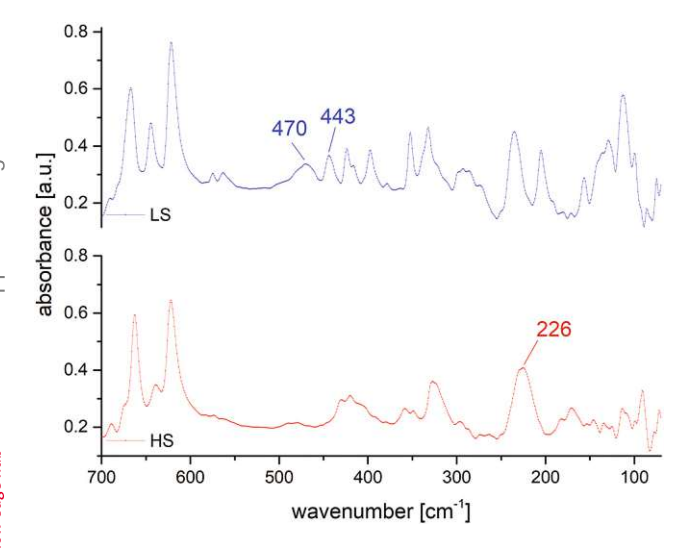
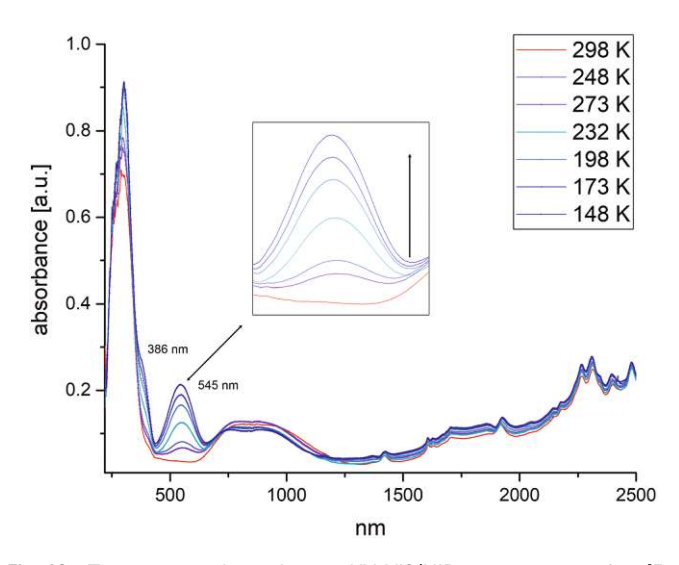


Fig. 11 Comparison of FIR spectra for [Fe(2COOHTz)₆](ClO₄)₂·2MeCN (7) in the HS-state (red) and LS-state (blue).



UV-VIS/NIR Fig. 12 Temperature-dependent spectra [Fe (2COOHTz)₆](ClO₄)₂·2MeCN (7). Inset: Increase of the corresponding to the ${}^{1}\!A_{1} \rightarrow {}^{1}\!T_{1}$ transition on cooling and increasing number of LS Fe-centres.

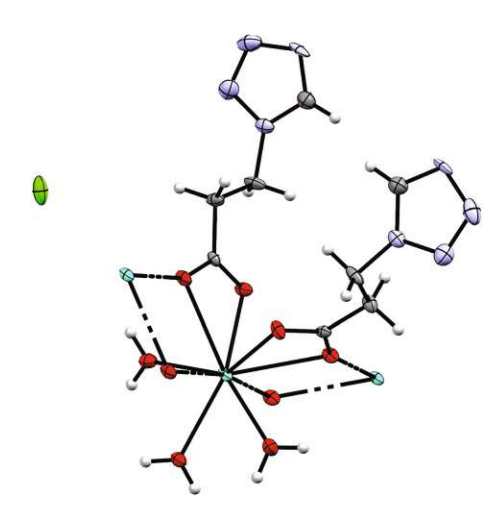


Fig. 13 μ_2 - η^2 : η^1 coordination pattern of the carboxylate-ligands in [Gd (3COOTz)2(H2O)3]Cl (10).

coordinate as bidentate, and one 3COOTz-ligand of each adjacent Gd-centre on both sides coordinates in an η^1 -fashion (see Fig. 14). H₂O molecules occupy the remaining coordination sites (3). The η^1 -interaction of the carboxylate-ligands with the adjacent Gd-atoms is remarkable, as the Gd-O-bond is the shortest of all three: the η^1 Gd-O interaction is 2.350 Å (Gd-O1), whereas the η^2 Gd–O bonds are with 2.432 Å (Gd–O2) and 2.685 Å (Gd-O1) 3.48% and 14.3% longer. The tetrazoles establish channels parallel to the gadolinium-oxo chains. Their tetrazolic CH groups are directed to the inner of the voids, the N2 and N3 atoms of the ring interacting with the H2O ligands of the nearby gadolinium-oxo chain. In the voids the Cl⁻-anions are stabilized by a zig-zag H-bond structure, originating from the H₂O-ligands at the Gd-centre (see Fig. 15). The crystallographic parameters for 10 are given in Table 2.

print at TU Wien Bibliothek

.⊑

Paper

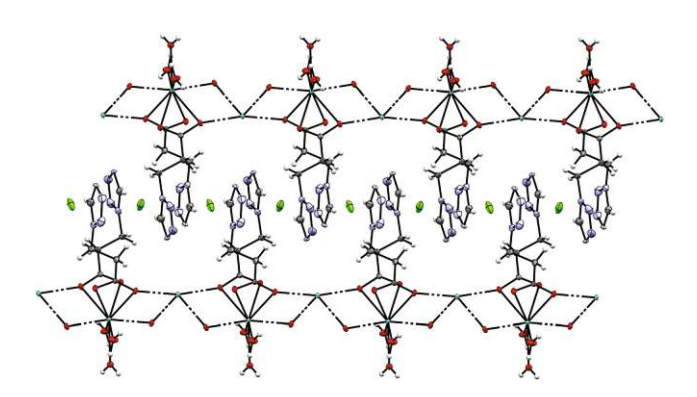


Fig. 14 One-dimensional chains in [Gd(3COOTz)₂(H₂O)₃]Cl (10) with Cl⁻-atoms parallel to the c-axis, seen along the a-axis.

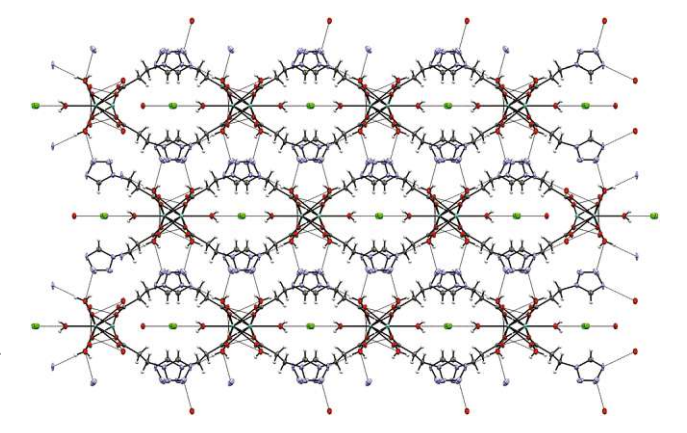


Fig. 15 Cl - Atoms located in the voids formed by the tetrazole rings stabilized by H-bonds to the H₂O ligands in the molecular structure of 10, view along c-axis.

10

Table 2 Crystallographic parameters for 10

	10
Formula	C ₈ H ₁₆ ClGdN ₈ O
Weight [g mol ⁻¹]	528.96
T[K]	100
Colour	Clear colourles
Shape	Plate
Crystal system	Monoclinic
Space group	C2/c
a [Å]	18.0057(4)
b [Å]	11.2323(6)
c [Å]	8.0169(9)
α [°]	90
β [\circ]	91.838(3)
γ [ο]	90
$V[A^3]$	1620.5(2)
z	4
$r_{\rm calc.} [\rm g \ cm^{-3}]$	2.1674
$m [\mathrm{mm}^{-1}]$	4.311
Measured refl's	9983
Indep't refl's	2927
Refl's $I \ge 2s(I)$	2505
$R_{ m int}$	0.0618
GooF	1.67
wR_2	0.0367
R_1	0.0331
CCDC†	2024832

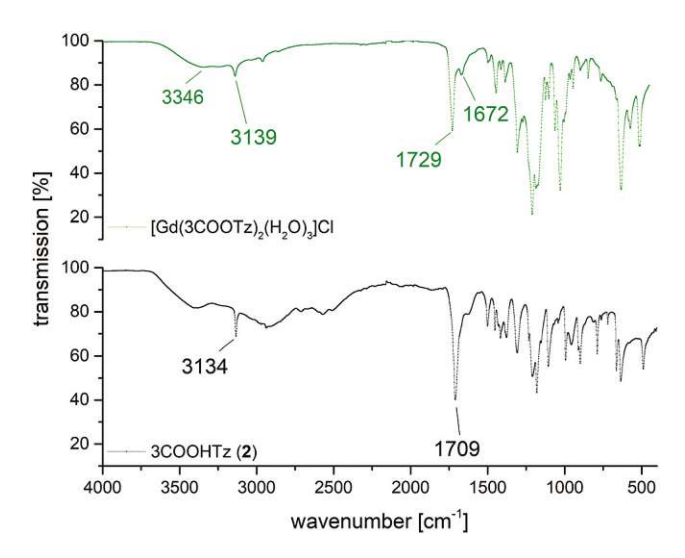


Fig. 16 Comparison of MIR spectra of 3COOHTz (2) and [Gd (3COOTz)2(H2O)3]Cl (10).

Fig. 16 shows a comparison between the MIR spectrum of 2 and a single crystal of [Gd(3COOTz)₂(H₂O)₃]Cl. Whereas the tetrazolic CH-band is only slightly shifted after the coordination to the Gd3+, the deprotonated and coordinated carbonyl-vibration is shifted by 20 cm⁻¹. The three coordinated H₂O-ligands appear in the MIR, resulting the OH-stretching mode at 3346 cm⁻¹ and the OH-scissoring vibration at 1672 cm⁻¹.

Experimental

Materials and methods

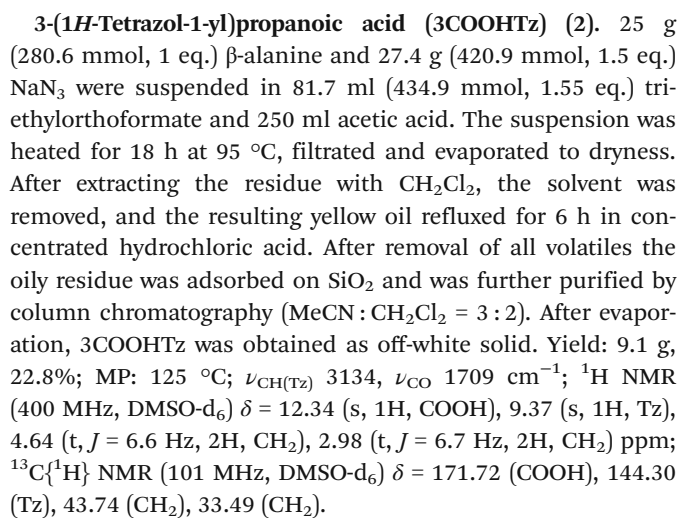
All operations involving Fe(II) were carried out under inert gas atmosphere (argon 5.0). The glassware used was oven dried at 120 °C before use for at least 2 hours. All solvents for the complexation reactions were dried before use and stored over molecular sieve 3 Å under argon.³⁹ Unless otherwise stated, all starting materials were commercially obtained and used without further purification. All NMR spectra were recorded in dry deuterated solvents on a Bruker Avance UltraShield 400 MHz. Chemical shifts are reported in ppm; ¹H and ¹³C shifts are referenced against the residual solvent resonance. For the measurement of MIR and FIR spectra, a PerkinElmer Spectrum 400, fitted with a coolable/heatable PIKE Gladi ATR unit was used within the range of 4000-100 cm⁻¹. Solid state UV/Vis/NIR spectra were recorded with a PerkinElmer Lambda 900 spectrophotometer between 300 and 1600 nm in diffuse reflectance against BaSO₄. A Harrick coolable/heatable powder sample holder in "Praying Mantis" configuration was used. Melting points were determined by differential scanning calorimetry, using a Netzsch STA 449 C Jupiter® with heating rates of 2 K min⁻¹, see Fig. S1-S3.† The magnetic moment of the Fe(II) complexes was measured using a Physical Property Measurement System (PPMS®) by Quantum Design. The **Dalton Transactions Paper**

experimental setup consisted of a vibrating sample magnetometer attachment (VSM), bearing a brass sample holder with a quartz-glass powder container. The magnetic moment was determined in an external field of 1 T in the range of 10 K to 300 K, measuring all 5 K with a previous thermal stabilization of 5 minutes. Variable temperature mid-range (4000–450 cm⁻¹) infrared spectra were recorded by the ATR technique on a PerkinElmer Spectrum 400, fitted with a coolable/heatable PIKE Gladi ATR Unit.²⁵ Single crystals were attached to a glass fiber by using perfluorinated oil and were mounted on a Bruker KAPPA APEX II diffractometer equipped with a CCD detector with Mo K_{α} radiation (Incoatec Microfocus Source IμS: 30 W, multilayer mirror, $\lambda = 0.71073$ Å). For all measurements data were reduced to intensity values by using SAINT Plus, 40 and an absorption correction was applied by using the multi scan method implemented by SADABS. 40 For the iron(II) complexes, protons were placed at calculated positions and refined as riding on the parent C atoms. All non-H atoms were refined with anisotropic displacement parameters. For 2024832 (10), a Bruker KAPPA APEX II diffractometer equipped with a CCD detector was used and data were collected at 100 K. The powder X-ray diffraction measurements were carried out on a PANalytical X'Pert Pro diffractometer in Bragg-Brentano geometry using Cu $K_{\alpha 1,2}$ radiation filtered with a BBHD mirror and an X'Celerator linear detector. For in situ experiments below ambient temperature an Oxford PheniX Cryochamber from Oxford Cryosystems was used. The powder sample were mounted on a copper sample holder on top of a background-free silicon support. The sample chamber was evacuated, and all measurements were carried out under vacuum. The actual sample temperature is directly monitored by a thermocouple on the sample holder. The diffractograms were evaluated using the PANalytical program suite HighScorePlus, correcting for the background.

Synthesis of ligands

Tetrazoles and their derivatives - especially in combination with perchlorates - are potentially shock sensitive or explosive compounds and should, therefore, be handled with great care and with the appropriate safety precautions!

2-(1*H*-Tetrazol-1-yl)acetic acid (2COOHTz) (1). 25 (333 mmol, 1 eq.) glycine and 32.4 g (499.6 mmol, 1.5 eq.) NaN₃ were suspended in 97 ml (516.2 mmol, 1.55 eq.) triethylorthoformate and 250 ml acetic acid. The suspension was heated for 18 h at 95 °C, filtrated and evaporated to dryness. After extracting the residue with CH2Cl2, the solvent was removed, and the resulting yellow oil refluxed for 6 h in concentrated hydrochloric acid. After removal of all volatiles the oily residue was adsorbed on SiO2 and was further purified by column chromatography (MeCN: CH2Cl2 = 3:2). After evaporation, 1 was obtained as beige crystalline material. Yield: 7.9 g, 18.5%; MP: 130 °C; $\nu_{\text{CH(Tz)}}$ 3156, ν_{CO} 1731/1712 cm⁻¹; ¹H NMR (400 MHz, DMSO-d₆) δ = 13.43 (s, 1H, COOH), 9.38 (s, 1H, Tz), 5.43 (s, 2H, CH₂) ppm; $^{13}\text{C}\{^1\text{H}\}$ NMR (101 MHz, DMSO-d₆) δ = 167.94 (COOH), 144.99 (Tz), 48.52 (CH₂) ppm.



4-(1H-Tetrazol-1-yl)butanoic acid (4COOHTz) (3). 25 g (242.4 mmol, 1 eq.) 4-aminobutanoic acid and 23.6 g (363.7 mmol, 1.5 eq.) NaN3 were suspended in 70.6 ml (375.8 mmol, 1.55 eq.) triethylorthoformate and 250 ml acetic acid. The suspension was heated for 18 h at 95 °C, filtrated and evaporated to dryness. After extracting the residue with CH₂Cl₂, the solvent was removed, and the resulting yellow oil refluxed for 6 h in concentrated hydrochloric acid. After removal of all volatiles the oily residue crystallized in the freezer overnight. The yellow solid was adsorbed on SiO2 and further purified by column chromatography (MeCN: $CH_2Cl_2 =$ 3:2) After evaporation, 4COOHTz was obtained as off-white solid. Yield: 11.24 g, 29.7%; MP: 86 °C; $\nu_{\rm CH(Tz)}$ 3114, $\nu_{\rm CO}$ 1714 cm⁻¹; ¹H NMR (400 MHz, DMSO-d₆) δ = 12.21 (s, 1H, COOH), 9.41 (s, 1H, Tz), 4.48 (t, J = 7.1, 2H, CH₂), 2.27 (t, J = 7.1) 7.3, 2H, CH₂), 2.06 (p, J = 7.2, 2H, CH₂) ppm; ${}^{13}C\{{}^{1}H\}$ NMR (101 MHz, DMSO-d₆) δ = 173.52 (COOH), 143.99 (Tz), 46.91 (CH₂), 30.37 (CH₂), 24.72 (CH₂).

Synthesis of Fe(II)-complexes

 $[Fe(2COOHTz)_6][BF_4]_2 \cdot 2MeCN$ (4). $Fe(BF_4)2 \cdot 6H_2O$ (100 mg, 296.3 μmol, 1 eq.) and 1 (231.5 mg, 1.81 mmol, 6.1 eq.) were dissolved in 10 ml MeCN and stirred at 50 °C for 18 h. After evaporation of the solvent, the residual oil was triturated in 10 ml THF for 1 h to remove the excess of ligand. The precipitated material was separated, washed with further THF (10 ml) and dried in a stream of N₂. Yield: 98.8 mg, 33.4%; $\nu_{\rm CH(Tz)}$ 3138, $\nu_{\rm CO}$ 1744 cm⁻¹.

 $[Fe(3COOHTz)_6][BF_4]_2$ (5). Same procedure as for 4. 5 was isolated as off-white, sticky solid. Yield: 75.7 mg, 23.6%; $\nu_{\rm CH(Tz)}$ 3135, $\nu_{\rm CO}$ 1714 cm⁻¹.

[Fe(4COOHTz)6][BF4]2 (6). Same procedure as for 4. 6 was isolated as white solid. Yield: 122 mg, 35.3%; $\nu_{\rm CH(Tz)}$ 3144, $\nu_{\rm CO}$ 1733 cm⁻¹.

[Fe(2COOHTz)₆][ClO₄]₂·2MeCN (7). Fe(ClO₄)₂·6H₂O (100 mg, 275.6 µmol, 1 eq.) was dissolved under Ar together with a tiny amount of ascorbic acid in 2 ml MeCN and added by filtration through a syringe filter (PTFE, 0.45 µm) to a degassed solution of 1 (215.4 mg, 1.68 mmol, 6.1 eq.) in 8 ml MeCN. The resulting mixture was stirred at 50 °C for 18 h. After evaporation of the solvent, the residual oil was triturated in 10 ml THF for 1 h to remove the excess of ligand. The precipitated material was separated, washed with further THF (10 ml) and dried in a stream of N₂. Yield: 51.5 mg, 18.2%; $\nu_{\rm CH(Tz)}$ 3159/3152, $\nu_{\rm CO}$ 1733/1715 cm⁻¹.

 $[Fe(3COOHTz)_6][ClO_4]_2$ (8). Same procedure as for 7. 8 was isolated as white sticky solid. Yield: 127.1 mg, 41.6%; $\nu_{\text{CH(Tz)}}$ 3137, $\nu_{\rm CO}$ 1740/1715 cm⁻¹.

 $[Fe(4COOHTz)_6][ClO_4]_2$ (9). Same procedure as for 7. 9 was isolated as white solid. Yield: 118.9 mg, 36.2%; $\nu_{\rm CH(Tz)}$ 3134, $\nu_{\rm CO}$ 1728 cm⁻¹.

 $[Gd(3COOTz)_2(H_2O)_3]Cl$ (10). $Fe(ClO_4)_2 \cdot 6H_2O$ (42.55 mg, 117.27 µmol, 1 eq.) was dissolved under Ar together with a tiny amount of ascorbic acid in 2 ml MeOH and added by filtration through a syringe filter (PTFE, 0.45 µm) to a degassed solution of 2 (100 mg, 703.64 mmol, 6 eq.) in 8 ml of a 1:1 mixture MeOH: H2O. The resulting mixture was stirred at 50 °C for 10 minutes, then 43.6 mg (117.27 μmol, 1 eq.) GdCl₃·6H₂O was added. The mixture was further stirred for 6 h at 50 °C. After evaporation of the solvent, the residual slightly yellow oil was kept at 50 °C for 6 h under vacuum and afterwards left for 3 weeks at 4 °C. A few tiny colourless crystals formed.

Conclusions

Fe(π)–SCO complexes with bifunctional ω-(1*H*-tetrazol-1-yl) carboxylic acids allow formation of supramolecular hydrogen bonding networks that enhance the cooperativity of the material. Furthermore, the COOH-group can act as anchorgroup for deposition on oxidic surfaces, or for formation of multi-metallic coordination polymers. Three ligands bearing a COOH-group with alkyl-chain lengths of C2-C4 were synthesized and coordinated to Fe(II) with BF₄ and ClO₄ as weak-coordinating anions. Complete and sharp spin state transitions were observed in the cases of 4, 6, 7 and 9. An initial attempt to prepare a 3d-4f mixed-metallic coordination polymer with Gd³⁺ resulted in the unexpected formation of one-dimensional Gd-oxo chains with the 3COOHTz-ligand having been deprotonated and coordinating to the Gd³⁺-atoms in a chelating-bridging μ_2 - η^2 : η^1 fashion. Future work will focus on a more suitable synthetic approach to realise a coordination on both ligand functional groups.

Conflicts of interest

There are no conflicts to declare.

Acknowledgements

We acknowledge financial support of the Austrian Science Fund (FWF Der Wissenschaftsfond) project P 31076-N28. The X-Ray center (XRC) of the Vienna University of Technology provided access to the powder X-Ray diffractometer.

References

- 1 P. Gütlich, H. A. Goodwin, Topics in Current Chemistry, Spin Crossover in Transition Metal Compounds I-III, Springer Berlin Heidelberg, 2004.
- 2 P. Gütlich, Eur. J. Inorg. Chem., 2013, 581-591, DOI: 10.1002/ejic.201300092.
- 3 H. J. Shepherd, C. Bartual-Murgui, G. Molnar, J. A. Real, M. C. Munoz, L. Salmon and A. Bousseksou, New J. Chem., 2011, 35, 1205-1210.
- 4 S. Decurtins, P. Gutlich, C. P. Kohler, H. Spiering and A. Hauser, Chem. Phys. Lett., 1984, 105, 1-4.
- 5 A. C. Aragonès, D. Aravena, J. I. Cerdá, Z. Acís-Castillo, H. Li, J. A. Real, F. Sanz, J. Hihath, E. Ruiz and I. Díez-Pérez, Nano Lett., 2016, 16, 218-226.
- 6 C. Lefter, V. Davesne, L. Salmon, G. Molnár, P. Demont, A. Rotaru and A. Bousseksou, Magnetochemistry, 2016, 2, 18.
- 7 C. Lefter, S. Rat, J. S. Costa, M. D. Manrique-Juárez, C. M. Quintero, L. Salmon, I. Séguy, T. Leichle, L. Nicu, P. Demont, A. Rotaru, G. Molnár and A. Bousseksou, Adv. Mater., 2016, 28, 7508-7514.
- 8 C. Lefter, R. Tan, J. Dugay, S. Tricard, G. Molnár, L. Salmon, J. Carrey, W. Nicolazzi, A. Rotaru and A. Bousseksou, Chem. Phys. Lett., 2016, 644, 138–141.
- 9 L. Cambi and A. Cagnasso, Atti R. Accad. Naz. Lincei, Mem. Cl. Sci. Fis., Mat. Nat., 1931, 13, 809.
- 10 L. Cambi and L. Szegö, Ber. Dtsch. Chem. Ges. (A and B), 1933, 66, 656-661.
- 11 L. Cambi and L. Szegö, Ber. Dtsch. Chem. Ges. (A and B), 1931, 64, 2591-2598.
- 12 M. Ohba, K. Yoneda and S. Kitagawa, CrystEngComm, 2010, 12, 159-165.
- 13 C. J. Kepert, Chem. Commun., 2006, 695, DOI: 10.1039/ b515713g.
- 14 A. Holovchenko, J. Dugay, M. Giménez-Marqués, R. Torres-Cavanillas, E. Coronado and H. S. J. van der Zant, Adv. Mater., 2016, 28, 7228-7233.
- Dugay, M. Gimenez-Marques, Т. H. W. Zandbergen, E. Coronado and H. S. J. van der Zant, Adv. Mater., 2015, 27, 1288-1293.
- 16 H. J. Shepherd, I. Y. A. Gural'skiy, C. M. Quintero, S. Tricard, L. Salmon, G. Molnár and A. Bousseksou, Nat. Commun., 2013, 4, 2607.
- 17 M. Matsuda, H. Isozaki and H. Tajima, Thin Solid Films, 2008, **517**, 1465–1467.
- 18 C. Lochenie, K. Schötz, F. Panzer, H. Kurz, B. Maier, F. Puchtler, S. Agarwal, A. Köhler and B. Weber, J. Am. Chem. Soc., 2018, 140, 700-709.
- 19 C. Bartual-Murgui, A. Akou, C. Thibault, G. Molnar, C. Vieu, L. Salmon and A. Bousseksou, J. Mater. Chem. C, 2015, 3, 1277-1285.
- 20 W.-Q. Gao, Y.-S. Meng, C.-H. Liu, Y. Pan, T. Liu and Y.-Y. Zhu, Dalton Trans., 2019, 48, 6323-6327.
- 21 J. Ru, F. Yu, P.-P. Shi, C.-Q. Jiao, C.-H. Li, R.-G. Xiong, T. Liu, M. Kurmoo and J.-L. Zuo, Eur. J. Inorg. Chem., 2017, **2017**, 3144-3149.

- 22 K. E. Burrows, S. E. McGrath, R. Kulmaczewski, O. Cespedes, S. A. Barrett and M. A. Halcrow, Chem. - Eur. *J.*, 2017, 23, 9067–9075.
- 23 I. A. Gass, S. Tewary, G. Rajaraman, M. Asadi, D. W. Lupton, B. Moubaraki, G. Chastanet, J.-F. Létard and K. S. Murray, Inorg. Chem., 2014, 53, 5055-5066.
- 24 A. Absmeier, M. Bartel, C. Carbonera, G. N. L. Jameson, F. Werner, M. Reissner, A. Caneschi, J. F. Letard and W. Linert, Eur. J. Inorg. Chem., 2007, 3047-3054, DOI: 10.1002/ejic.200601096...
- 25 M. Muttenthaler, M. Bartel, P. Weinberger, G. Hilscher and W. Linert, J. Mol. Struct., 2005, 741, 159-169.
- 26 M. Seifried, C. Knoll, G. Giester, J. M. Welch, D. Müller and P. Weinberger, Eur. J. Org. Chem., 2017, 2017, 2416-2424.
- 27 M. Seifried, C. Knoll, G. Giester, M. Reissner, D. Müller and P. Weinberger, Magnetochemistry, 2016, 2, 1-13.
- 28 M. Nihei, Y. Yanai, I. J. Hsu, Y. Sekine and H. Oshio, Angew. Chem., Int. Ed., 2017, 56, 591-594.
- 29 C. Lochenie, J. Heinz, W. Milius and B. Weber, Dalton Trans., 2015, 44, 18065-18077.
- 30 W. Bauer, C. Lochenie and B. Weber, Dalton Trans., 2014, 43, 1990-1999.

- 31 A. Absmeier, M. Bartel, C. Carbonera, G. N. L. Jameson, P. Weinberger, A. Caneschi, K. Mereiter, J. F. Letard and W. Linert, Chem. - Eur. J., 2006, 12, 2235-2243.
- 32 P. L. Franke and W. L. Groeneveld, Transition Met. Chem., 1981, 6, 54-56.
- 33 T. Kamiya and Y. Saito, US3767667A, 1971.
- 34 T. Kamiya and Y. Saito, DE2147023A1, 1971.
- 35 O. H. Jústiz, R. Fernández-Lafuente, J. M. Guisán, P. Negri, G. Pagani, M. Pregnolato and M. Terreni, J. Org. Chem., 1997, 62, 9099-9106.
- 36 D. Müller, C. Knoll, M. Seifried and P. Weinberger, Vib. Spectrosc., 2016, 86, 198-205.
- 37 P. Gütlich, A. Hauser and H. Spiering, Angew. Chem., Int. Ed. Engl., 1994, 33, 2024-2054.
- 38 A. Abhervé, M. J. Recio-Carretero, M. López-Jordà, J. M. Clemente-Juan, J. Canet-Ferrer, A. Cantarero, M. Clemente-León and E. Coronado, Inorg. Chem., 2016, **55**, 9361-9367.
- 39 D. D. Perrin and W. L. F. Armarego, Purification of Laboratory Chemicals, 4th ed., Butterworth-Heinemann, Oxford, 1997.
- 40 I. Bruker, Bruker AXS Inc., Madison, Wisconsin, USA,

Supporting Information

Bifunctional Fe(II) spin crossover-complexes based on ω -(1*H*-tetrazol-1-yl) carboxylic acids

Willi Zeni,^a Marco Seifried,^a Christian Knoll,^a Jan M. Welch,^b Gerald Giester,^c Berthold Stöger,^d Werner Artner,^d Michael Reissner, e Danny Müller, a* and Peter Weinbergera*

- a. Institute of Applied Synthetic Chemistry, TU Wien, Getreidemarkt 9/163-AC, 1060 Vienna, Austria E-mail: danny.mueller@tuwien.ac.at: peter.e163.weinberger@tuwien.ac.at
- b. Center for Labelling and Isotope Production, TRIGA Center Atominstitut, TU Wien, Stadionallee 2, 1020 Vienna, Austria.
- ^c Department of Mineralogy and Crystallography, University of Vienna, Althanstraße 14 (UZA 2), 1090 Vienna, Austria.
- ^{d.} X-Ray Center, TU Wien, Getreidemarkt 9, 1060 Vienna, Austria
- e. Institute of Solid State Physics, TU Wien, Wiedner Hauptstraße 8-10/138, 1040 Vienna, Austria

- Fe-N bond lengths for 4, 6, 7, 9
- DSC / TGA data for 1, 2, 3

Table S1. Bond-lengths for $[Fe(2COOHTz)_6](BF_4)_2 \cdot 2$ MeCN (4) in HS and LS state

	4 , HS [Å]	4, LS [Å]
Fe-N ₄	2.176	1.987

Table S2. Bond-lengths for $[Fe(4COOHTz)_6](BF_4)_2 \cdot Et_2O$ (6) in HS and LS state

	6 , HS [Å]	6 , LS [Å]
Fe-N ₄	2.165	1.969
Fe-N _{4A}	2.182	1.979
Fe-N _{4B}	2.185	1.981

Table S3. Bond-lengths for $[Fe(2COOHTz)_6](CIO_4)_2 \cdot 2 MeCN$ (7) in HS and LS state

	7 , HS [Å]	7 , LS [Å]
Fe-N ₄	2.184	2.004

Table S4. Bond-lengths for [Fe(4COOHTz)₆](ClO₄)₂·Et₂O (9) in HS and LS state

	9 , HS [Å]	9 , LS [Å]
Fe ₁ -N ₄	2.181	1.984
Fe ₁ -N _{4A}	2.176	1.987
Fe ₁ -N _{4B}	2.173	1.992
Fe ₂ -N _{4C}	2.174	1.987
Fe ₂ -N _{4D}	2.185	1.997
Fe ₂ -N _{4E}	2.176	1.984

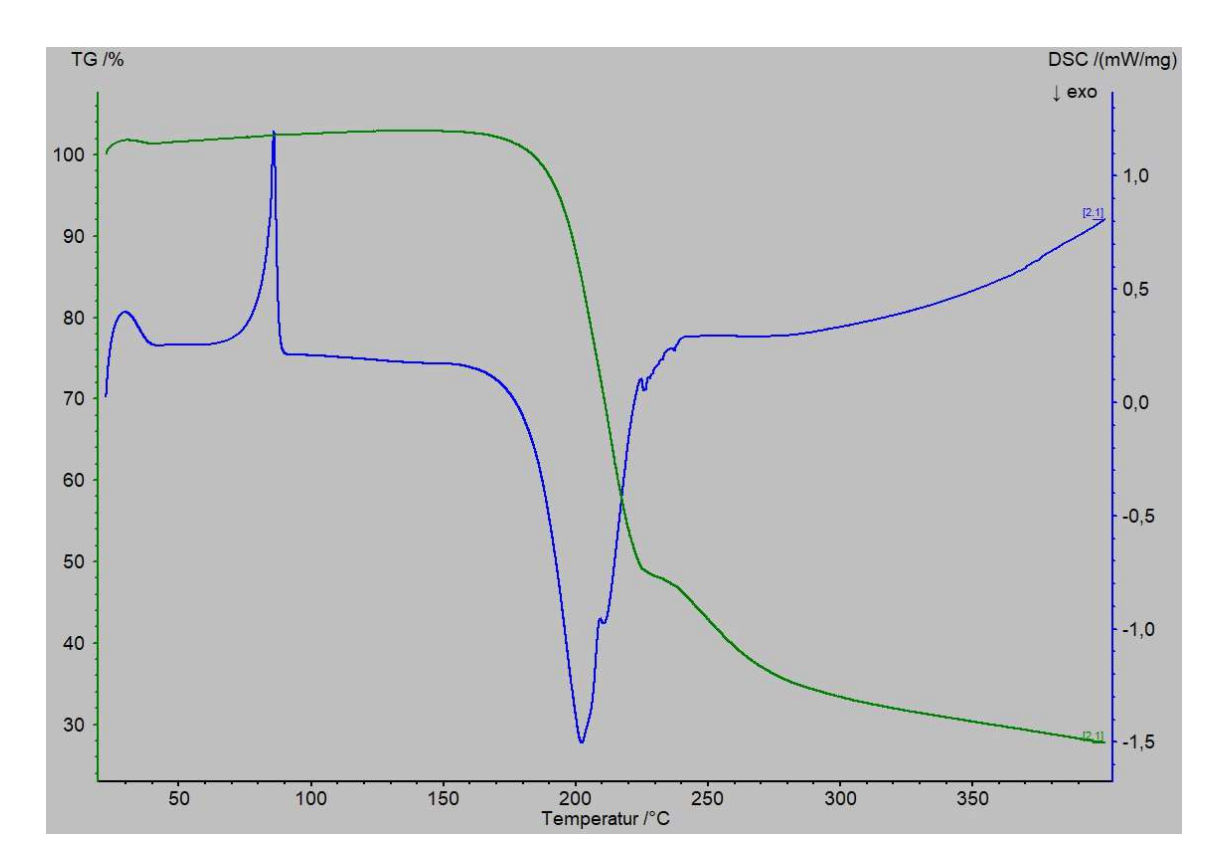


Figure S1. DSC / TGA analysis for 2COOHTz (1)

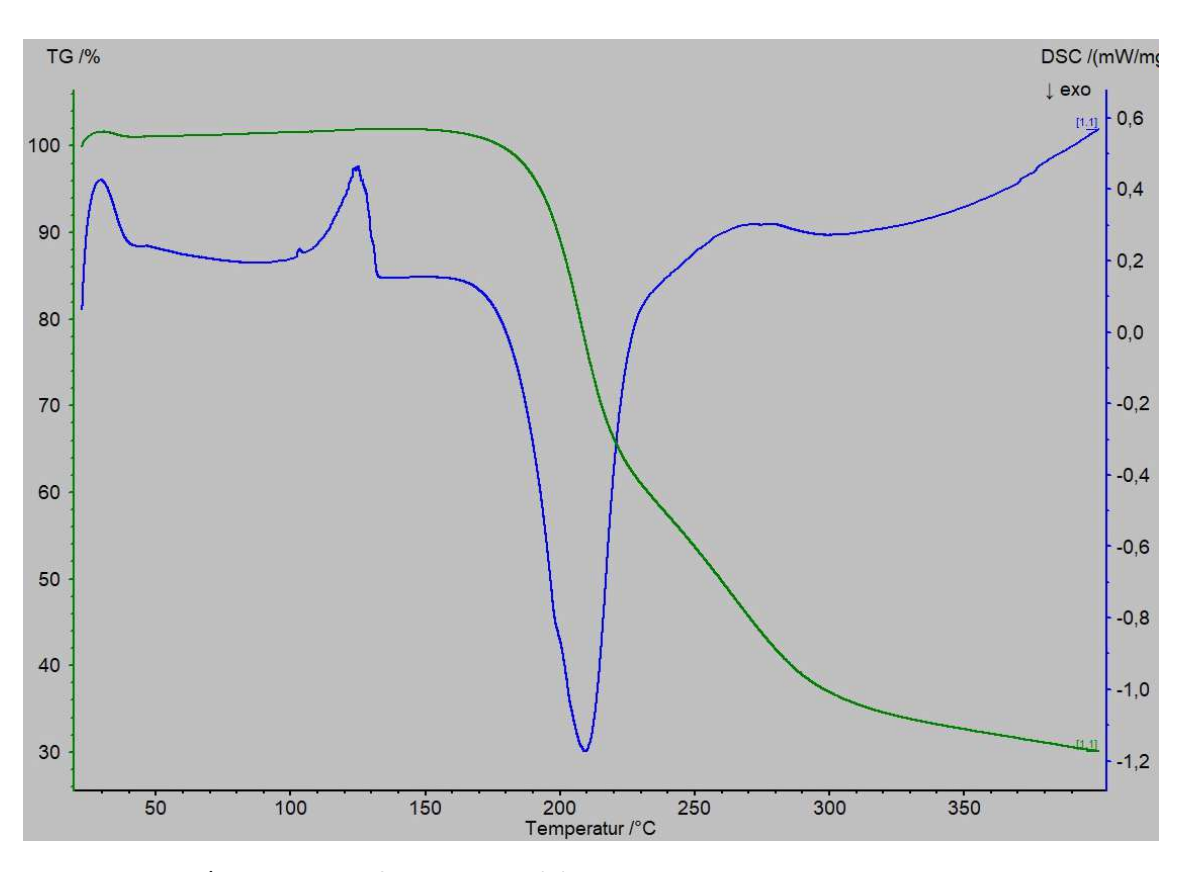


Figure S2. DSC / TGA analysis for 3COOHTz (2)

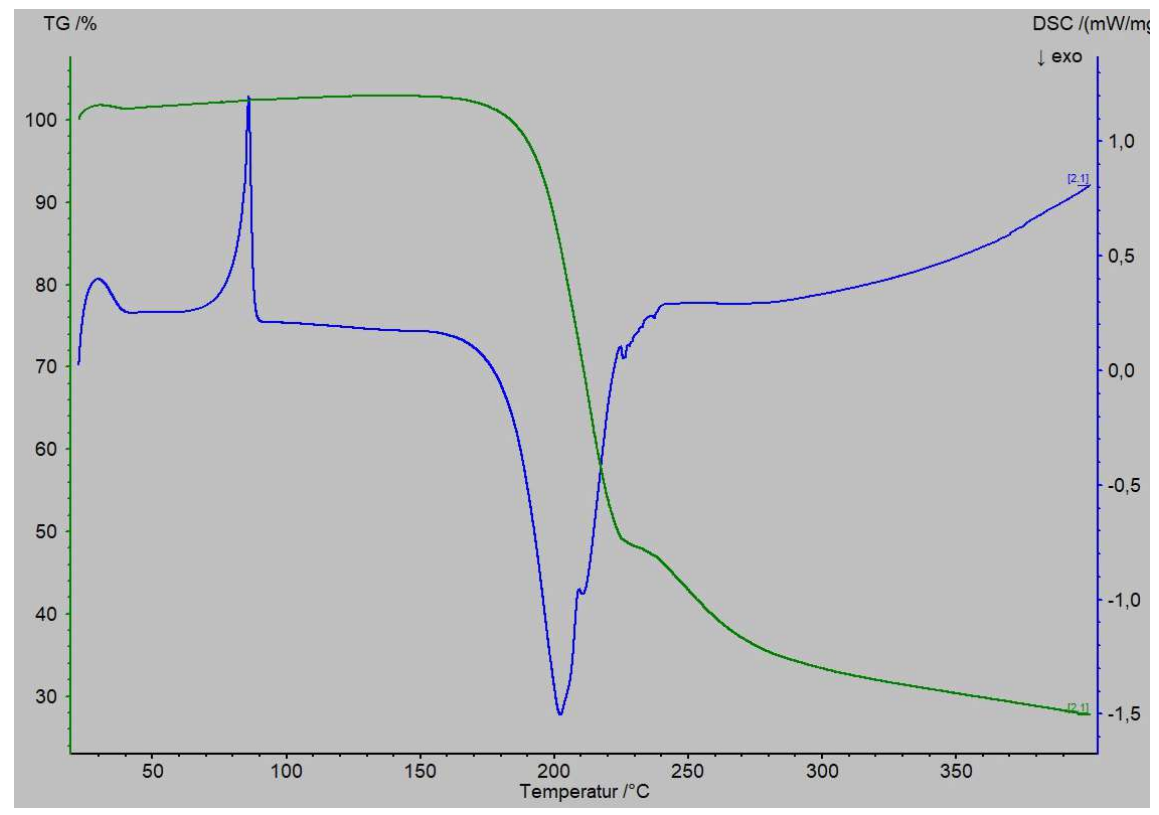


Figure S3. DSC / TGA analysis for 4COOHTz (3)

Tetrakis-cyanoacetylides as building block for a second generation of spin-switchable Hofmann type-networks with enhanced porosity

Willi Zeni^[a]*, Danny Müller^[a], Werner Artner^[b], Gerald Giester^[c], Michael Reissner^[d], Peter Weinberger^{[a]*}

[a] DI Willi Zeni, Dr. Danny Müller, Associate-Prof. Dr. Peter Weinberger Institute of Applied Synthetic Chemistry, TU Wien Getreidemarkt 9/163-01-3, 1060 Vienna, Austria

E-mail: willi.zeni@tuwien.ac.at; peter.e163.weinberger@tuwien.ac.at

[b] Dipl.- Ing. Werner Artner X-Ray Center, TU Wien, Getreidemarkt 9/057-4, 1060 Vienna, Austria

[c]Ao. Univ. Prof. Dr. Gerald Giester Department of Mineralogy and Crystallography University of Vienna, Josef-Holaubek-Platz 2, 1090 Vienna, Austria

> Ao. Univ. Prof. Dr. Michael Reissner Institute of Solid State Physics, TU Wien Wiedner Hauptstraße 8-10/138, 1040 Vienna, Austria

ABSTRACT

The combination of Spin Crossover (SCO) with guest incorporation properties has attracted the interest of researchers in the last couple of decades, and lead to the design of numerous SCO-porous coordination polymers (SCO-PCP). The most famous class of SCO-PCP is the one of Hofmann-type networks, which are very promising materials for (chemo)sensing applications. Different strategies have been carried out to expand the classic structure Fe(pz)[M(CN)₄] (M=Ni, Pd, Pt) to get larger cavities, but the resulting compounds often showed poor magnetic behavior. In this work, we present wide mesh size spin-switching Hofmann-type networks based on tetrakis(cyanoacetylides) synthesized with a newly developed method, resulting in compounds of the general formula Fe(pz)[M(C₃N)₄]. The compounds were characterized in their structural, magnetic, and spectroscopic properties. They present five-fold larger cavities and a drastic increase in porosity. The desired hysteretic and guest-dependent Spin-crossover behavior is retained, in-situ chemoswitching of the spin state and memory effect are also observed.

INTRODUCTION

Porous coordination polymers (PCPs) gained considerable interest in the last couple decades as a class of porous materials which, thanks to their permanent and designable regular porosity, showed great versatility and created prospects for their application in different fields, from hydrogen storage, natural gas storage, gas separation, and capturing of harmful gases⁸ to an application in catalysis⁹ or as stationary phase in gaschromatography. 10 A current research focus in the field of multifunctionality is the creation of systems in which the guest adsorption process is accompanied by a change in solid state properties (e.g. optics, conductivity, magnetism). In this context, the coupling of the porous properties with the spin-crossover (SCO) phenomenon is particularly attractive, especially since in the last two decades the research in the SCO field has been focused on multifunctional materials. SCO is well known for Fe(II) coordination compounds, showing spin-state interconversions between the low-spin (LS) and high-spin (HS) states under external stimuli (temperature, ^{11, 12} pressure, ¹¹⁻¹³ light, ^{14, 15}, etc.). The change of the metal centre's spin-state affects key-properties of the material including magnetic moment, ^{11, 12} colour, ¹⁶ dielectric constant, ^{17, 18} lattice extension, ¹⁹ etc. The most famous class of spin-switchable porous networks is the one of Hofmann-type networks, based on the compound M1(L)₂[M2(CN)₄] (M1=M2=Ni²⁺ L=NH₃) reported in 1897 by Hofmann and Küspert.²⁰ The first SCO-PCP, namely the 2D PCP Fe(py)₂[Ni(CN)₄] (py=pyridine), was reported in 1996 by Kitazawa et al.²¹, and represented the first milestone in SCO-PCPs research. In 2001 the second milestone was reached, with Fe(pz)[M^{II}(CN)₄] (pz=pyrazine, M^{II}=Ni²⁺, Pd²⁺, Pt²⁺) reported by Real et al. ²². The substitution of py with pz resulted in $\{Fe[M^{II}(CN)_4]\infty\}$ layers stacked by pz ligands, giving the network 3D dimensionality. Since then, this class of compounds rapidly gained interest for a variety of reasons: a) the highly cooperative and often hysteretic spin transition around room temperature; b) the guest-responsive SCO, guest-dependent magnetic behavior, and memory effect; c) robustness to absorption and desorption of a wide range of small molecule guests, and d) the possibility to tailor the design of the frameworks, making these systems very flexible and adaptable to the desired application. In 2009, Ohba et al. published a study in which they reported the bidirectional

chemoswitching of the spin-state in Fe(pz)[Pt(CN)₄] (=pzPt), demonstrating how this class of PCPs are truly environment responsive materials. Furthermore, the presence of memory effect was observed, for which the guest-induced spin state was retained even after guest-desorption.²³. A synergistic interplay between SCO and guest-exchange was also demonstrated for Fe(pz)[Ni(CN)₄] (=pzNi) by Kepert et al.²⁴

Numerous modifications of the Fe(pz)[M^{II}(CN)₄] (=pzM) scaffold have been reported, mainly with the goal of increasing the pores' volume and enhance the porosity of the PCPs, which would allow for the incorporation of larger guest molecules, instead of only small, passive molecules. The extension of the pores size has been mostly achieved by substituting pz with longer ditopic N-ligands, such as bpac²⁵ or bpeben²⁶ (bpac=bis(4pyridyl)acetylene, bpeben=1,4-bis(4-pyridylethynyl)benzene). While the desired 3D structure was preserved, and the pores' volume was indeed increased (10 times increase in the case of bpeben compared to pz), these compounds showed gradual and nonhysteretic spin transition, suggesting that the effectiveness of transmission of SCO cooperativity decreases with increasing length of the pillar ligand. Furthermore, incorporation of the ligand in the pores was observed. Another strategy to increase the pores' volume is the substitution of the [M^{II}(CN)₄]²- linkers with [M^I(CN)₂]- (M=Ag⁺, Cu⁺, Au⁺); the use of [Ag(CN)₂] yields [Fe(L)_n{Ag(CN)₂}₂], with a structure consisting of two interpenetrating 3D networks with edge-shared {Fe[Ag(CN)₂]₄} rhombuses in the 2D sheets²⁷. In the case of Au, 3D triply interpenetrated networks are formed.²⁸⁻³⁰ This approach successfully enlarged the voids so that even a ferrocene molecule could be incorporated³⁰, but again, the compounds showed poor magnetic behavior. Furthermore,

network interpenetration takes away the regular porosity, making the system less flexible for possible modifications.

In this work we present a previously unreported method for the synthesis of a new generation of expanded Hofmann-type networks. The elongation is performed by the insertion of an acetylenic-subunit to the M-CN bond, resulting in square-planar tetrakiscyanoacetylides [MII(C₃N)₄]² spacer with nearly doubled extension compared to $[M^{II}(CN)_4]^{2-}$, leading to Hofmann-type SCO-PCPs of the general formula $Fe(pz)[M^{II}(C_3N)_4]$. The absence of additional metallic nodes preserves the desired 3D structure with regular porosity avoiding networks' interpenetration. The magnetic properties are retained featuring hysteretic SCO near room-temperature, as well as the guest-dependency of the spin-state, guest-induced spin transition (=chemoswitching) and the memory effect showed by Fe(pz)[M^{II}(CN)₄], but in comparison the here reported compounds feature five-fold larger pores and a drastic increase in porosity.

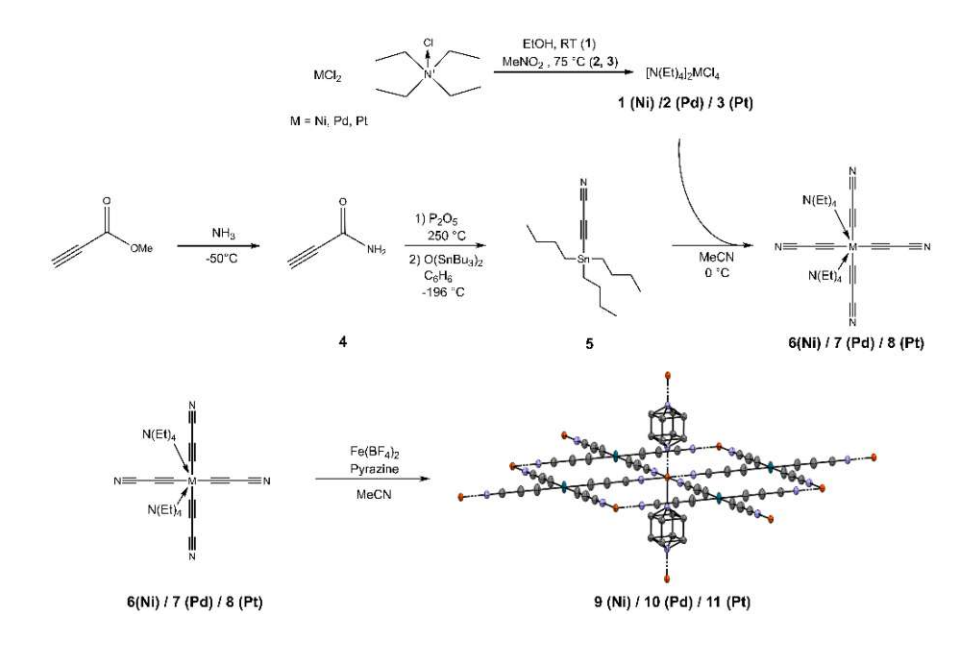
RESULTS AND DISCUSSION

Synthesis

The preparation of the [MII(C₃N)₄]²⁻ species (M=Ni, Pd, Pt) was achieved with a slight modification of a literature known procedure, 31 where instead of Me₃SnC₃N, the tributyl analogue nBu₃SnC₃N was used, and MeCN was used as solvent instead of DMF. The first step consisted in the synthesis $[NEt_4]_2[MCl_4]$ (1/2/3 for Ni, Pd and Pt respectively) by reaction of MCl₂ with NEt₄Cl. The synthesis of nBu₃SnC₃N was also done by modifying a literature reported procedure:³² reaction of methylpropiolate with NH₃ at -50 °C led to



2-propynamide (4), which was first treated with phosphorous-pentoxide for dehydration subsequently with bis-(tributyltin)-oxide, 3and leading to (tributylstannyl)propiolonitrile (5). Ultimately, reaction of 1/2/3 with 5 in MeCN at 0 °C resulted in $[NEt_4][M(C_3N)_4]$ (6/7/8 for Ni, Pd and Pt respectively). As reported in literature, 31 the compounds are air-stable in the solid state, but in contrast to literature reports, the species are stable in solution for longer than 24h, if inert atmosphere is provided. After longer time, a small deposit forms. The PCPs were synthesized by mixing 6-8 with anhydrous $Fe(BF_4)_2$ and pyrazine in MeCN, where compounds 9,10 and 11precipitated as amorphous powders. After centrifugation and solvent removal, the powders were dried in vacuum. In the HS state the PCPs appear as yellow/orange powders, in the LS state the color changes to deep red. A schematic representation of the synthesis is depicted in Scheme 1, for detailed experimental procedures see the Experimental section.



Scheme 1. Synthetic route for the preparation of $Fe(pz)[M(C_3N)_4]$

~35 °C.

The synthesis of 6/7/8 with the use of nBu₃SnC₃N allowed for lower volumes of solvents and easier precipitation of the products in Et₂O. Strict exclusion of oxygen and moisture are crucial for a successful synthesis, especially for the more reactive compound 6, which shows a tendency for homo-polymerization of the propargylnitrile fragment when these criteria are not met. The only drawback is a somewhat difficult work-up, caused by the muddy texture of the reaction mixture which makes the filtration a bit tedious. Another suboptimal synthetic aspect, which also regards 5, is the use of trialkyl-Sn(IV) species, whose toxicity is well known. To avoid its use, other synthetic pathways were tried out (e.g. isolation of HC₃N, deprotonation to form an acetylide and subsequent reaction with 1-3) but they were unsuccessful. Since organolithium reagents cannot be used due to the presence of the CN group, sodium amide was utilized as base, but some problems were encountered: on one hand, it is very hard to find a solvent (or solvent-mixture) in which NaNH₂ is -even slightly- soluble (NH₃ would be the best choice in that sense, but here it is inconvenient since it is also the by-product of the reaction), on the other hand one must deal with the very high thermal instability of acetylides. To overcome the second problem, syntheses at low temperatures (up to -90 °C) were carried out but they were again unsuccessful, since seconds after mixing the reagents the product decomposed. Even lower temperature conditions could be tried out, but that poses again a solubility problem and finding a solvent that is still liquid at such temperatures is also challenging. Finally, it must be mentioned that compound 9 is very temperature-sensitive, and decomposes at

Structural Characterization

Single crystals suitable for X-ray diffraction could solely be grown for compound 10 via electrocrystallization and could only be measured for the LS state at 200 K, due to degradation of the crystals at higher temperatures. Structural confirmation for compounds 9 and 11 was obtained via p-XRD, exploiting the isostructurality of the PCPs resulting in identical p-XRD patterns. A layering technique with very diluted solution was used to obtain crystalline powder. A detailed description of the experimental setup is given in the Experimental section.

Compound 10 may be described in the tetragonal space group P4/mmm (no. 123) with one molecule per unit cell ($a = 10.795(2) \text{ Å}, c = 6.759(2) \text{ Å}, V = 787.6 \text{ Å}^3$) with disordered pz moieties. However, taking into account rather weak additional X-ray reflections, a superstructure results in the space group P4/mbm (no. 127) with two molecules per unit cell (a = 15.266 (3) Å, c = 6.759 (2) Å, V = 1575.2 Å³). This now allows an ordered arrangement of the pyrazine molecules as shown in the Supplementary Figure 1. For further details, the reader is referred to the methodology chapter. For the sake of simplicity, the following further structure description will only be done in the small unit cell in space group P4/mmm.

As expected, the structure is formed by alternate octahedral $[FeN_6]^{2+}$ cations and square planar $[Pd(C_3N)_4]^{2-}$ anions. Four equivalent $[Pd(C_3N)_4]^{2-}$ groups coordinate via the Natoms at the equatorial positions of the octahedron, thus acting as bridges linking four Fe atoms and generating $\{\text{Fe}[\text{Pd}(C_3N)_4]\} \infty$ layers. The layers lie on top of each other and are stacked by pyrazine molecules which occupy the axial position of the octahedron,

generating an open 3D framework. The octahedral coordination geometry around the Fe(II) presents no distortions, due to the site symmetry 4/mmm all angles between cisligands are 90°. The Fe-N distances are 1.928 Å for the Fe-N1 bonds (equatorial) and 1.989 Å for the Fe-N2 bonds (axial), which are in agreement with typical Fe-N bond lengths for Fe(II) complexes in the LS state. The structure of 10 is depicted in Figure 1.

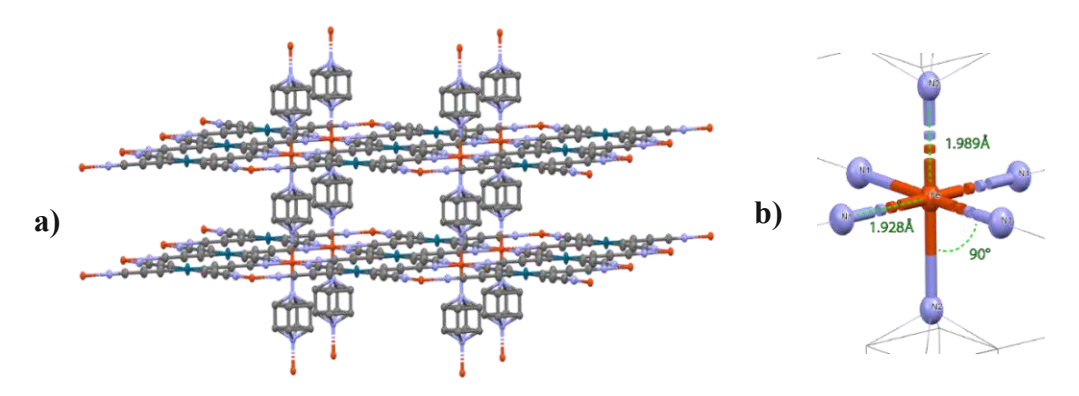
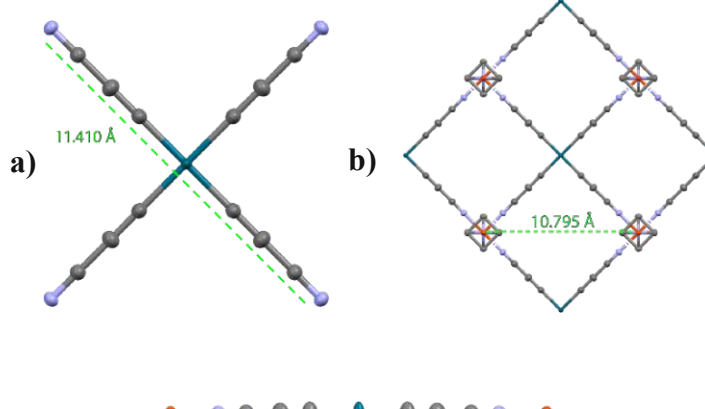


Figure 1. a) Perspective view of 10 with disordered pyrazine molecules, hydrogens are omitted for clarity. b) detail on the Fe-center with selected bond lengths and angles. Color code: orange=Fe, grey=C, blue=N, petrol=Pd

Comparison of 10 with pzNi and pzPt (no deposited structure for pzPd could be found) gives a good sense of the increase in guest accessible volume for this second generation of spin switchable Hofmann-type networks: the N-N distances in the linker are 6.029 Å and 6.279 Å for $[Ni(CN)_4]^{2-}$ and $[Pt(CN)_4]^{2-}$ respectively, whereas in $[Pd(C_3N)_4]^{2-}$ it is almost double, namely 11.410 Å. As a result, the Fe-Fe distance in the $\{\text{Fe}[\text{Pd}(C_3N)_4]\}$ alone (which then determines the size of the pores) increases from 6.911 / 7.114 Å in pzNi and 7.184 Å in pzPt to 10.795 Å in 10. The Fe-Fe distance between different layers remains practically the same, 6.780 and 6,783 Å in pzNi and pzPt respectively, vs. 6.759 Å in 10 (see Figure 2).

The increase in the linkers length is reflected in the volume of guest-accessible voids (determined with Platon ³³) and the resulting porosity of the PCPs. With a guestaccessible volume of 454 Å³, compound 10 presents a fivefold increase compared to the reference cyanide-based systems, for which guest accessible voids have a volume of 94 $Å^3$ (pzNi) and 83.6 Å³ (pzPt)^{23, 24}. It is also worth to compare compound 10 with other reported expanded Hofmann-type SCO-PCPs. For example, an elongation on the c-axis using bpac instead of pz in a cyanide-based compound results in guest-accessible voids with a volume of 293.6 Å³, although the axial Fe-Fe distance is doubled compared to the pz analogue (13.662 Å)²⁵. Moreover, 10 shows a drastic increase in porosity: the voids in compound 10 constitute 57.7% of the unit cell's volume, whereas the value for $Fe(bpac)[Pt(CN)_4]^{25}$ is 41.7% and only 23.9% for $Fe(pz)[Pt(CN)_4]^{23}$. Similar values for the volume of guest-accessible voids are found in Fe(bpeben)[Pt(CN)₄] with 511 $Å^3$, but in this case they constitute only 48.9% of the cell's volume. 26 Powder-XRD diffraction patterns for structural confirmation of compounds 9 and 11 are depicted in Figure 3.



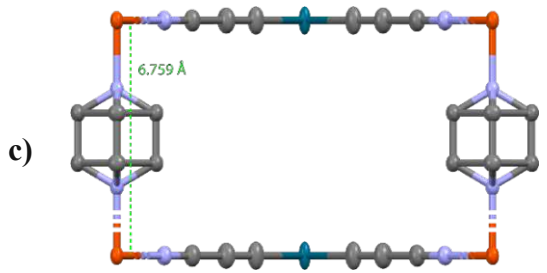


Figure 2. a) N-N distance in the $[Pd(C3N)4]^{2}$ -fragment, view along c axis b) Fe-Fe distance on the ab-plane, view along c-axis c) Fe-Fe distance between layers, view along a axis. Hydrogens are omitted for clarity. Color code: orange=Fe, grey=C, blue=N, dark cyan=Pd

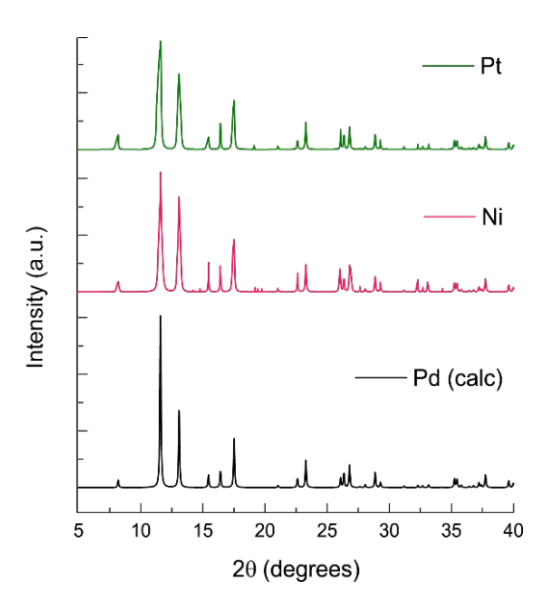


Figure 3. p-XRD diffractogram of compounds 9 and 11 measured at 200K, and the calculated pattern for $10\,$

Table 1: Crystallographic parameters for 10, described in the small unit cell

	10
Formula	C ₁₆ H ₄ FeN ₆ Pd
Weight [g mol-1]	442.5
T [K]	200
Colour	red
Shape	block
Crystal System	tetragonal
Space Group	P4/mmm
a [Å]	10.7946(15)
c [Å]	6.7591(14)
V [ų]	787.6(3)
Z	1
ρcalc. [g cm ⁻³]	0.933
μ [mm ⁻¹]	1.035
Measured Refl's.	12722
Unique Refl's	522
F(000)	214
Rint	0.0616
GooF	1.169
R1	0.0582
wR2	0.1893
No. of parameters	32
CCDC	2366166

Magnetic Characterization and guest-dependent magnetic behavior

Temperature dependent magnetic susceptibility was measured for compounds 9, 10 and 11 in a temperature range 10-305 K (9) and 10-350 K (10, 11). Due to the significant temperature sensitivity of 9, magnetic measurements of the PCP-guest composites were not performed for this compound because the resulting data would be incomplete and thus would not provide additional information. The PCPs exhibit different behavior based on the presence/absence and nature of guest-molecules. Compound 9 undergoes a gradual and incomplete spin transition (LS state is not fully reached) with hysteresis and $\chi_{mol}T$ values between 1.5 and 3.7 cm³Kmol⁻¹, typical for Fe(II) in the HS state. Compounds 10 and 11 show a gradual but complete spin transition with a 10 K hysteresis and χ_{mol} T values between 0.5 and 3.6 cm³Kmol⁻¹, again typical values for Fe(II). T↑ are 285 and 275 K and $T\downarrow$ are 275 and 265 K for 10 and 11, respectively. Results are depicted in Figure 4. It must be mentioned that the measurements were performed on the material obtained after the synthesis; considering its amorphous nature, the observed magnetic behavior is remarkable, especially for the presence of a small hysteresis.

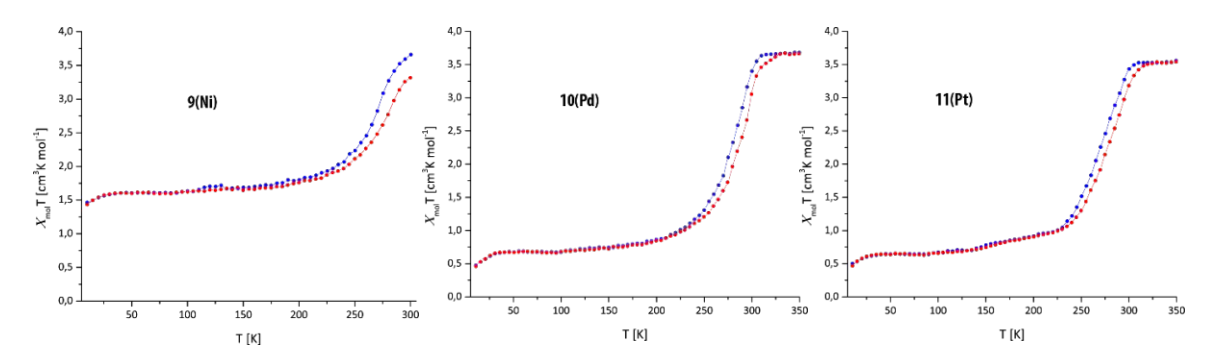


Figure 4. Temperature dependent magnetic susceptibility of compounds 9-11, red=heating blue=cooling

Guest-absorption causes a drastic change of the magnetic behavior, which is also dependent on the nature of the guest. An uptake of MeCN results in a complete and abrupt spin transition with larger hysteresis for both 10 and 11. T↑ are 315 and 300 K and $T\downarrow$ are 280 and 285 K for 10 and 11, respectively. In both cases the guest improves the quality of the spin transition and broadens the hysteresis, which especially for 10 is noteworthy. The same type of behavior is observed when the PCPs adsorb acetone, although the hysteresis is not as large as for MeCN. Absorption of MeOH results in a gradual and incomplete spin transition without hysteresis. As observed for other compounds of this class, certain guest molecules induce the stabilization of one spin state: for 10 and 11 water stabilizes the HS state at all temperatures, whereas benzene stabilizes the LS state at all temperatures. Although magnetic measurements were not carried out, this still seems to be valid for 9 as well: when exposed to water the powder maintained a bright yellow color even after cooling in liquid nitrogen, and when exposed to benzene it immediately turned from yellow to deep red, and the color was maintained after heating (up to 35 °C). Results are reported in Figure 5.

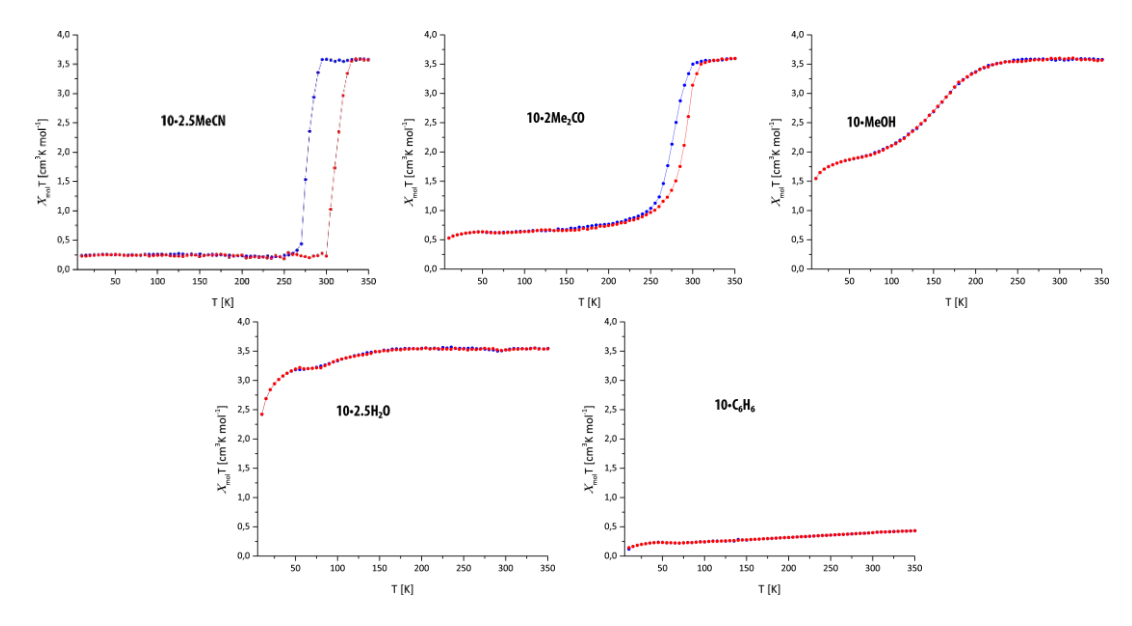


Figure 5. Temperature dependent magnetic susceptibility of 10-guest

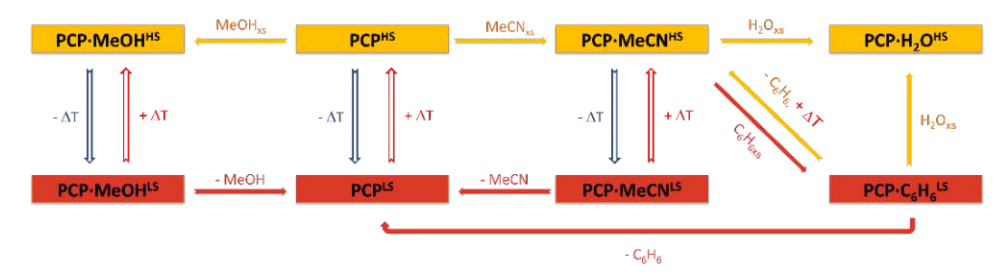
Manuscript

Comparison of these results with the ones reported in literature for pzM highlights some differences between the two families of compounds. The empty pzM networks show a rather abrupt spin transition with a larger hysteresis, in the range 20-30 K.²²⁻²⁴ The difference in abruptness and width of hysteresis has probably two reasons: the additional flexibility provided by the longer C₃N fragment, resulting in a decrease of cooperativity, and the fact that pzM precipitate as microcrystalline powders, whereas 9,10 and 11 are amorphous. The PCP-guest composites also show different behavior compared to pzM·guest. The two main factors influencing the magnetic behavior of the PCPs·guest composites are guest-size and host-guest interactions. In pzM, benzene absorption stabilizes the HS state at all temperatures, thus showing an opposite behavior as that of 9-11. Reason for this different behavior lies with all probability in the different pore size: 10,11 and pzM all absorb one molecule of benzene per Fe centre, and in pzM the benzene ring is large enough to prevent a shrinkage, thus the stabilization of the HS state, whereas for 10 and 11 it is reasonable to assume that $\pi - \pi$ interactions between bz and pz prevail and stabilize the system in the LS state. The stabilization of the HS state by water is presumably of dual nature: water weakens the ligand field strength of Fe(II), and also the small H₂O molecules completely fill the voids, providing a rigidity stabilizing the HS state.^{24, 34}



Bidirectional chemoswitching and memory effect

In-situ bidirectional chemo-switching of the spin state and memory effect were observed for all the PCPs, confirming a synergistic behavior between guest-absorption/-desorption and spin transition as in pzM. A schematic illustration of the results is depicted in Scheme 2.



Scheme 2. Schematic representation of the in-situ bidirectional chemoswitching and memory effect of compounds 9-11

Exposure of the PCPs to MeCN at room temperature yields PCP·MeCN^{HS}. Lowering the temperature triggers the spin-transition to PCP·MeCNLS, as already showed by magnetic susceptibility measurements. Exposing PCP·MeCNHS to an excess of MeOH, results in the replacement of MeCN with MeOH and, again, lowering the temperature brings PCP·MeOH in the LS state (despite the incomplete transition, a color change could be observed). After exposing both guest-free PCPs and PCP·MeCNHS to benzene without changing the temperature, a chemo-switching is observed, giving PCP·C₆H₆LS. Moreover, the PCPs show a memory effect: exposing PCP·C₆H₆LS to MeCN at room temperature leads to PCP·MeCNLS. The LS state is also retained after benzene desorption, yielding PCPLS. Exposing PCP·C₆H₆LS to water results in another chemoswitching to PCP·H₂OHS.

Infrared spectroscopy

FTIR-MIR spectra were measured for all the reported compounds, variable temperature measurements were recorded for compounds 9-11 to monitor changes in the IR absorption bands upon spin transition. Compound 4 shows an intense and broad ν_{NH2} absorption band with two peaks (typical for primary amides) located at 3286 and 3178 cm⁻¹, the $\nu_{C=C}$ band at 2109 cm⁻¹ and the $\nu_{C=O}$ band at 1645 cm⁻¹. Compound 5 presents the $\nu_{\rm CH}$ of the butyl groups in the range 2957-2854 cm⁻¹ and the $\nu_{\rm CN}$ at 2247 cm⁻¹. Compound 6-8 show the $\nu_{\rm CH}$ of the ethyl groups in the range 2980-2990 cm⁻¹, the $\nu_{\rm CN}$ band at 2203, 2214 and 2209 cm⁻¹ and the $\nu_{C=C}$ at 2038, 2049 and 2050 cm⁻¹ for 6, 7 and 8 respectively, which are in accordance with literature reported data³¹. Coordination to Fe(II) causes a shift of the absorption bands in 9-11, and for these compounds a shift is also observed by changing the measurement temperature, since it triggers the spin transition. Results are reported in Table 1, for the spectra see the Supporting Information.

Table 2: IR absorption bands for compounds 6-11

IR mode	6 (cm ⁻¹)	7 (cm ⁻¹)	8 (cm ⁻¹)
VCN	2203	2208	2214
VC≡C	2038	2049	2050
VM-C	517	516	517

	9 (cm ⁻¹)		10 (cm ⁻¹)		11(cm ⁻¹)	
IR mode	HS	LS	HS	LS	HS	LS
VCN	2215	2220	2223	2218	2214	2212
VC=C	2038	2038	2050	2053	2048	2049

For 6-8, the C≡C bands shift to higher wavenumber with increasing stability of the M-C bond. As expected, the $\nu_{\rm CN}$ band is affected by coordination to Fe(II), and in 9-11 shifts to higher wavenumbers compared to 6-8. A band broadening is also observed for both bands, which is characteristic for successful coordination. In 9-11, a small shift of the $\nu_{\rm CN}$ band is also observed upon spin-transition, with lower wavenumbers for the HS state due to the increase in the Fe-N bond length. A comparison of the IR spectra of 8, 11HS and 11LS is depicted in Figure 6.

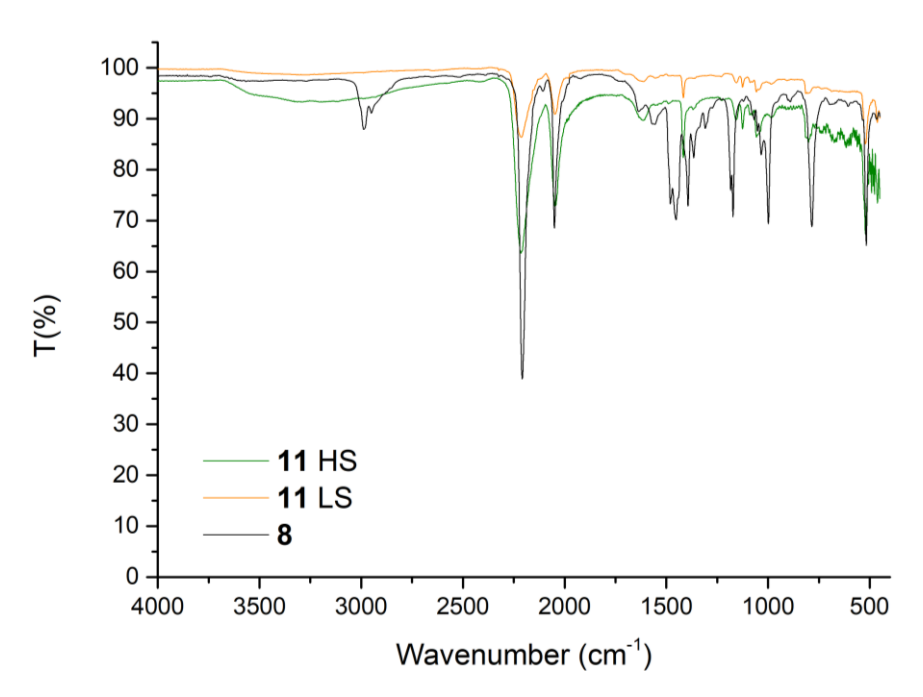


Figure 6: MIR spectra comparison of 8, 11-HS and 11-LS

CONCLUSIONS

The target compounds Fe(pz)[M(C₃N)₄] (M=Ni, Pd, Pt) were successfully synthesized and characterized in their structure, magnetic properties, and host-guest chemistry interactions. The newly developed synthetic method to produce $Fe[M(C_3N)_4] \infty$ layers proved to be successful, and for the first time, an elongation of the networks within the

equatorial plane was performed without recurring to aromatic (multi-)ring systems or linear M^ICN₂ linkers. As a result, the desired regular 3D structure of the pzM analogues was retained without networks interpenetration. The addition of an acetylenic unit to the CN fragment confirmed to be an advantageous strategy, because, due to the linearity and low steric hindrance of the C₃N fragment, the elongation by just two carbon atoms results in a drastic increase of both volume of guest accessible voids and porosity of the resulting PCPs. Elongation along the c-axis with longer pillar ligands is not as effective, since these are based on multi-ring systems which are bulky and take away part of the pores' space. Consequently, extremely long ligands are needed to reach the same characteristics of voids volume and porosity of 9-11, but this often results in poor magnetic behavior and/or ligand incorporation. Another drawback is that enlarging the pores only along the c-axis can still prevent the uptake of larger guests, since they are not necessarily flat and rod-shaped. Most importantly, compounds 9-11 retained the desired SCO properties, showing hysteretic SCO as well as guest-dependent magnetic behavior, in-situ bidirectional chemo-switching of the spin state and memory effect, two properties that make this class of compounds particularly attractive. A negative aspect is of course the sensitivity of 9 towards temperature, which makes it very difficult to handle. As mentioned in the "Synthesis" paragraph, some synthetic aspects need to be improved, by finding new reaction pathways to obtain species containing the $[M(C_3N)_4]^{2-}$ fragment without recurring to the use of highly toxic trialkyl-Sn(IV) species. Another hindering feature is the amorphous nature of the materials and the consequent difficulty of growing single crystals. Different methods were tried out (solvent-diffusion, layering techniques, slow reaction-diffusion, hydrothermal crystallization, non-aqueous geldiffusion), but none worked. Since all these methods entail a fast introduction of Fe^{2+} , thinking of alternative methods with slow Fe^{2+} diffusion led to electrocrystallization, which finally was successful. Slow diffusion of Fe^{2+} seems to be a crucial step for crystal growth. A layering method with extremely diluted solutions was fortunately good enough to obtain crystalline powders, but despite countless attempts, no single crystals suitable for measurement could be grown with this method. Nonetheless, with this work we showed proof of principle for the synthesis of the materials, and we believe to have paved the way for a new approach to Hofmann-type SCO-PCPs. The present work is a starting point for further improvement of this new family of Hofmann-type SCO-PCPs. The next steps include ulterior extension of the frameworks, both in the ab plane through additional $C\equiv C$ subunits and also on the c-axis with longer pillar ligands. Lastly, functionalization of the pillar ligands will be an important step, because it could allow for a selective guestabsorption of large and functional guest.

KEYWORDS: Spin Crossover, Porous coordination polymer, chemo-switching, multifunctional materials

EXPERIMENTAL

Methodology

All operations involving Fe(II) were carried out under inert gas atmosphere (argon 5.0). The glassware was oven dried at 120 °C before use for at least 2 hours. All solvents for the complexation reactions were dried before use and stored over molecular sieve 3 Å under argon.³⁵ Unless otherwise stated, all starting materials were commercially obtained

and used without further purification. All NMR spectra were recorded in dry deuterated solvents on a Bruker Avance UltraShield 400 MHz. Chemical shifts are reported in ppm; ¹H and ¹³C shifts are referenced against the residual solvent resonance. For the measurement of MIR spectra, a Perkin-Elmer Spectrum 400, fitted with a coolable/heatable PIKE Gladi ATR unit was used within the range of 4000-100 cm⁻¹. The magnetic moment of the Fe(II) complexes was measured using a Physical Property Measurement System (PPMS®) by Quantum Design. The experimental setup consisted of a vibrating sample magnetometer attachment (VSM), bearing a brass sample holder with a quartz-glass powder container. The magnetic moment was determined in an external field of 1 T in the range of 10 K to 350 K. Quantification of guest-uptake was made by NMR measurements, dissolving the samples in DMSO and using the peak of pyrazine as reference. Variable temperature mid-range (4000 - 450 cm⁻¹) infrared spectra were recorded by the ATR technique on a Perkin Elmer Spectrum 400, fitted with a coolable/heatable PIKE Gladi ATR Unit.³⁶ Single crystals attached to a glass fiber by using perfluorinated oil, were examined at 200 K on a Bruker KAPPA APEX II diffractometer equipped with a CCD detector with Mo K_α radiation (Incoatec Microfocus Source IµS: 30 W, multilayer mirror, $\lambda=0.71073$ Å) and an Oxford Cryosystems Cryostream 800 Plus LT device. Data handling with integration and absorption correction by evaluation of multi-scans was done with the Bruker Apex5 suite³⁷. The structures were solved by direct methods³⁸; subsequent difference Fourier syntheses and least-squares refinements yielded the positions of the remaining atoms using the SHELXL software³⁹ implemented in the shelXle GUI tool.⁴⁰ For the iron(II) complexes, protons were placed at calculated positions and refined as riding on the parent C atoms. All non-

H atoms were refined with anisotropic displacement parameters. The refinement of the crystal structure in the averaged small unit cell in space group P4/mmm achieved R values (R1 = 0.058, wR2 = 0.189) as compared to (R1 = 0.085, wR2 = 0.286) for superstructure in the space group P4/mbm. Apart from the specific arrangement of the Pz molecules, there were no significant differences in the general atomic arrangement as well as interatomic atomic bond distances when comparing the two structure models. The powder X-ray diffraction measurements were carried out on a PANalytical X'Pert Pro diffractometer in Bragg–Brentano geometry using Cu $K_{\alpha 1,2}$ radiation filtered with a BBHD mirror and an X'Celerator linear detector. For in situ experiments below ambient temperature an Oxford PheniX Cryochamber from Oxford Cryosystems was used. The powder samples were mounted on an Anton Paar domed sample holder. The actual sample temperature was directly monitored by a thermocouple on the sample holder. The diffractograms were evaluated using the PANalytical program suite HighScorePlus, correcting for the background. For the single crystal growth via electrocrystallization an ISO-TECH IPS1810H DC laboratory power supply was used.

Single-crystal growth

The experimental setup for the crystal growth consisted of an H-tube with a frit, loaded with a MeCN solution of (n-Bu)₄N(BF₄) on one side (cathode) and a MeCN solution of pyrazine and 7 (after filtration on activated charcoal) on the other side (anode). An Fe wire was introduced on both sides and the H-tube was closed with two septa. A voltage of 1.5 V was applied between the two iron wires causing the slow anodic dissolution of the Fe wire. Square shaped, dark red single crystals formed on the glass walls anodic side. The setup is depicted in Figure 7.



Figure 7: experimental setup for the single-crystal growth via electrocrystallization

Synthesis

Synthesis tetraethylammoniumtetrachloronickelate (1): Nickel(II)chloride hexahydrate (10 g, 1 eq.) and tetraethylammoniumchloride (14.01 g, 2.01 eq.) were suspended in 50 mL EtOH and stirred for 18 h at RT. The bright green solution was concentrated until crystallization started and cooled to 0 °C. The precipitated turquoise solid was separated, washed with cold CH₂Cl₂ and dried under vacuum (11.1 g, 79,8% yield.).

Synthesis of tetraethylammoniumtetrachloropalladate (2): Palladium(II)chloride (1.5 g, 1 eq.) and tetraethylammoniumchloride (2.8 g, 2 eq.) were suspended in 20 mL MeNO₂ and heated for 18 h at 75 °C. The solvent was evaporated, and the dark red residue triturated in 10 mL CH₂Cl₂, cooled to 0 °C and filtrated. The solid was dried under vacuum and the product was isolated as a dark red powder (3.9 g, 90,7% yield).

Synthesis of tetraethylammoniumtetrachloroplatinate(3): Platinum(II)chloride (1.25 g, 1 eq.) and tetraethylammoniumchloride (1.56 g, 2 eq.) were suspended in 20 mL MeNO₂ and heated for 18 h at 75 °C. The solvent was evaporated, and the dark red residue triturated in 10 mL CH₂Cl₂, cooled to 0 °C and filtrated. The solid was dried under vacuum and the product isolated as a dark-red/brown powder (2.5 g, 90% yield).

Synthesis of 2-propynamide (4): a 250 mL single-neck round-bottom flask was cooled to -50 °C. Gaseous NH₃ was insufflated through a septum and condensed in the flask. Methyl propiolate (10 g, 1eq.) was added dropwise, and the reaction was left stirring at -40 °C for 4 h. After quick warming under N2 stream Et₂O was added to the orange solution, the precipitated solid was separated and the solvent was removed under reduced pressure yielding the product as an orange solid. (quantitative yield).

IR (neat, cm^{-1}): ν_{NH2} 3286, 3178; $\nu_{C=C}$ 2109; $\nu_{C=O}$ 1645, 1594

¹H NMR (400 MHz, DMSO) δ (ppm)=8.08 (s, 1H, NH₂), 7,62 (s, 1H, NH₂), 4.07

(s, 1H, CH)

Synthesis of 3-(tributylstannyl)propiolonitrile (5): The synthesis was conducted under inert atmosphere with standard Schlenk technique. A 100 mL Schlenk-flask was charged with bis(tributyltin) oxide (31.16 g, 1 eq.), dry benzene (20 mL) and 3 Å molecular sieves, and cooled to -196 °C. The flask was connected via a glas tube to a 500 mL Schlenk flask charged with 4 (8.21 g, 0.12 mol, 2 eq.). The system was evacuated and filled with Ar three times respectively, and finally P₂O₅ (50.6 g, 6 eq) was added in the 500 mL flask under Ar stream. The system was evacuated to 1mbar and kept under vacuum for the whole reaction time. The reaction mixture was heated to 200 °C with a heating mantle, and vigorous reaction was observed, and the formation of large amounts of vapor indicated the formation of 2-propynenitrile. This was accompanied by a foaming of the pentoxide mixture. After approximately 15 min the dehydration of the amide was complete (no further gas evolution was observed), and the reaction mixture turned to a black tar. The system was vented with Ar and the solid product was left to warm up to room temperature and further stirred for 10 min. All solids were filtered off and the crude (dark brown liquid) was distilled under reduced pressure (b.p. 110 °C at 0.7 mbar) to isolate the product as a colorless liquid with a pungent smell (19 g, 94% yield).

IR (neat, cm⁻¹): ν_{CN} 2247, $\nu_{C\equiv C}$ 2038

 1 H NMR (400 MHz, CD₂Cl₂): δ (ppm) = 1.65 - 1.56 (m, 6H, -Sn-CH2-), 1.41 -

 $1.29 \text{ (m, 6H, - CH2C} + 2CH2-), } 1.17 - 1.12 \text{ (m, 6H, }$

-CH2CH3), 0.93 (t, J = 7.3 Hz, 9H, -CH3)

¹³C NMR (101 MHz, CD₂Cl₂): δ (ppm) = 105.41, 100.72, 29.34, 27.55, 13.97, 12.39

Synthesis of Tetraethylammonium tetrakis(cyanoethynyl)nickelate (6): The reaction was conducted under inert atmosphere with standard Schlenk technique. 1 (2,5 g, 1eq.) was dissolved in 25 mL dry MeCN and the solution was cooled to 0 °C. 5 (11.07g, 6eq) was added under cooling and the solution was left stirring for 18 h. The mixture was filtered with a pressure filter to separate the solid deposit and the filtrate was poured in dry Et₂O (ca 200 mL). A precipitate formed and it was again separated via pressure filtration and washed 3 times with small portions of Et₂O. The solid was finally dried under vacuum, to isolate the product as a dark-grey solid (1.5 g, 53.3% yield).

IR (neat, cm⁻¹): $\nu_{\text{C}=\text{N}} 2203$, $\nu_{\text{C}=\text{C}} 2038$, $\nu_{\text{Ni-C}} 517$

Synthesis of Tetraethylammonium tetrakis(cyanoethynyl)palladate (7): Same procedure as for 6, with 2 g (1 eq.) of 2 and 6 g (6 eq) of 5. The product was isolated as a brown solid (1.2 g, 71.8% yield).

IR (neat, cm⁻¹):
$$\nu_{C=N} 2208$$
, $\nu_{C=C} 2049$, $\nu_{Pd-C} 516$

Synthesis of Tetraethylammonium tetrakis(cyanoethynyl)platinate (8): Same procedure as for 6, with 2 g (1 eq.) of 3 and 6.83 g (6 eq) of 5. The product was isolated as a brown solid (1.7 g, 86.5% yield).

IR (neat, cm⁻¹):
$$\nu_{\text{C}=\text{N}} 2214, \nu_{\text{C}=\text{C}} 2050, \nu_{\text{Pt-C}} 517$$

Synthesis of anhydrous Fe(BF₄)₂: A three-neck Schlenk-flask was charged with reduced iron powder in 40 mL THF and equipped with a reflux condenser and a septum. HBF₄·Et₂O was added dropwise and the mixture was heated to reflux and let stirring for 5 days (until all iron powder was consumed). The mixture consisting of solvent and undissolved Fe(BF₄)₂ was cooled in an ice bath to let the solid settle, and the solvent was removed. The solid was washed three times with dry Et₂O and dried under vacuum to isolate the product as a white powder (quant. yield).

Synthesis of $[Fe(pz)][Ni(C_3N)_4]$ (9): a microwave vial was charged with 2 mL dry MeCN, pyrazine (4.63 mg, 1 eq) and $Fe(BF_4)_2$ (13.25 mg, 1 eq). 30 mg (0.06 mmol, 1 eq) of 6 were dissolved in 2 mL dry MeCN and the solution was filtered over activated charcoal in a Pasteur pipette directly into the vial. Immediate precipitation of a yellow powder was observed. The suspension was centrifuged, the solvent removed with a syringe, and the solid was dried under vacuum. The product was isolated as a yellow-orange powder (15.1 mg, 65.8% yield).

IR (neat,
$$cm^{-1}$$
):

$$\nu_{\rm C=N} \ 2215, \ \nu_{\rm C=C} \ 2038, \ \nu_{\rm Ni-C} \ 517$$

Synthesis of $[Fe(pz)][Pd(C_3N)_4]$ (10): Same procedure as for 9, with 4.24 mg (1 eq.) pyrazine, 12.14 mg (1 eq.) of $Fe(BF_4)_2$ and 30 mg (0.053 mmol, 1 eq.) of 7. The product was isolated as a yellow-orange powder (18 mg, 76.9% yield).

IR (neat,
$$cm^{-1}$$
):

$$\nu_{C=N} 2223, \nu_{C=C} 2050, \nu_{Pd-C} 516$$

Synthesis of [Fe(pz)][Pt(C₃N)₄] (11): Same procedure as for 9, with 3.66 mg (1 eq.) pyrazine, 10.5 mg (1 eq.) of Fe(BF₄)₂ and 30 mg (0.046 mmol, 1 eq.) of 8. The product was isolated as a orange powder (21.3 mg, 87.6% yield).

IR (neat,
$$cm^{-1}$$
):

$$\nu_{C \equiv N} 2214, \nu_{C \equiv C} 2048, \nu_{Pt-C} 517$$

REFERENCES

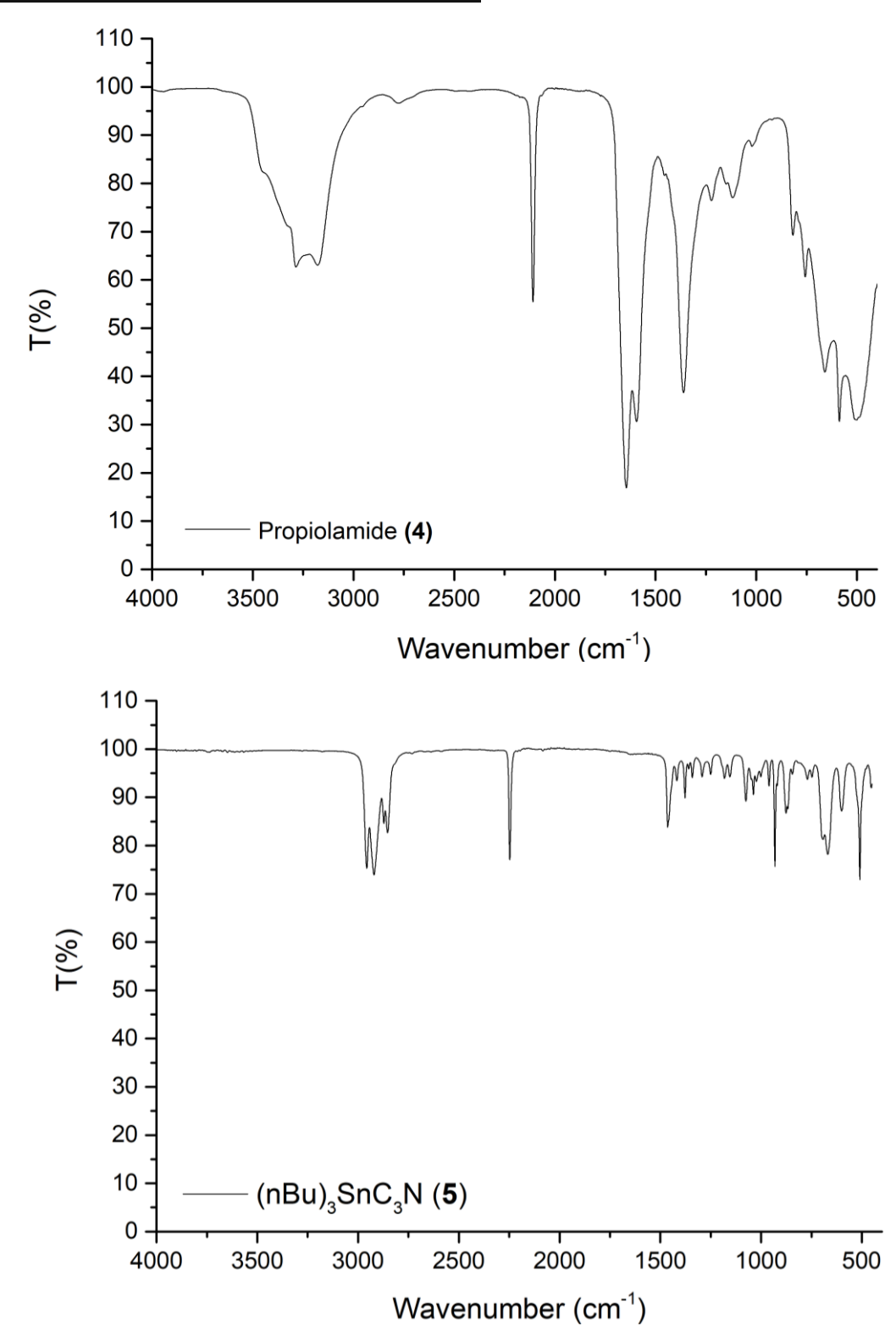
- 1. Hou, C.-C.; Xu, Q., Metal-Organic Frameworks for Energy. Advanced Energy *Materials* **2018**, 1801307.
- Kumar, K. V.; Preuss, K.; Titirici, M.-M.; Rodríguez-Reinoso, F., Nanoporous Materials for the Onboard Storage of Natural Gas. Chemical Reviews 2017, 117 (3), 1796-1825.
- Yu, J.; Xie, L.-H.; Li, J.-R.; Ma, Y.; Seminario, J. M.; Balbuena, P. B., CO2 3. Capture and Separations Using MOFs: Computational and Experimental Studies. Chemical Reviews 2017, 117 (14), 9674-9754.
- Lin, R.-B.; Xiang, S.; Xing, H.; Zhou, W.; Chen, B., Exploration of porous 4. metal-organic frameworks for gas separation and purification. Coordination Chemistry Reviews 2017.
- Adil, K.; Belmabkhout, Y.; Pillai, R. S.; Cadiau, A.; Bhatt, P. M.; Assen, A. H.; Maurin, G.; Eddaoudi, M., Gas/vapour separation using ultra-microporous metalorganic frameworks: insights into the structure/separation relationship. Chemical Society Reviews 2017, 46 (11), 3402-3430.
- Li, H.; Wang, K.; Sun, Y.; Lollar, C. T.; Li, J.; Zhou, H.-C., Recent advances in gas storage and separation using metal-organic frameworks. Materials Today 2018, 21 (2), 108-121.
- Li, J.-R.; Kuppler, R. J.; Zhou, H.-C., Selective gas adsorption and separation in 7. metal-organic frameworks. Chemical Society Reviews 2009, 38 (5), 1477.
- Kim, K. C., Design strategies for metal-organic frameworks selectively capturing harmful gases. Journal of Organometallic Chemistry 2018, 854, 94-105.
- Jiao, L.; Wang, Y.; Jiang, H.-L.; Xu, Q., Metal-Organic Frameworks as Platforms for Catalytic Applications. Adv Mater 2018, 30 (37), 1703663.
- Zhang, J.; Chen, Z., Metal-organic frameworks as stationary phase for application in chromatographic separation. Journal of Chromatography A 2017, 1530, 1-18.
- 11. Gütlich, P.; Goodwin, H. A., Spin Crossover in Transition Metal Compounds I-III. In Topics in Current Chemistry, [Online] Springer Berlin Heidelberg,: Berlin, Heidelberg, 2004. SpringerLink http://dx.doi.org/10.1007/b40394-9 MIT Access Only.
- Gütlich, P., Spin Crossover Quo Vadis? European Journal of Inorganic 12. Chemistry **2013**, (5-6), 581-591.
- Shepherd, H. J.; Bartual-Murgui, C.; Molnar, G.; Real, J. A.; Munoz, M. C.; 13. Salmon, L.; Bousseksou, A., Thermal and pressure-induced spin crossover in a novel three-dimensional Hoffman-like clathrate complex. New J Chem 2011, 35 (6), 1205-1210.
- 14. Decurtins, S.; Gutlich, P.; Hasselbach, K. M.; Hauser, A.; Spiering, H., Light-Induced Excited-Spin-State Trapping in Iron(Ii) Spin-Crossover Systems - Optical Spectroscopic and Magnetic-Susceptibility Study. Inorg Chem 1985, 24 (14), 2174-2178.
- Decurtins, S.; Gutlich, P.; Kohler, C. P.; Spiering, H., New Examples of Light-Induced Excited Spin State Trapping (Liesst) in Iron(Ii) Spin-Crossover Systems. J Chem Soc Chem Comm 1985, (7), 430-432.
- Kahn, O.; Martinez, C. J., Spin-transition polymers: From molecular materials toward memory devices. Science 1998, 279 (5347), 44-48.

- Mahfoud, T.; Molnar, G.; Cobo, S.; Salmon, L.; Thibault, C.; Vieu, C.; Demont, P.; Bousseksou, A., Electrical properties and non-volatile memory effect of the [Fe(HB(pz)(3))(2)]spin crossover complex integrated in a microelectrode device. Appl Phys Lett 2011, 99 (5).
- 18. Zhu, L.; Zou, F.; Gao, J. H.; Fu, Y. S.; Gao, G. Y.; Fu, H. H.; Wu, M. H.; Lu, J. T.; Yao, K. L., The integrated spintronic functionalities of an individual high-spin state spin-crossover molecule between graphene nanoribbon electrodes. Nanotechnology **2015,** 26 (31).
- 19. Manrique-Juarez, M. D.; Rat, S.; Mathieu, F.; Saya, D.; Séguy, I.; Leïchlé, T.; Nicu, L.; Salmon, L.; Molnár, G.; Bousseksou, A., Microelectromechanical systems integrating molecular spin crossover actuators. Appl Phys Lett 2016, 109 (6), 061903.
- Hofmann, K. A.; Küspert, F., Verbindungen von Kohlenwasserstoffen mit Metallsalzen. Zeitschrift für anorganische Chemie 1897, 15 (1), 204-207.
- Kitazawa, T.; Gomi, Y.; Takahashi, M.; Takeda, M.; Enomoto, M.; Miyazaki, 21. A.; Enoki, T., Spin-crossover behaviour of the coordination polymer FeII(C5H5N)2NiII(CN)4. Journal of Materials Chemistry 1996, 6 (1), 119-121.
- Niel, V.; Martinez-Agudo, J. M.; Muñoz, M. C.; Gaspar, A. B.; Real, J. A., Cooperative Spin Crossover Behavior in Cyanide-Bridged Fe(II)-M(II) Bimetallic 3D Hofmann-like Networks (M = Ni, Pd, and Pt). *Inorg Chem* **2001**, *40* (16), 3838-3839.
- Ohba, M.; Yoneda, K.; Agustí, G.; Muñoz, M. C.; Gaspar, A. B.; Real, J. A.; Yamasaki, M.; Ando, H.; Nakao, Y.; Sakaki, S.; Kitagawa, S., Bidirectional Chemo-Switching of Spin State in a Microporous Framework. Angewandte Chemie *International Edition* **2009**, 48 (26), 4767-4771.
- Southon, P. D.; Liu, L.; Fellows, E. A.; Price, D. J.; Halder, G. J.; Chapman, K. 24. W.; Moubaraki, B.; Murray, K. S.; Letard, J. F.; Kepert, C. J., Dynamic Interplay between Spin-Crossover and Host-Guest Function in a Nanoporous Metal-Organic Framework Material. J Am Chem Soc 2009, 131 (31), 10998-11009.
- Bartual-Murgui, C.; Ortega-Villar, N. A.; Shepherd, H. J.; Muñoz, M. C.; Salmon, L.; Molnár, G.; Bousseksou, A.; Real, J. A., Enhanced porosity in a new 3D Hofmann-like network exhibiting humidity sensitive cooperative spin transitions at room temperature. Journal of Materials Chemistry 2011, 21 (20), 7217-7222.
- Muñoz-Lara, F. J.; Gaspar, A. B.; Muñoz, M. C.; Ksenofontov, V.; Real, J. A., 26. Novel Iron(II) Microporous Spin-Crossover Coordination Polymers with Enhanced Pore Size. *Inorg Chem* **2012**, *52* (1), 3-5.
- Niel, V.; Muñoz, M. C.; Gaspar, A. B.; Galet, A.; Levchenko, G.; Real, J. A., 27. Thermal-, Pressure-, and Light-Induced Spin Transition in Novel Cyanide-Bridged FeIIbAgI Bimetallic Compounds with Three-Dimensional Interpenetrating Double Structures {FeIILx[Ag(CN)2]2}·G. Chemistry - A European Journal 2002, 8 (11), 2446.
- 28. Clements, J. E.; Price, J. R.; Neville, S. M.; Kepert, C. J., Perturbation of Spin Crossover Behavior by Covalent Post-Synthetic Modification of a Porous Metal-Organic Framework. Angewandte Chemie International Edition 2014, 53 (38), 10164-10168.
- 29. Li, J.-Y.; Ni, Z.-P.; Yan, Z.; Zhang, Z.-M.; Chen, Y.-C.; Liu, W.; Tong, M.-L., Cyanide-bridged bimetallic 3D Hoffman-like coordination polymers with tunable magnetic behaviour. Crystengcomm 2014, 16 (28), 6444-6449.
- Li, J.-Y.; Chen, Y.-C.; Zhang, Z.-M.; Liu, W.; Ni, Z.-P.; Tong, M.-L., Tuning the Spin-Crossover Behaviour of a Hydrogen-Accepting Porous Coordination Polymer

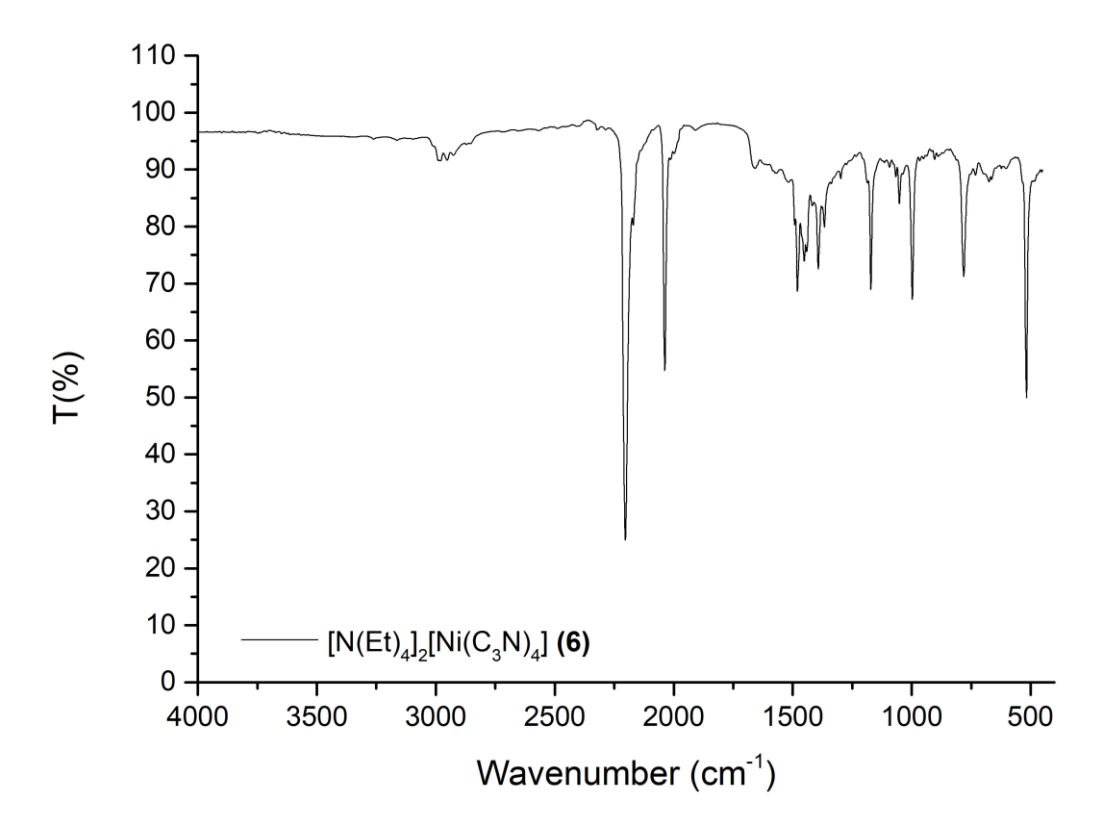
- by Hydrogen-Donating Guests. Chemistry A European Journal 2015, 21 (4), 1645-1651.
- 31. Zhou, Y.; Arif, A. M.; Miller, J. S., The preparation and characterization of square-planar tetrakis(cyanoacetylide) complexes: $[MII(C \square C - C \square N)4]2 - (M = Ni, Pd,$ Pt). Chem Commun 1996, (16), 1881-1882.
- 32. France, S. c. d.; chimie, S. f. d., Bulletin de la Société chimique de France. Société française de chimie: 1993.
- Spek, A., Structure validation in chemical crystallography. Acta 33. *Crystallographica Section D* **2009**, *65* (2), 148-155.
- Ohtani, R.; Hayami, S., Guest-Dependent Spin-Transition Behavior of Porous Coordination Polymers. Chemistry - A European Journal 2017, 23 (10), 2236-2248.
- W. L. F. Armarego, D. D. P., Purification of Laboratory Chemicals, 4th ed.,. 35. Butterworth-Heinemann, Oxford 1997.
- Müller, D.; Knoll, C.; Seifried, M.; Weinberger, P., ATR or transmission—A variable temperature study comparing both techniques using [Fe(3ditz)3](BF 4)2 as model system. Vibrational Spectroscopy 2016, 86, 198-205.
- Bruker (2023) APEX5 software suite. Bruker AXS Inc., Madison, Wisconsin, 37. USA.
- 38. Sheldrick, G., SHELXT - Integrated space-group and crystal-structure determination. Acta Crystallographica Section A 2015, 71 (1), 3-8.
- Sheldrick, G., Crystal structure refinement with SHELXL. Acta Crystallographica Section C 2015, 71 (1), 3-8.
- Hübschle, C. B.; Sheldrick, G. M.; Dittrich, B., ShelXle: a Qt graphical user interface for SHELXL. Journal of Applied Crystallography 2011, 44 (6), 1281-1284.

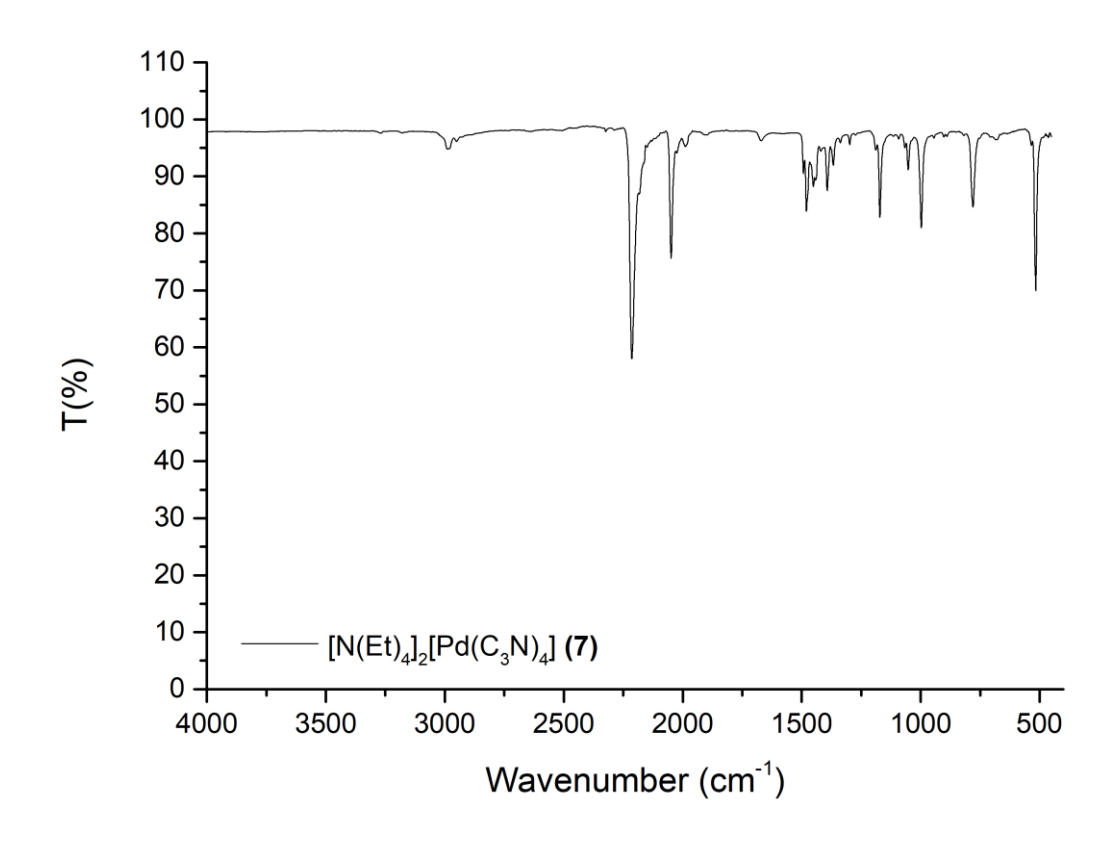
SUPPORTING INFORMATION

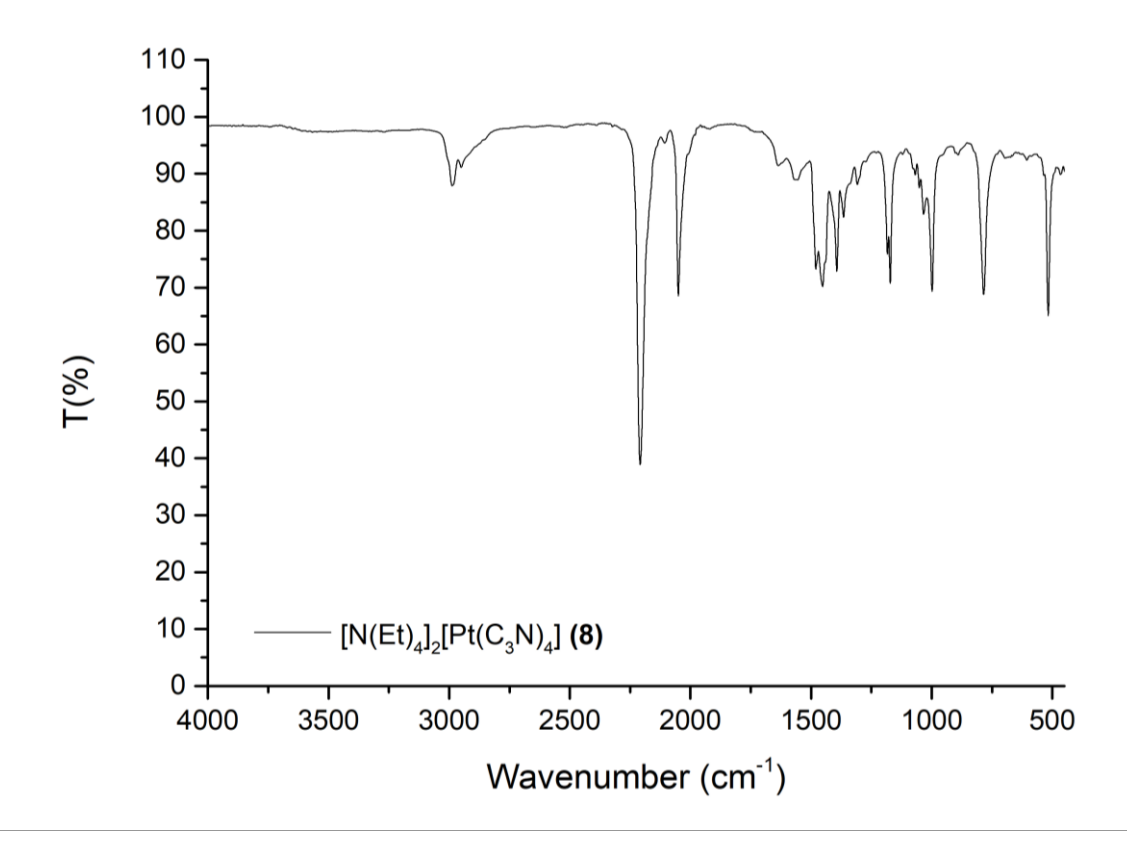
INFRARED SPECTRA OF COMPOUNDS 4-11

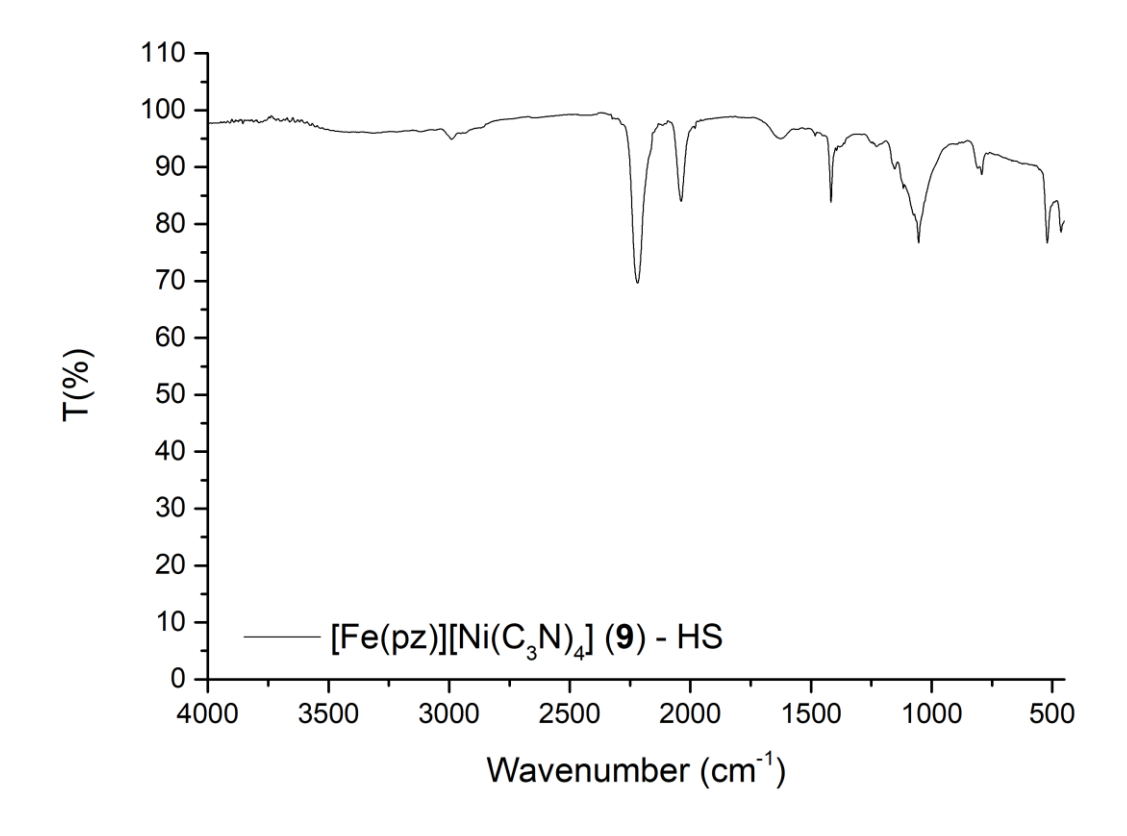


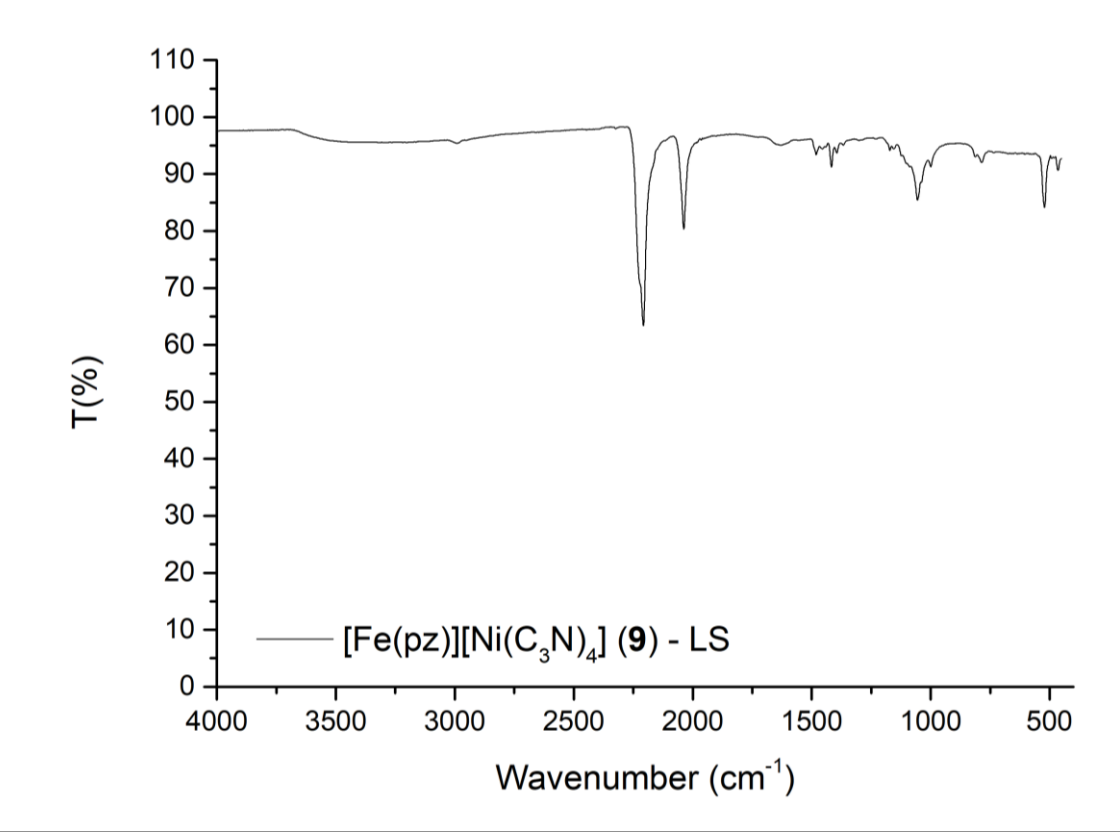


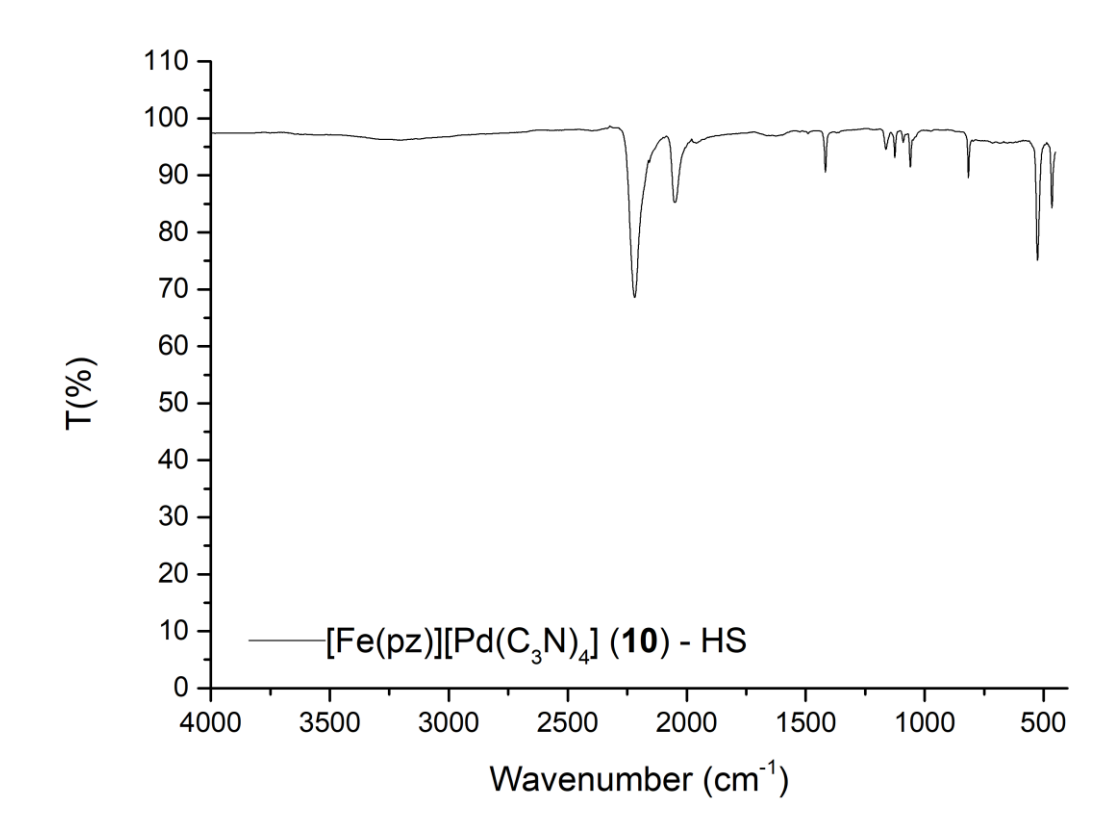


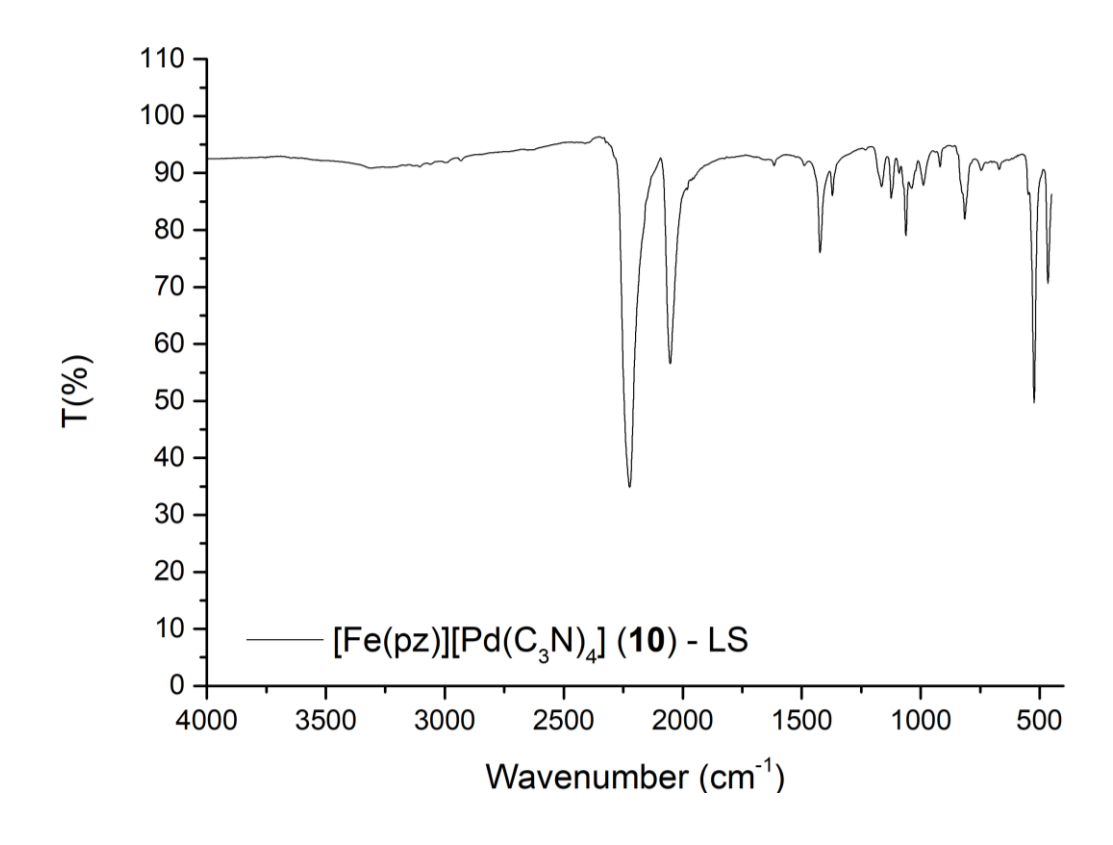


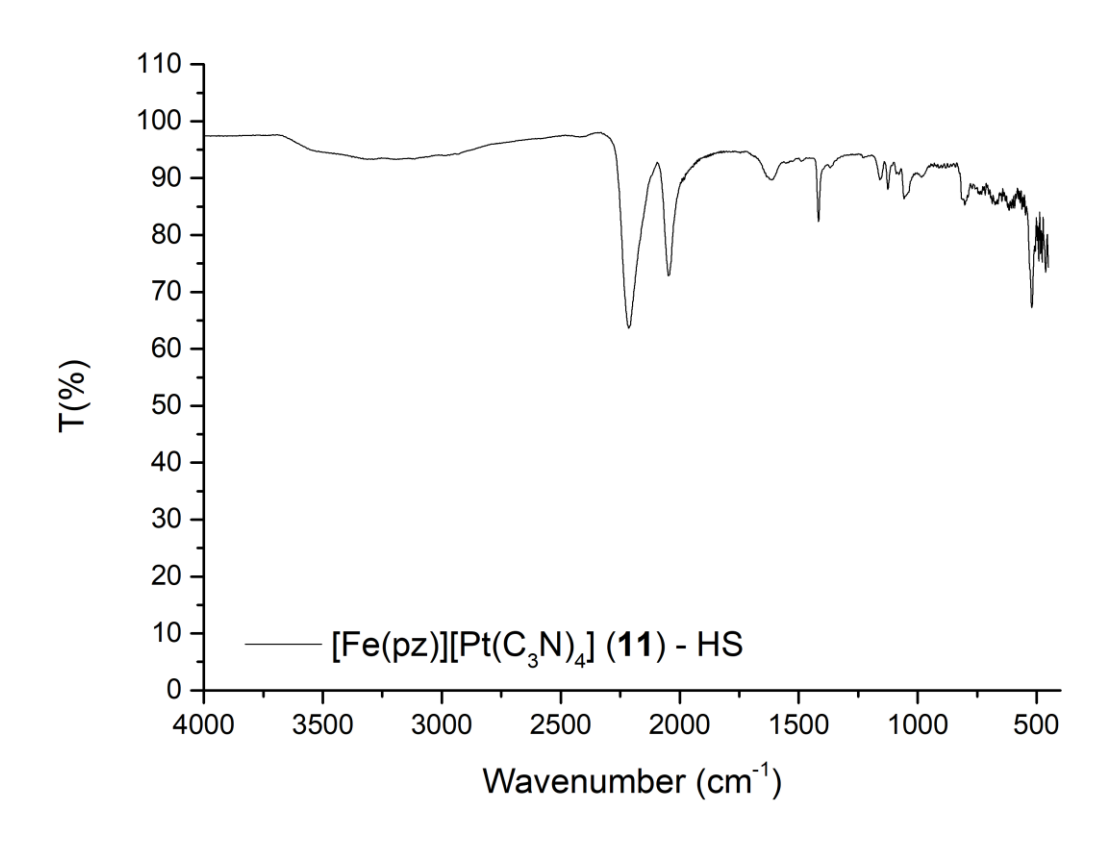


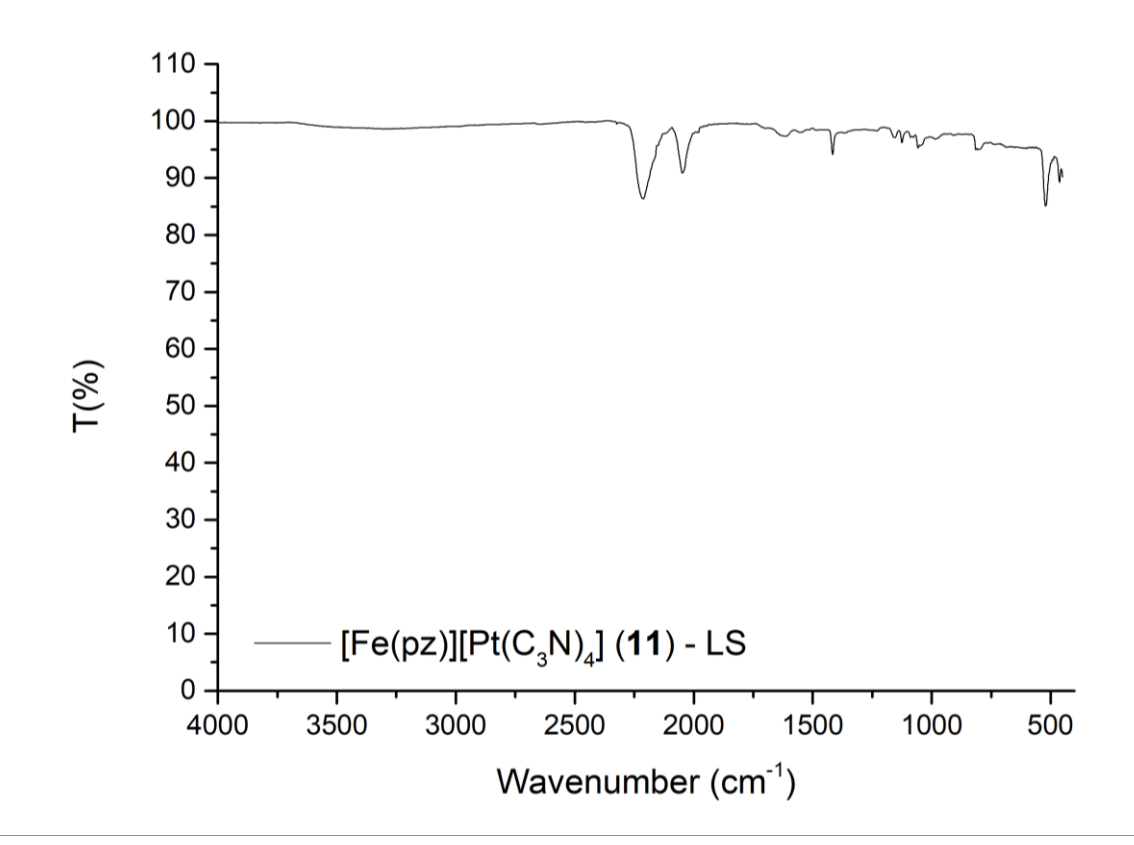




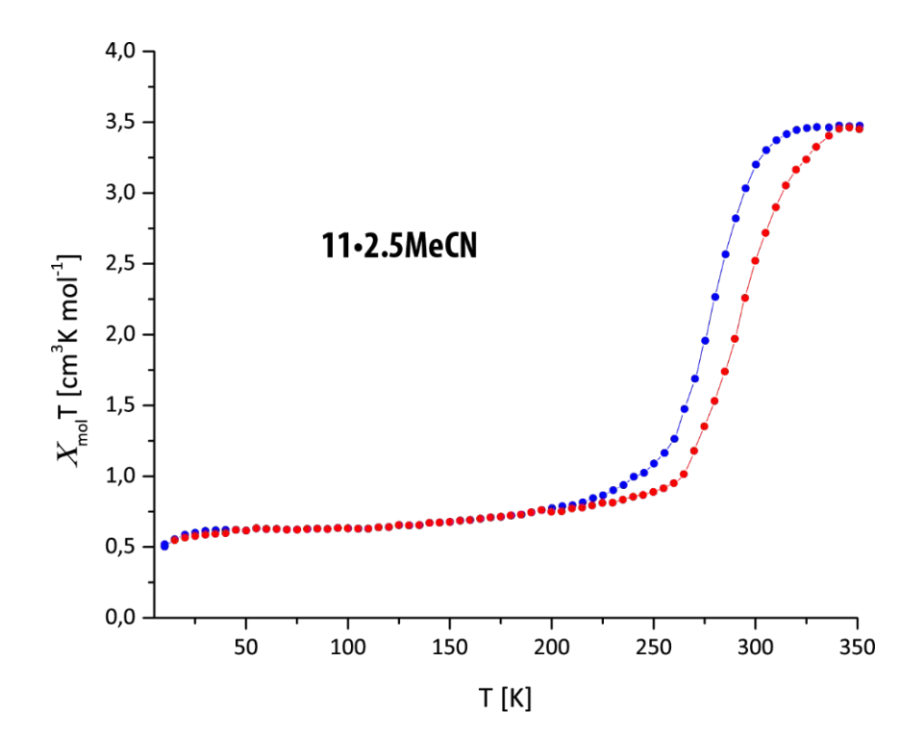


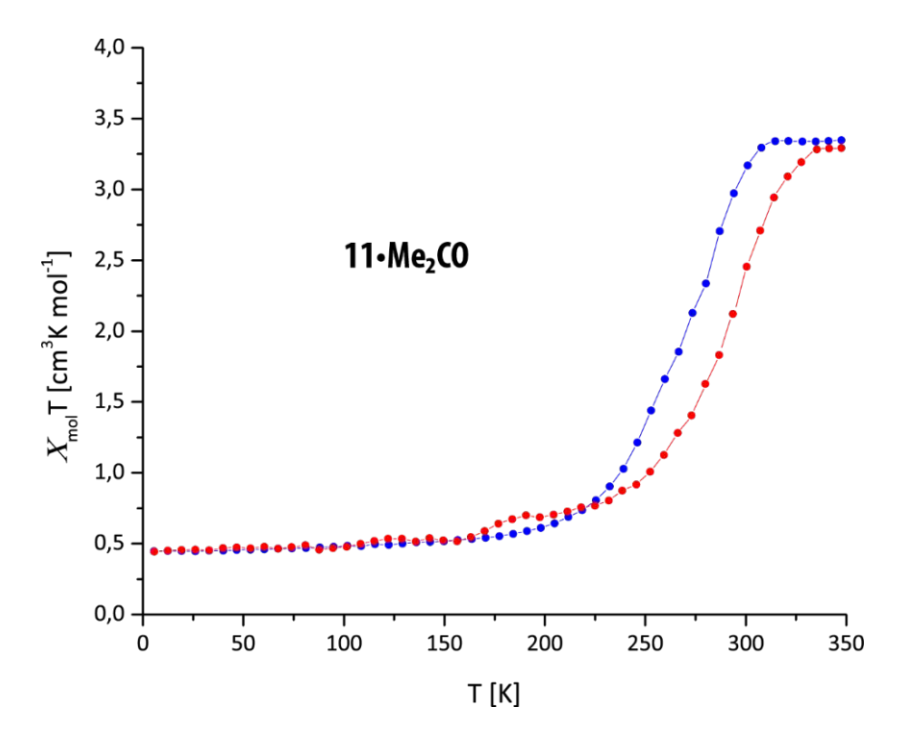


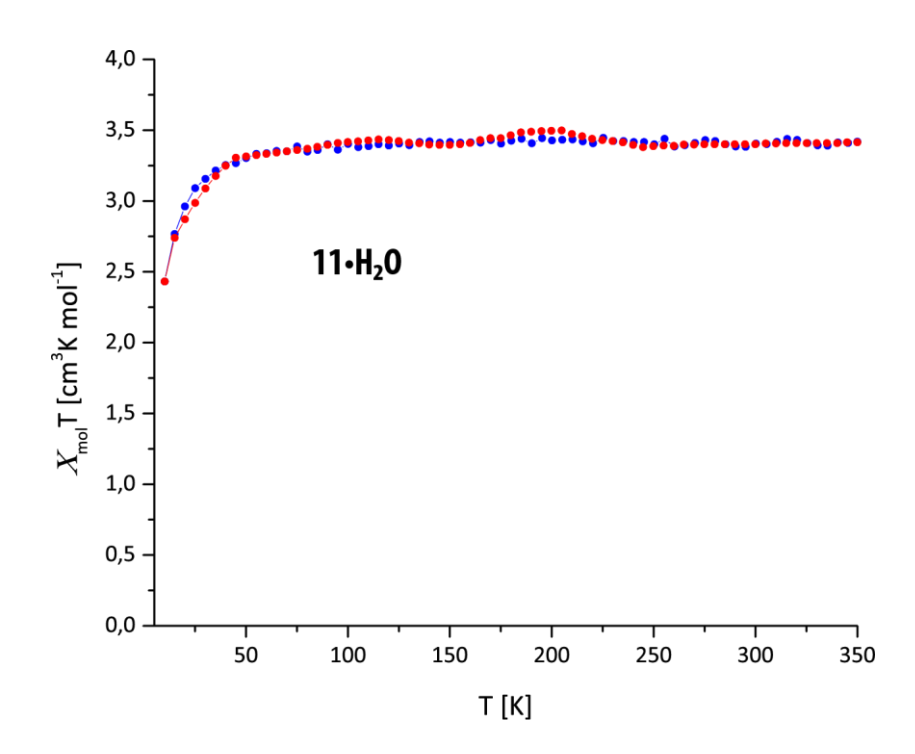


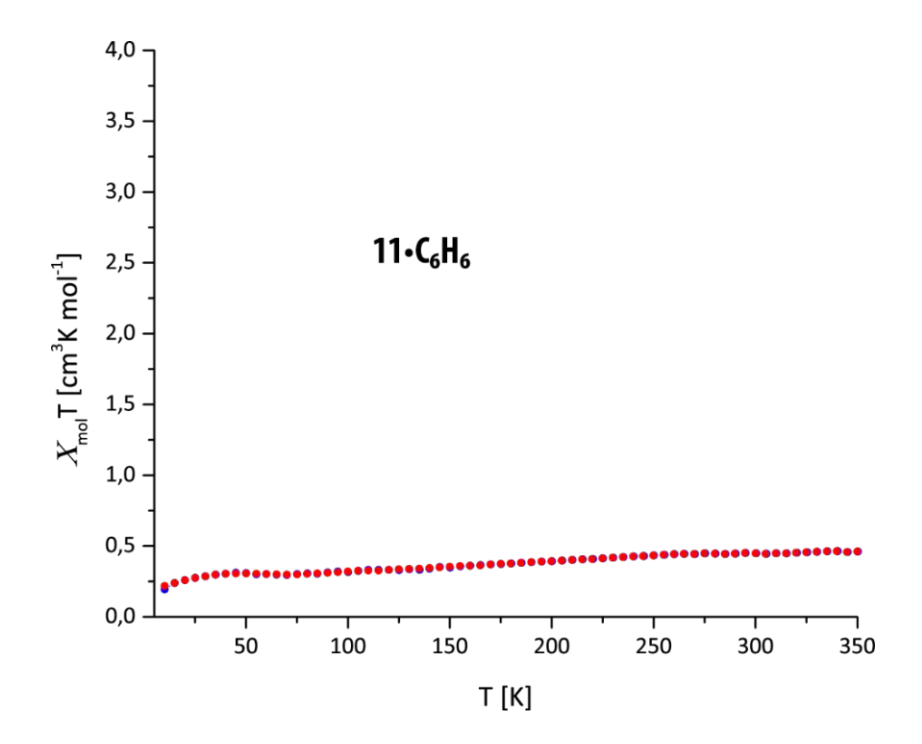


TEMPERATURE DEPENDENT MAGNETIC SUSCEPTIBILITY OF **PCP•GUEST COMPOSITES**







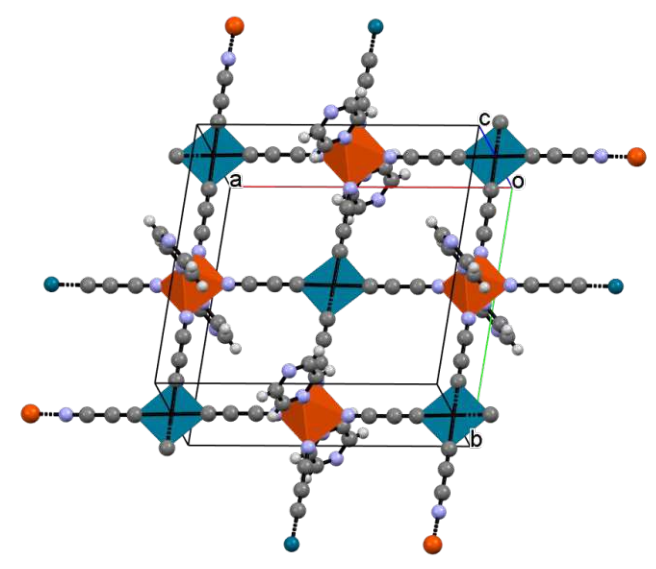


SELECTED BOND-LENGTHS FOR 10

Table S1: Selected bond-lengths for 10 in the small unit cell

-	
Atom2	Length
C3	1.982
N1	1.928
N2	1.99
C1	1.137
C2	1.38
C3	1.21
	C3 N1 N2 C1 C2

SUPERSTRUCTURE-SPACE GROUP P4/mbm



Supplementary Figure 1: Superstructure of 10 in the space group P4/mbm with specific arrangement of the pz rings. The coordination figures around Fe and Pd are indicated with orange and petrol color, respectively. Grey =C, blue=N, white=H

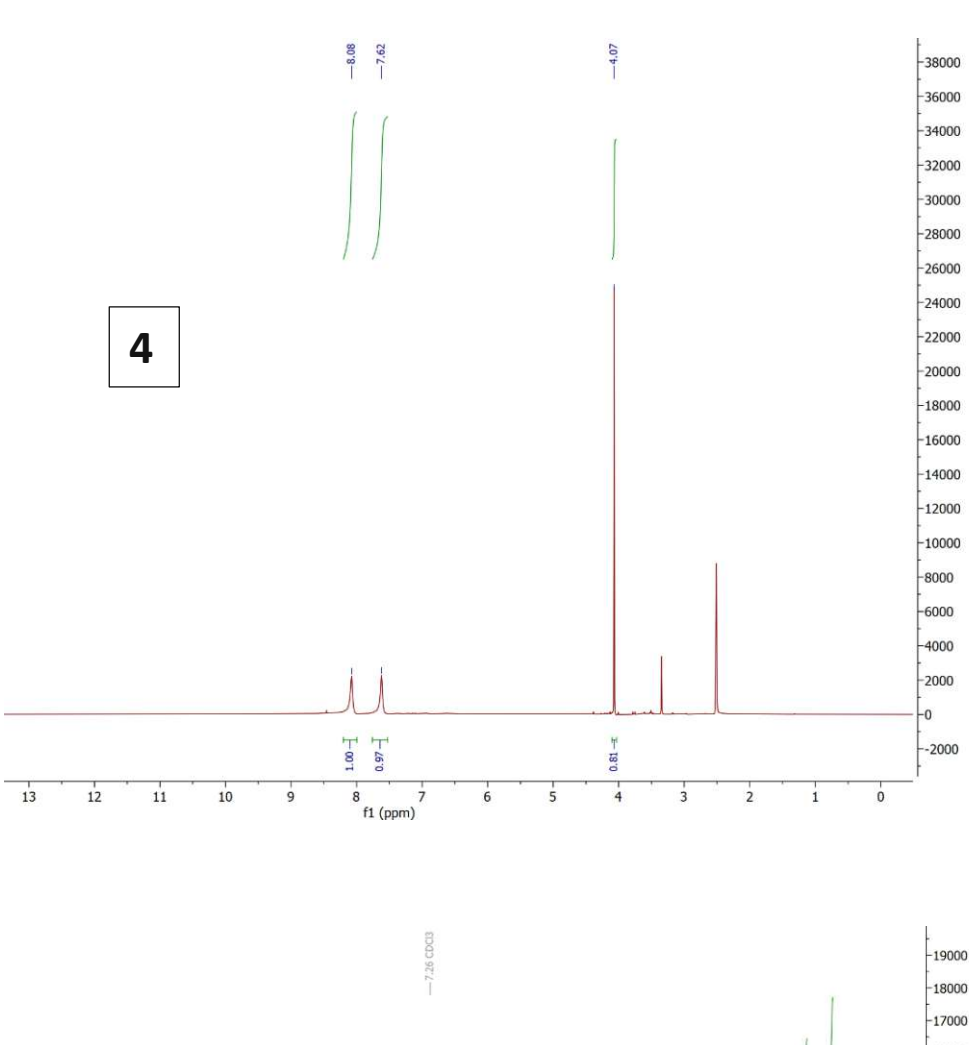
Table S1: Selected bond-lengths for 10 in the large unit cell

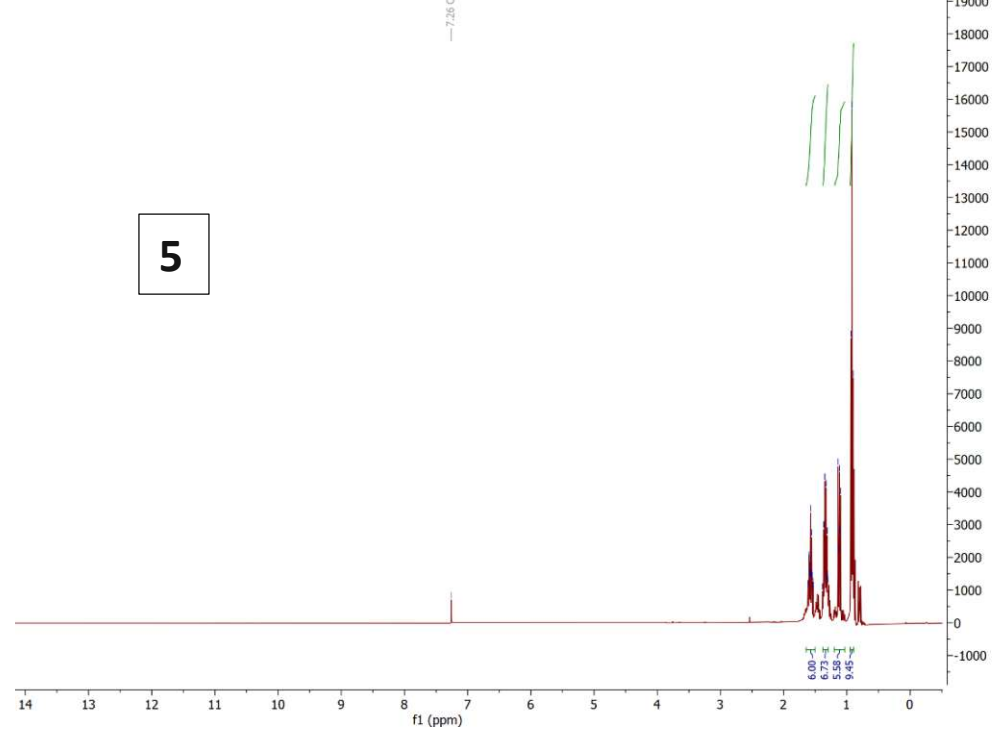
Atom1	Atom2	Length
Pd	C3	1.984
Fe	N1	1.93
Fe	N2	1.986
N1	C1	1.137
C1	C2	1.374
C2	C3	1.209

Table S2: Crystallographic parameters for 10 in the large unit cell

	10
Formula	C ₁₆ H ₄ FeN ₆ Pd
Weight [g mol-1]	442.5
T [K]	200
Colour	red
Shape	block
Crystal System	tetragonal
Space Group	P4/mbm
a [Å]	15.266 (3)
c [Å]	6.759(2)
V [ų]	1575.2
Z	2
ρcalc. [g cm-3]	0.933
μ [mm-1]	1.035
Measured Refl's.	24045
Unique Refl's	926
F(000)	428
Rint	0.0919
GooF	1.131
R1	0.0855
wR2	0.2859
No. of parameters	41
CCDC	2366167

NMR SPECTRA OF COMPOUNDS 4-5







CONCLUSIONS

With the present work, all the objectives defined in the abstract could be achieved, since all the target compounds were successfully prepared and characterized.

The first part of the work yielded an unexpected result: 1-propyl-1H-imidazole was revealed as an extreme versatile ligand for Fe(II) compounds, and a simple change in solvent and/or reaction temperature can lead to very different products, so much that a whole new family of complexes with different nuclearity was obtained.

The homoleptic complex, which was the main subject of the study, was unfortunately not susceptible of thermal spin-transition, nor were the other complexes. The comparison between $[Fe(PrIm)_6](BF_4)_2$ with $[Fe(PrTz)_6](BF_4)_2$ seems to indicate that the different behavior of the two complexes has a dual nature. By changing the azole ring, ligand fields of different strength were expected, but UV-vis measurements show almost equal values of 10Dq for the two complexes: this means that the energy difference between the HS and the LS state in the imidazole complex is too high to be overcome by thermal energy input. Another factor that needs to be taken into consideration is the very poor molecular packing, as showed by SC-XRD measurements: even at 100 K the thermal ellipsoids of the propyl group show high disorder, which translates in poor cooperativity. Highpressure experiments suggest that this second aspect has a major impact in the magnetic behavior of the complex; when a crystalline specimen was subjected to 11GPa hydrostatic pressure, hence a tighter packing was imposed, the color change from white to magenta, typical for the HS to LS transition, could be observed.

The most interesting aspect of the study was without doubt the Fe₄O₄ cubane-like cluster. A screening of different reaction conditions suggests that it is the thermodynamic product of the reaction, whereas the homoleptic complex is the kinetic one. Further investigation of the compound needs to be done, especially in regard of its potential redox properties.

The second paper showed that using ligands bearing a second functionality capable of creating an H-bond network is a successful strategy to improve cooperativity in SCOcompounds. The only exception is represented by the 3-COOH-Tz ligand, and the cause is with all probability of structural nature: the ligand itself could not be easily isolated as a fine powder as the other ones, it had an oily and gluey texture and only after several washing steps a solid could be obtained, and its complexes were the only one for which single crystals could not be grown. The second part of the study was unfortunately not successful, although a previously unreported Gd-oxo complex was isolated. A different synthetic strategy is needed to prepare the desired mixed-metallic complexes.

The last part of the work was for sure the most challenging and demanding, but it was also the most satisfactory, since all the goals could be reached.

The synthetic protocols for the preparation of the $[M(C_3N)_4]^{2-}$ linkers were optimized and the yields improved, and the desired Hofmann-type SCO-PCPs were successfully synthesized. The expansion on the ab-plane was performed without additional metal linker, and as a result, the desired 3D structure was retained. Although single crystals could solely be grown for the Pd-species, crystalline powders were obtained for the Ni and Pt species, which gave structural confirmation for these complexes as well.

Both pore volume and porosity show a substantial increase, not only in respect to the parent compounds based on $[M(CN)_4]^2$ linkers, but also in comparison to other enlarged Hofmann-type SCO-PCPs. The proposed elongation on the ab-plane is a successful strategy because thanks to the linearity and low steric hindrance of the C₃N fragment, the linear elongation is very well reflected in the volume of guest accessible voids and porosity. To the best of our knowledge, the compounds presented the highest value of porosity reported so-far for this class of compounds.

In addition to that, the observed magnetic behavior proved to be guest dependent, and as for $[Fe(pz)][M(CN)_4]$ the guest molecules govern the spin transition and the spin temperature, with some cases where the guest stabilizes one spin state at all temperatures. Finally, bidirectional chemo-switching and a memory effect were observed, giving confirmation of the environment-responsive nature of the compounds.

Building on these results, the next steps will consist in further expansion of the networks and functionalization of the pillar ligands for a selective absorption of large, functional guests.

With the present work, both fundamental and application-oriented aspects of SCOcompounds were investigated, and although some minor negative aspects are present, the main set goals could all be reached.

The reported result will hopefully help the advancement of research in the field, and especially with the last part of the work, the implementation of SCO-compounds for chemosensing applications is nearer to become reality.

References

- [1] P. Gütlich and H. A. Goodwin in Spin Crossover in Transition Metal Compounds I, Vol. Springer Berlin Heidelberg, Berlin, Heidelberg, 2004, pp. 1 online resource (xiii, 341 pages).
- [2] P. Gütlich and H. A. Goodwin, Spin Crossover in Transition Metal Compounds II, Springer, 2004, p.
- [3] P. Gütlich and H. A. Goodwin, Spin Crossover in Transition Metal Compounds III, Springer, 2004, p.
- [4] M. A. Halcrow in Spin-crossover materials properties and applications, Vol. Wiley-Blackwell, Oxford, 2013, p. 1 online resource.
- [5] L. Cambi and L. Szego, Berichte Der Deutschen Chemischen Gesellschaft 1931, 64, 2591-2598.
- [6] D. F. Evans, Journal of the Chemical Society (Resumed) 1959, 2003-2005.
- [7] O. Kahn and C. J. Martinez, Science 1998, 279, 44-48.
- [8] P. Weinberger and M. Grunert, Vibrational Spectroscopy 2004, 34, 175-186.
- [9] P. Gütlich, E. Bill and A. X. Trautwein, Mössbauer Spectroscopy and Transition Metal Chemistry: Fundamentals and Applications, Springer Berlin Heidelberg, 2010, p.
- [10] P. Gütlich, V. Ksenofontov and A. B. Gaspar, Coordination Chemistry Reviews 2005, *249*, 1811-1829.
- [11] A. H. Ewald, R. L. Martin, E. Sinn and A. H. White, Inorganic Chemistry 1969, 8, 1837-1846.
- [12] S. Klokishner, J. Linares and F. Varret, Chemical Physics 2000, 255, 317-323.
- [13] A. B. Gaspar, G. Molnár, A. Rotaru and H. J. Shepherd, Comptes Rendus Chimie 2018, *21*, 1095-1120.
- [14] J. J. McGravey and I. Lawthers, Journal of the Chemical Society, Chemical Communications 1982, 906-907.
- [15] S. Decurtins, P. Gutlich, C. P. Kohler, H. Spiering and A. Hauser, Chemical Physics Letters 1984, 105, 1-4.
- [16] S. Decurtins, P. Gutlich, K. M. Hasselbach, A. Hauser and H. Spiering, *Inorganic* Chemistry 1985, 24, 2174-2178.
- [17] S. Decurtins, P. Gutlich, C. P. Kohler and H. Spiering, Journal of the Chemical Society-Chemical Communications 1985, 430-432.
- [18] P. Gütlich in Nuclear Decay Induced Excited Spin State Trapping (NIESST), Eds.: P. Gütlich and H. A. Goodwin), Springer Berlin Heidelberg, Berlin, Heidelberg, 2004, pp. 231-260.
- [19] G. Vankó, F. Renz, G. Molnár, T. Neisius and S. Kárpáti, Angewandte Chemie International Edition 2007, 46, 5306-5309.
- [20] C. Roux, J. Zarembowitch, B. Gallois, T. Granier and R. Claude, *Inorganic* Chemistry 1994, 33, 2273-2279.
- [21] M.-L. Boillot, J. Zarembowitch and A. Sour in Ligand-Driven Light-Induced Spin Change (LD-LISC): A Promising Photomagnetic Effect, Eds.: P. Gütlich and H. A. Goodwin), Springer Berlin Heidelberg, Berlin, Heidelberg, 2004, pp. 261-276.
- [22] B. Brachňaková and I. Šalitroš, Chemical Papers 2018, 72, 773-798.

- [23] A. Real, J. Zarembowitch, O. Kahn and X. Solans, Inorganic Chemistry 1987, 26, 2939-2943.
- [24] J. A. Real, A. B. Gaspar, M. C. Muñoz, P. Gütlich, V. Ksenofontov and H. Spiering in Bipyrimidine-Bridged Dinuclear Iron(II) Spin Crossover Compounds, Eds.: P. Gütlich and H. A. Goodwin), Springer Berlin Heidelberg, Berlin, Heidelberg, 2004, pp. 167-193.
- [25] G. Vos, R. A. Le Febre, R. A. G. De Graaff, J. G. Haasnoot and J. Reedijk, Journal of the American Chemical Society 1983, 105, 1682-1683.
- [26] J. A. Kolnaar, G. van Dijk, H. Kooijman, A. L. Spek, V. G. Ksenofontov, P. Gütlich, J. G. Haasnoot and J. Reedijk, Inorganic Chemistry 1997, 36, 2433-2440.
- [27] G. Psomas, N. Bréfuel, F. Dahan and J.-P. Tuchagues, *Inorganic Chemistry* 2004, 43, 4590-4594.
- [28] E. Breuning, M. Ruben, J.-M. Lehn, F. Renz, Y. Garcia, V. Ksenofontov, P. Gütlich, E. Wegelius and K. Rissanen, Angewandte Chemie International Edition 2000, 39, 2504-
- [29] R. W. Hogue, S. Singh and S. Brooker, Chemical Society Reviews 2018, 47, 7303-7338.
- [30] I. Boldog, F. J. Muñoz-Lara, A. B. Gaspar, M. C. Muñoz, M. Seredyuk and J. A. Real, Inorganic Chemistry 2009, 48, 3710-3719.
- [31] R. C. Stoufer, D. H. Busch and W. B. Hadley, Journal of the American Chemical Society 1961, 83, 3732-3734.
- [32] W. Kläui, Inorganica Chimica Acta 1980, 40, X22-X23.
- [33] T. Zhu, C. H. Su, B. K. Lemke, L. J. Wilson and K. M. Kadish, *Inorganic Chemistry* 1983, 22, 2527-2530.
- [34] L. G. Marzilli and P. A. Marzilli, Inorganic Chemistry 1972, 11, 457-461.
- [35] W. Klaeui, W. Eberspach and P. Guetlich, Inorganic Chemistry 1987, 26, 3977-3982.
- [36] J. Zarembowitch and O. Kahn, Inorganic Chemistry 1984, 23, 589-593.
- [37] S. Brooker, D. J. de Geest, R. J. Kelly, P. G. Plieger, B. Moubaraki, K. S. Murray and G. B. Jameson, Journal of the Chemical Society, Dalton Transactions 2002, 2080-2087.
- [38] I. H. Wasbotten and A. Ghosh, Inorganic Chemistry 2007, 46, 7890-7898.
- [39] S. Hayami, Y. Komatsu, T. Shimizu, H. Kamihata and Y. H. Lee, Coordination Chemistry Reviews 2011, 255, 1981-1990.
- [40] P. G. Sim and E. Sinn, Journal of the American Chemical Society 1981, 103, 241-243.
- [41] P. N. Martinho, B. Gildea, M. M. Harris, T. Lemma, A. D. Naik, H. Müller-Bunz, T. E. Keyes, Y. Garcia and G. G. Morgan, Angewandte Chemie International Edition 2012, 51, 12597-12601.
- [42] B. Gildea, M. M. Harris, L. C. Gavin, C. A. Murray, Y. Ortin, H. Müller-Bunz, C. J. Harding, Y. Lan, A. K. Powell and G. G. Morgan, Inorganic Chemistry 2014, 53, 6022-6033.
- [43] A. J. Fitzpatrick, E. Trzop, H. Müller-Bunz, M. M. Dîrtu, Y. Garcia, E. Collet and G. G. Morgan, Chemical Communications 2015, 51, 17540-17543.
- [44] I. A. Kühne, K. Esien, L. C. Gavin, H. Müller-Bunz, S. Felton and G. G. Morgan, Molecules 2020, 25, 5603.

- [45] I. A. Kühne, L. C. Gavin, M. Harris, B. Gildea, H. Müller-Bunz, M. Stein and G. G. Morgan, Journal of Applied Physics 2021, 129.
- [46] M. M. Harris, I. A. Kühne, C. T. Kelly, V. B. Jakobsen, R. Jordan, L. O'Brien, H. Müller-Bunz, S. Felton and G. G. Morgan, Crystal Growth & Design 2023, 23, 3996-4012.
- [47] G. G. Morgan, K. D. Murnaghan, H. Müller-Bunz, V. McKee and C. J. Harding, Angewandte Chemie International Edition 2006, 45, 7192-7195.
- [48] E. Dobbelaar, V. B. Jakobsen, E. Trzop, M. Lee, S. Chikara, X. Ding, H. Müller-Bunz, K. Esien, S. Felton, M. A. Carpenter, E. Collet, G. G. Morgan and V. S. Zapf, Angewandte Chemie International Edition 2022, 61, e202114021.
- [49] Proceedings of the Chemical Society 1961, 357-396.
- [50] V. V. Rostovtsev, L. G. Green, V. V. Fokin and K. B. Sharpless, Angewandte Chemie International Edition 2002, 41, 2596-2599.
- [51] A. Einhorn, E. Bischkopff, B. Szelinski, G. Schupp, E. Spröngerts, C. Ladisch and T. Mauermayer, Justus Liebigs Annalen der Chemie 1905, 343, 207-305.
- [52] P. L. Franke, J. G. Haasnoot and A. P. Zuur, Inorganica Chimica Acta 1982, 59, 5-9.
- [53] P. N. Gaponik, S. V. Voitekhovich and O. A. Ivashkevich, Uspekhi Khimii 2006, 75, 569-603.
- [54] H. Zhao, Z.-R. Qu, H.-Y. Ye and R.-G. Xiong, Chemical Society Reviews 2008, 37, 84-100.
- [55] F. R. Benson, Chemical Reviews 1947, 41, 1-61.
- [56] A. O. Koren, P. N. Gaponik, O. A. Ivashkevich and T. B. Kovalyova, Mendeleev Communications 1995, 5, 10-11.
- [57] D. Müller, C. Knoll, B. Stöger, W. Artner, M. Reissner and P. Weinberger, European Journal of Inorganic Chemistry 2013, 2013, 984-991.
- [58] M. Quesada, F. Prins, O. Roubeau, P. Gamez, S. J. Teat, P. J. van Koningsbruggen, J. G. Haasnoot and J. Reedijk, Inorganica Chimica Acta 2007, 360, 3787-3796.
- [59] P. J. van Koningsbruggen, Y. Garcia, H. Kooijman, A. L. Spek, J. G. Haasnoot, O. Kahn, J. Linares, E. Codjovi and F. Varret, Journal of the Chemical Society, Dalton Transactions 2001, 466-471.
- [60] C. M. Grunert, J. Schweifer, P. Weinberger, W. Linert, K. Mereiter, G. Hilscher, M. Müller, G. Wiesinger and P. J. van Koningsbruggen, Inorquite Chemistry 2004, 43, 155-
- [61] D. Müller, C. Knoll and P. Weinberger, Monatshefte für Chemie Chemical Monthly 2017, 148, 131-137.
- [62] D. Müller, C. Knoll, B. Stoger, W. Artner, M. Reissner and P. Weinberger, European Journal of Inorganic Chemistry 2013, 984-991.
- [63] M. Seifried, C. Knoll, J. M. Welch, D. Müller and P. Weinberger, Synthesis (Germany) 2018, 50, 1007-1014.
- [64] M. Seifried, C. Knoll, G. Giester, J. M. Welch, D. Müller and P. Weinberger, European Journal of Organic Chemistry 2017, 2017, 2416-2424.
- [65] W. L. Driessen and P. H. van der Voort, Inorganica Chimica Acta 1977, 21, 217-222.
- [66] W. Hibbs, A. M. Arif, P. J. van Koningsbruggen and J. S. Miller, CrystEngComm 1999, 1, 12-14.

- [67] W. Hibbs, P. J. van Koningsbruggen, A. M. Arif, W. W. Shum and J. S. Miller, Inorganic Chemistry 2003, 42, 5645-5653.
- [68] A. Bhattacharjee, P. J. van Koningsbruggen, W. Hibbs, J. S. Miller and P. Gütlich, Journal of Physics: Condensed Matter 2007, 19, 406202-406202.
- [69] M. A. Halcrow, Coordination Chemistry Reviews 2009, 253, 2493-2514.
- [70] J. Olguín and S. Brooker, Coordination Chemistry Reviews 2011, 255, 203-240.
- [71] O. G. Shakirova and L. G. Lavrenova, Crystals 2020, 10, 843.
- [72] Y. Sunatsuki, M. Sakata, S. Matsuzaki, N. Matsumoto and M. Kojima, Chemistry Letters 2003, 30, 1254-1255.
- [73] H. Ohta, Y. Sunatsuki, M. Kojima, S. Iijima, H. Akashi and N. Matsumoto, Chemistry Letters 2004, 33, 350-351.
- [74] N. Bibi, E. G. R. de Arruda, A. Domingo, A. A. Oliveira, C. Galuppo, Q. M. Phung, N. M. Orra, F. Béron, A. Paesano, Jr., K. Pierloot and A. L. B. Formiga, *Inorganic* Chemistry 2018, 57, 14603-14616.
- [75] P. Gütlich, Structure and Bonding 1981, 44, 83-195.
- [76] A. F. Stassen, M. Grunert, E. Dova, M. Müller, P. Weinberger, G. Wiesinger, H. Schenk, W. Linert, J. G. Haasnoot and J. Reedijk, European Journal of Inorganic Chemistry 2003, 2273-2282.
- [77] D. Müller, C. Knoll, M. Seifried, J. M. Welch, G. Giester, M. Reissner and P. Weinberger, Chemistry – A European Journal 2018, 24, 5271-5280.
- [78] A. B. Koudriavtsev, A. F. Stassen, J. G. Haasnoot, M. Grunert, P. Weinberger and W. Linert, Physical Chemistry Chemical Physics 2003, 5, 3676-3683.
- [79] P. J. van Koningsbruggen, M. Grunert and P. Weinberger, Monatshefte Fur Chemie 2003, *134*, 183-198.
- [80] M. Muttenthaler, M. Bartel, P. Weinberger, G. Hilscher and W. Linert, Journal of Molecular Structure 2005, 741, 159-169.
- [81] A. Absmeier, M. Bartel, C. Carbonera, G. N. L. Jameson, F. Werner, M. Reissner, A. Caneschi, J. F. Letard and W. Linert, European Journal of Inorganic Chemistry 2007, 3047-3054.
- [82] M. Quesada, H. Kooijman, P. Gamez, J. S. Costa, P. J. van Koningsbruggen, P. Weinberger, M. Reissner, A. L. Spek, J. G. Haasnoot and J. Reedijk, Dalton Transactions 2007, 5434-5440.
- [83] N. Hassan, P. Weinberger, F. Kubel, G. Molnar, A. Bousseksou, L. Dlhan, R. Boca and W. Linert, Inorganica Chimica Acta 2009, 362, 3629-3636.
- [84] N. Hassan, J. Stelzl, P. Weinberger, G. Molnar, A. Bousseksou, F. Kubel, K. Mereiter, R. Boca and W. Linert, Inorganica Chimica Acta 2013, 396, 92-100.
- [85] N. T. Madhu, P. K. Radhakrishnan, M. Grunert, P. Weinberger and W. Linert, Thermochimica Acta 2003, 407, 73-84.
- [86] A. Absmeier, M. Bartel, C. Carbonera, G. N. L. Jameson, P. Weinberger, A. Caneschi, K. Mereiter, J. F. Letard and W. Linert, Chemistry-a European Journal 2006, 12, 2235-2243.
- [87] P. Baran, R. Boča, I. Chakraborty, J. Giapintzakis, R. Herchel, Q. Huang, J. E. McGrady, R. G. Raptis, Y. Sanakis and A. Simopoulos, *Inorganic Chemistry* 2008, 47, 645-655.
- [88] K. L. Taft, A. Caneschi, L. E. Pence, C. D. Delfs, G. C. Papaefthymiou and S. J. Lippard, Journal of the American Chemical Society 1993, 115, 11753-11766.

- [89] T. A. Hudson, K. J. Berry, B. Moubaraki, K. S. Murray and R. Robson, *Inorganic* Chemistry 2006, 45, 3549-3556.
- [90] J. M. Clemente-Juan, C. Mackiewicz, M. Verelst, F. Dahan, A. Bousseksou, Y. Sanakis and J.-P. Tuchagues, Inorganic Chemistry 2002, 41, 1478-1491.
- [91] M. Seifried, F. M. Kapsamer, M. Reissner, J. M. Welch, G. Giester, D. Müller and P. Weinberger, Magnetochemistry 2022, 8, 95.
- [92] W. Zeni, D. Müller, M. Seifried, J. Welch, B. Stöger, G. Giester, M. Reissner, R. Miletich and P. Weinberger, European Journal of Inorganic Chemistry n/a, e202400358.
- [93] Z.-G. Gu, C.-Y. Pang, D. Qiu, J. Zhang, J.-L. Huang, L.-F. Qin, A.-Q. Sun and Z. Li, Inorganic Chemistry Communications 2013, 35, 164-168.
- [94] D.-H. Ren, X.-L. Sun, L. Gu, D. Qiu, Z. Li and Z.-G. Gu, Inorganic Chemistry Communications 2015, 51, 50-54.
- [95] K. Nishi, S. Arata, N. Matsumoto, S. Iijima, Y. Sunatsuki, H. Ishida and M. Kojima, Inorganic Chemistry 2010, 49, 1517-1523.
- [96] A. D. Ivanova, E. V. Korotaev, V. Y. Komarov, T. S. Sukhikh, S. V. Trubina, L. A. Sheludyakova, S. A. Petrov, A. Y. Tikhonov and L. G. Lavrenova, Inorganica Chimica Acta 2022, 532, 120746.
- [97] T. Kosone, R. Kosuge, M. Tanaka, T. Kawasaki and N. Adachi, New Journal of Chemistry 2022, 46, 10540-10544.
- [98] G. Lemercier, N. Bréfuel, S. Shova, J. A. Wolny, F. Dahan, M. Verelst, H. Paulsen, A. X. Trautwein and J.-P. Tuchagues, Chemistry – A European Journal 2006, 12, 7421-7432.
- [99] Dalton Transactions 2007, 697-710.
- [100] L. Salmon, G. Molnár, D. Zitouni, C. Quintero, C. Bergaud, J.-C. Micheau and A. Bousseksou, Journal of Materials Chemistry 2010, 20, 5499-5503.
- [101] A. B. Gaspar, V. Ksenofontov, M. Seredyuk and P. Gütlich, Coordination Chemistry Reviews 2005, 249, 2661-2676.
- [102] H. J. Shepherd, I. y. A. Gural'skiy, C. M. Quintero, S. Tricard, L. Salmon, G. Molnár and A. Bousseksou, *Nature Communications* 2013, 4, 2607.
- [103] B. Tondu, M. Piedrahita-Bello, L. Salmon, G. Molnár and A. Bousseksou, Sensors and Actuators A: Physical 2022, 335, 113359.
- [104] G. J. Halder, C. J. Kepert, B. Moubaraki, K. S. Murray and J. D. Cashion, Science 2002, 298, 1762-1765.
- [105] J. A. Real, E. Andrés, M. C. Muñoz, M. Julve, T. Granier, A. Bousseksou and F. Varret, Science 1995, 268, 265-267.
- [106] S. M. Neville, G. J. Halder, K. W. Chapman, M. B. Duriska, B. Moubaraki, K. S. Murray and C. J. Kepert, Journal of the American Chemical Society 2009, 131, 12106-12108.
- [107] E. Coronado, M. Giménez-Marqués, G. Mínguez Espallargas, F. Rey and I. J. Vitórica-Yrezábal, Journal of the American Chemical Society 2013, 135, 15986-15989.
- [108] Z. Arcís-Castillo, F. J. Muñoz-Lara, M. C. Muñoz, D. Aravena, A. B. Gaspar, J. F. Sánchez-Royo, E. Ruiz, M. Ohba, R. Matsuda, S. Kitagawa and J. A. Real, *Inorqunic* Chemistry 2013, 52, 12777-12783.
- [109] P. D. Southon, L. Liu, E. A. Fellows, D. J. Price, G. J. Halder, K. W. Chapman, B. Moubaraki, K. S. Murray, J.-F. Létard and C. J. Kepert, Journal of the American Chemical Society 2009, 131, 10998-11009.

- [110] X. Bao, H. J. Shepherd, L. Salmon, G. Molnár, M.-L. Tong and A. Bousseksou, Angewandte Chemie International Edition 2013, 52, 1198-1202.
- [111] M. Ohba, K. Yoneda, G. Agustí, M. C. Muñoz, A. B. Gaspar, J. A. Real, M. Yamasaki, H. Ando, Y. Nakao, S. Sakaki and S. Kitagawa, Angewandte Chemie International Edition 2009, 48, 4767-4771.
- [112] F. J. Muñoz-Lara, A. B. Gaspar, M. C. Muñoz, A. B. Lysenko, K. V. Domasevitch and J. A. Real, *Inorganic Chemistry* 2012, 51, 13078-13080.
- [113] C. Faulmann, K. Jacob, S. Dorbes, S. Lampert, I. Malfant, M.-L. Doublet, L. Valade and J. A. Real, *Inorganic Chemistry* 2007, 46, 8548-8559.
- [114] P. G. Lacroix, I. Malfant, J.-A. Real and V. Rodriguez, European Journal of Inorganic Chemistry 2013, 2013, 615-627.
- [115] F. J. Muñoz-Lara, A. B. Gaspar, M. C. Muñoz, M. Arai, S. Kitagawa, M. Ohba and J. A. Real, Chemistry - A European Journal 2012, 18, 8013-8018.
- [116] S. Titos-Padilla, J. M. Herrera, X.-W. Chen, J. J. Delgado and E. Colacio, Angewandte Chemie International Edition 2011, 50, 3290-3293.
- [117] M. Matsuda, H. Isozaki and H. Tajima, Chemistry Letters 2008, 37, 374-375.
- [118] A. B. Gaspar, M. Seredyuk and P. Gütlich, Coordination Chemistry Reviews 2009, 253, 2399-2413.
- [119] Y. Garcia, F. Robert, A. D. Naik, G. Zhou, B. Tinant, K. Robeyns, S. Michotte and L. Piraux, Journal of the American Chemical Society 2011, 133, 15850-15853.
- [120] O. I. Kucheriv, V. V. Oliynyk, V. V. Zagorodnii, V. L. Launets and I. A. Gural'Skiy, Scientific Reports 2016, 6.
- [121] C. Bartual-Murgui, A. Akou, C. Thibault, G. Molnár, C. Vieu, L. Salmon and A. Bousseksou, Journal of Materials Chemistry C 2015, 3, 1277-1285.
- [122] F. Averseng, C. Lepetit, P. G. Lacroix and J. P. Tuchagues, Chemistry of Materials 2000, 12, 2225-2229.
- [123] K. A. Hofmann and F. Küspert, Zeitschrift für anorganische Chemie 1897, 15, 204-
- [124] T. Kitazawa, Y. Gomi, M. Takahashi, M. Takeda, M. Enomoto, A. Miyazaki and T. Enoki, Journal of Materials Chemistry 1996, 6, 119-121.
- [125] V. Niel, J. M. Martinez-Agudo, M. C. Muñoz, A. B. Gaspar and J. A. Real, Inorganic Chemistry 2001, 40, 3838-3839.
- [126] C. Bartual-Murgui, N. A. Ortega-Villar, H. J. Shepherd, M. C. Muñoz, L. Salmon, G. Molnár, A. Bousseksou and J. A. Real, Journal of Materials Chemistry 2011, 21.
- [127] F. J. Munoz-Lara, A. B. Gaspar, M. C. Munoz, V. Ksenofontov and J. A. Real, Inorganic Chemistry 2013, 52, 3-5.
- [128] V. Niel, M. C. Muñoz, A. B. Gaspar, A. Galet, G. Levchenko and J. A. Real, Chemistry - A European Journal 2002, 8, 2446.
- [129] J. E. Clements, J. R. Price, S. M. Neville and C. J. Kepert, Angewandte Chemie International Edition 2014, 53, 10164-10168.
- [130] J.-Y. Li, Z.-P. Ni, Z. Yan, Z.-M. Zhang, Y.-C. Chen, W. Liu and M.-L. Tong, CrystEngComm 2014, 16, 6444-6449.
- [131] J.-Y. Li, Y.-C. Chen, Z.-M. Zhang, W. Liu, Z.-P. Ni and M.-L. Tong, Chemistry -A European Journal 2015, 21, 1645-1651.
- [132] M. M. Dîrtu, A. Rotaru, D. Gillard, J. Linares, E. Codjovi, B. Tinant and Y. Garcia, Inorganic Chemistry 2009, 48, 7838-7852.

[133] C. J. Johnson, G. G. Morgan and M. Albrecht, Journal of Materials Chemistry C $2015,\ 3,\ 7883\text{-}7889.$

[134] D. Müller in Iron (II) spin crossover complexes: from chirality to multifunctionality, Vol. Technische Universität Wien, 2015.

6 Appendix



6.1 Reprint Permissions and copyright



This is a License Agreement between Willi Zeni ("User") and Copyright Clearance Center, Inc. ("CCC") on behalf of the Rightsholder identified in the order details below. The license consists of the order details, the Marketplace Permissions General Terms and Conditions below, and any Rightsholder Terms and Conditions which are included

All payments must be made in full to CCC in accordance with the Marketplace Permissions General Terms and Conditions below.

Order Date Order License ID 01-Jul-2024 1500117-1 1434-1948

Type of Use Publisher

Portion

Republish in a thesis/ dissertation WILEY - VCH Chapter/article

LICENSED CONTENT

Publication Title

European journal of inorganic chemistry

Article Title

A New Family of Fe(II) 1-Propvl-1H-Imidazole Complexes with Mono-. Bi-, and Tetra-Nuclear

Members

Author / Editor

Gesellschaft Deutscher Chemiker., Koninklijke Nederlandse Chemische Vereniging., Koninklijke Vlaamse Chemische Vereniging., Société royale de chimie (Belgium), Società chimica italiana., Société française de

chimie.

01/01/1998

Language Country Rightsholder English Germany

John Wiley & Sons - Books **Publication Type**

Journal

REQUEST DETAILS

Portion Type Page Range(s)

Total Number of Pages Format (select all that

apply)

Date

Who Will Republish the

Content?

Duration of Use

Lifetime Unit Quantity

1-10

Chapter/article

10

Print, Electronic

Academic institution

Life of current edition

Up to 499

Rights Requested Distribution Translation

Copies for the Disabled? Minor Editing Privileges?

Incidental Promotional

Use?

Currency

Main product Worldwide

Original language of publication

No No

EUR

NEW WORK DETAILS

Institution Name

TU Wien - Institute of Applied Synthetic Chemistry

Title

Iron(II) Spin Crossover Complexes: a multifaceted approach to rational design, tailor cooperativity, enhance complexity and advanced multifunctionality.

Instructor Name

Date

Expected Presentation

2024-07-19

ADDITIONAL DETAILS

The Requesting Person / Organization to Appear on the License

Willi Zeni

Willi Zeni



6.2 Curriculum vitae

Willi Zeni

Dipl.-Ing., BSc.

- 05.10.1992, Trento (ITA)
- Große Pfarrgasse 21/14 A-1020 Vienna
- zeni.wil92@gmail.com
- +43 68120355885

SKILLS **EDUCATION**

SEP 2019 - CURRENT

PHD PROGRAMME Technical Chemistry.

University of Technology, Vienna - AUT

Dissertation on: Iron(II) Spin Crossover Complexes: a multifaceted approach to rational design, tailor cooperativity, enhance complexity and advanced multifunctionality.

MAR 2016 - JUL 2019

MASTER'S PROGRAMME Technical Chemistry.

University of Technology, Vienna - AUT

Master's thesis: "Iron(II) Spin-Crossover complexes based on alkyl imidazoles and pyrazoles'

OCT 2012 - SEP 2015

BACHELOR'S PROGRAMME Chemistry.

Università degli studi di Padova, Padova - ITA

Bachelors thesis: "Transition metal complexes with NHC ligands derived from caffeine".

SECONDARY SCHOOL

Fondazione Edmund Mach, San Michele all'Adige - ITA

Diploma di maturità (Qualification for university entrance) with the qualification "Oenologist". Final essay: "Deacidification of wines with the double salts method: theoretical principles, practical methodology, calculation scheme and organoleptic impact"

0	Italian	•	•	•	•	•
0	German	•	•	•	•	•
0	English	•	•	•	•	C
₽	MS Office	•	•	•	•	•
N	Origin Pro	•	•	•	•	0

Ps Photoshop Ai Ilustrator 000

.00 Indesign

EXPERIENCE

SEP 2018 - CURRENT

Research group Weinberger. Magneto- and Thermochemistry

Synthesis and Characterization of iron(II) based spin crossover materials.

University of Technology, Vienna - AUT ▼

APR 2017 - CURRENT

Teaching in undergraduate laboratory courses

University of Technology, Vienna - AUT ▼

Supervision in: Synthesis laboratory course, Advanced laboratory course in synthetic chemistry, Introductory laboratory and Preparative laboratory for chemical eingineers

SEP 2012 - NOV 2012

Internship at "Château Ferrière"

Margaux - FRA ♥

Co-oenologist, supervision and active participation in all the post-harvest operations and first vinification stages

SEP 2011 - NOV 2011

Internship at "Weingut Rolf Heinrich"

Heilbronn - DEU ♥

Helping with the harvest and in the first vinification stages

AUG 2010 - OCT 2010

Internship at "Contadi Castaldi"

Adro - ITA

Performing different tasks in the harvest phase as well as in the first vinification stages

2008 - 2020

Working at the winery "Azienda Agricola Zeni Giorgio"

San Michele all'Adige - ITA ♥

Involved in every aspect, from work in the vineyard and in the cellar to sales and management

FEB 2020

Workshop for Novel Materials and superconductors

Schladming, AUT

POSTER PRESENTATION on "Towards multifunctionality of a 3d-4f coordination polymer"

Workshop for Novel Materials and superconductors

Schladming, AUT

 $\textbf{POSTER PRESENTATION} \ on \ "Bifunctional Fe(II) SCO-complexes based on \ []-(IH-tetrazol-1-yl) \ carboxylic \ acids$

AUG 2022

ICCC (International Conference on Coordination Chemistry)

Rimini, ITA 🛡

POSTER PRESENTATION "Advanced Host-Guest Chemistry in Second-Generation Spin-Switchable Hofmann-type Networks'

SEP 2023

EICC (EuChemS Inorganic Chemistry Conference)

Vienna, AUT 🛡

 $\textbf{ORAL PRESENTATION} \quad \text{``Host-guest Chemistry in Second Generation Spin-Switchable Hofmann-type Networks: larger}$ pores for larger guests"

PEER-REVIEWED PUBLICATIONS

- 1) W. Zeni, M. Seifried, C. Knoll, J. M. Welch, G. Giester, B. Stöger, W. Artner, M. Reissner, D. Müller, P. Weinberger "Bifunctional Fe(II) spin crossovercomplexes based on ω -(1H-tetrazol-1-yl) carboxylic acids" Dalton transactions 2020, 49, 17183-17193.
- 2) W. Zeni, D. Müller, M. Seifried, J. M. Welch, G. Giester, B. Stöger, R. Miletich, M. Reissner, , P. Weinberger "A new family of Fe(II) 1-propyl-1H-imid azole complexes with mono-, bi-, and tetra-nuclear members" European Journal of Inorganic Chemistry, accepted June 18th, 2024
- W. Zeni, D. Müller, G. Giester, B. Stöger, M. Reissner, W. Artner, P. Weinberger "Tetrakis-cyanoacetylides as building block for a second generation of 3) spin-switchable Hofmann-type networks with enhanced porosity" Submitted to ACS - Inorganic Chemistry July 1st 2024